Modeling of Complex Reaction Systems

Steam Cracker

Zoetermeer, June 1998

M.W.M. van Goethem Jaagpad 81 2288CJ Rijswijk (ZH) Tel. 015-2190824 Delft University of Technology (TUD), Department of Chemical Technology and Material Science, Sub-Faculty Chemical Process Technology Section Process Control & Integration

Kinetic Technology International (KTI) B.V. Division Pyrotec Bredewater 26 2715 CA Zoetermeer The Netherlands

Supervisors:

Dr. ir. P.J.T. Verheijen (TUD) Dr. ir. C. van Leeuwen (KTI)

Preface

I would like to thank Cor van Leeuwen and Peter Verheijen for there considerable advice and efforts. I also enjoyed the collaboration with Nils van Velzen. Further I am grateful to all my colleagues at the Pyrotec division of KTI, in particular Barbie Hunt, Florian Kleinendorst, Peter Valkenburg. For the opportunity to obtain my masters degree in chemical technology I thank my parents. I appreciate the moral support and patients of my girl friend Karin Kostermans.

SPYRO* is a registered trademarks of KTI B.V.

By faith we perceive that the universe was fashioned by the word of God, so that the visible came forth from the invisible. Hebr. 11:3

Summary

Steam pyrolysis of ethane and naphtha is an important chemical bulk process. It produces ethylene and propylene, which are important base chemicals. In order to be competitive, crackers have to be operated at near optimal conditions. Hence, a simulation program of the process, particularly of the pyrolysis is very helpful. KTI uses and licenses such a program called SPYRO*. Development of this program has started over 20 years ago. Consequently, it uses a closed model.

It has been the objective of this study to investigate the feasibility of the development of an open version of SPYRO. Here open means that the equations are written in residual form . This enhances the flexibility of the program very much.

For our studies we have used the model of Froment for ethane cracking because the documentation to make an open SPYRO model was insufficient. This Froment model has been modified as to improve the modeling of the bends.

It has been checked, whether the solution of this model would pose any problems. It was found that the index might become more than 1 during integration. As yet no sound physical explanation has been found for this phenomena.

It also follows from investigation of the index that a start-up problem of the numerical integration exists for the original set of differential equations. We have found a more elegant method to circumvent this problem than Froment. Moreover, we were able to solve the set of equations for bad initial conditions (equal to the boundary conditions).

The ordinary differential equations of the model are turned into algebraic equations using orthogonal collocation on finite elements. This allows the model to be solved with an equation solver. The results were compared with various commercial numerical integrators. Excellent agreement was found for limited numbers of sections and collocation points.

The speed of solution of the linearized set of model equations depends on the size, the sparsity and structure of the Jacobian. The latter has an enormous effect on the fill-in of the L and U decomposition matrices. We found a very satisfying structure by modification of the equations and proper arrangement in the Jacobian.

On the basis of the above results we may draw the following conclusions regarding the feasibility of the development of an Open SPYRO model. Unfortunately we had to use a simple model of Froment rather than the SPYRO equations themselves. Nevertheless, we have concluded that such a development is feasible. Within a reasonable time an accurate solution will be found even with bad starting values. The computation time can be further reduced with a smart initialization procedure.

Table of Contents

Prefaceii					
Sun	nmary	*******	••••••	iii	
1	Intr	oduction	n	6	
2			cker Model		
	2.1	Introdu	uction	10	
	2.2	Ethane	Cracker Model Description	10	
		2.3	The Index of Ethane Cracker Model		
	2.4	Initiali	zation Problem	18	
	2.5	Solution	on of Initialization Problem	19	
		2.5.1	Froment Solution	19	
		2.5.2	Alternative Solution to the Initialization Problem	19	
	2.6		Problem During Solving of Test Model		
	2.7		al Meaning of Index		
3	Nun		Implementation		
	3.1		uterized model		
	3.2	_	gonal Collocation		
		3.2.1	Lagrange Polynomial		
		3.2.2	Orthogonal Collocation on Finite Elements		
		3.2.3	Collocation of Coupled Differential Equations		
		3.2.4	Collocation of Coupled ODE's with Finite Element Method		
		3.2.5	Form of the Residual Equations		
	3.3		uation Methods		
		3.3.1	Types of Homotopy		
		3.3.2	Solution of the homotopy equations		
		3.3.3	Homotopy Differential Equations		
4			Cthane Cracker Model		
	4.1		es		
	4.2		ntum Balance		
			Friction of the Bends		
		4.2.2	Comparison of Solution to Initialization Problem		
	4.3		y Balance	45	
		4.3.1	Comparison of Energy Balances without Kinetic Energy		
		4.3.2	Comparison of Energy Balances with Kinetic Energy		
5			e-up		
	5.1		uction		
	5.2	Validation of Collocation on Ethane Cracker Model			
	5.3	_	ged Ethane Cracker Model		
	5.4	Considerations over Mass Balance			
	5.5		on of Collocation Model with Homotopy		
		5.5.1	Initialization of Collocation Model	63	

	Conclusions and Recommendations	**************************************
	6.1 Collocation	
	6.2 Mass balances	
	6.3 Solving the collocation model	68
	6.4 Momentum Balance	
	6.5 Energy Balance	
7	References	
8	Nomenclature	74
-		
An		
_	pendix 1: Data of Froment Ethane cracker model	76
Ap	pendix 1: Data of Froment Ethane cracker modelpendix 2: Discussion over Momentum Equation used by Froment	76
Ap	pendix 1: Data of Froment Ethane cracker model pendix 2: Discussion over Momentum Equation used by Froment pendix 3: Differentiation of Lagrange Interpolation Polynomial	76 78
Ap Ap	pendix 1: Data of Froment Ethane cracker model pendix 2: Discussion over Momentum Equation used by Froment pendix 3: Differentiation of Lagrange Interpolation Polynomial pendix 4: Adaptive Collocation on Finite Elements	768082
Ap Ap Ap	pendix 1: Data of Froment Ethane cracker modelpendix 2: Discussion over Momentum Equation used by Fromentpendix 3: Differentiation of Lagrange Interpolation Polynomialpendix 4: Adaptive Collocation on Finite Elementspendix 5: Path Parameterization by Arclength	
Ap Ap Ap Ap	pendix 1: Data of Froment Ethane cracker model pendix 2: Discussion over Momentum Equation used by Froment pendix 3: Differentiation of Lagrange Interpolation Polynomial pendix 4: Adaptive Collocation on Finite Elements	

1 Introduction

The chemical process of steam pyrolysis for the production of ethylene is modeled for simulation purposes. Pyrolysis, the cracking of hydrocarbons diluted with steam, takes place between 650 - 850°C. The reactor (see Figure 1) which is used for this process consists of two sections: a convection section, in which the hydrocarbon feed is mixed with steam and heated to the temperature where the cracking starts (650°C), and the firebox section where the hydrocarbon feed flows through the radiant coils in which the cracking takes place. The residence time in the tubes is very short (0.5 - 1 s).

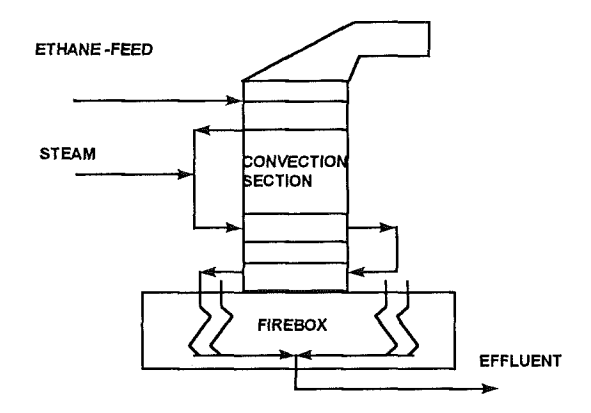


Figure 1: A schematic representation of an ethane cracker.

A number of requirements concerning the steam creaking process are:

- 1. Considerable heat input at a high level. At high temperatures a reasonable conversion can be obtained within short residence times.
- 2. Limitation of hydrocarbon partial pressure in the reactor. The equilibrium shifts to a less favorable composition (large molecules) at higher pressure. Steam is added for dilution; it also reduces the formation of coke.
- 3. Very short residence times. If the residence time is too long unfavorable products are obtained.
- 4. Rapid quench of the reactor product to preserve the composition

The production of ethylene is a large scale process with small profit margins. The plants must operate close to the optimal conditions, to be competitive with other companies. It is not surprising that a lot of effort is put in the development of a simulation program. Such a program is SPYRO. This simulation tool can help to provide answers to the following questions without the use of (a lot of) expensive experiments.

- Which feed gives the most profit?
- What is the maximum tube skin temperature?
- What is the maximum time on stream before decoking?

Furthermore the program can be used for:

- Influence of the variation of the heat input, outlet pressure, etc.
- Off-line optimization of the steam cracker.
- Design of a steam cracker.

In the early days of steam cracking, the feed was mainly ethane. Through the knowledge and the experience of the ethane steam cracking process, the ethylene producing companies started to use heavier feeds. In the past the driving force to release a new version of SPYRO was to improve the kinetic scheme that could handle the new feeds used by the ethylene production companies. The SPYRO simulation package is nowadays able to handle all kind of feeds used for the production of ethylene. A lot of work has been done to improve the kinetic scheme opposed to the algorithm that solves the cracker model. The driving force for the next release is an open SPYRO. This concerns the algorithm applied to obtain the solution of the SPYRO model. An open model is a model where the equations are written in the residual form. The advantage is illustrated with a simple example. In most current simulation packages for radiant coils, for example SPYRO, it is difficult to calculate the required coil length, that results in a given yield. The engineer has to apply a trial and error method through changing the length of the coil in order to get the desired yield. In the open SPYRO model the yield is a parameter and the length of the coil a variable. An engineer can easily decide what the variables are and what the parameters should be.

The target of the open SPYRO project is to model the steam cracking process. An open SPYRO model is wanted and therefor we need a solver and an open model that can be connected to the solver. For the open model we need the SPYRO equations, that is, the differential balances and all the algebraic equations to describe the steam cracking process. The SPYRO differential equations have to be transformed to algebraic equations by the collocation method. An overview of the project is schematically given below in Figure 2.

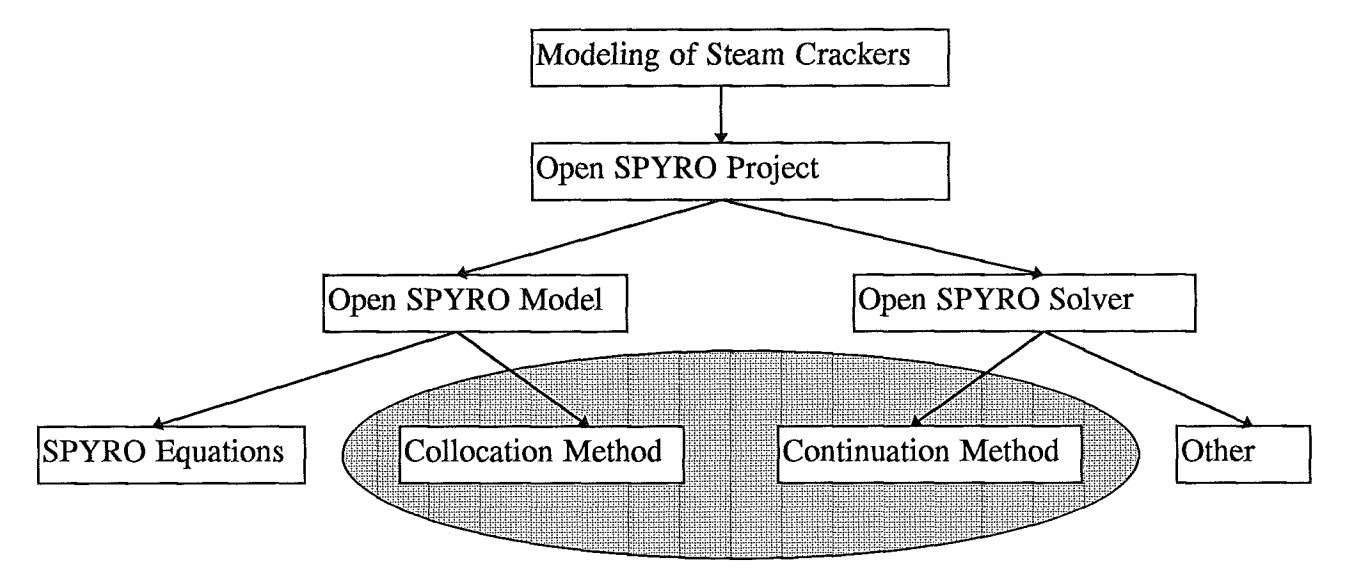


Figure 2: A schematic overview of open SPYRO project.

This report deals with topics of the open SPYRO model and solver as illustrated in Figure 2, it is part of the investigation to the feasibility of the creation of an open SPYRO model. It contains results that must lead to the answer if it is possible to create the open SPYRO model using the collocation method. The collocation method needs to be tested and validated, this requires a test model. The SPYRO equations are for certain reasons not available to test with. We use a small ethane steam cracker model to test and validate the collocation method, for experimental purposes we made a number of large 'steam cracker' models. These large models do not have a physical meaning like the SPYRO or ethane model, but are used to test the solver and to make statements relevant for solving SPYRO with collocation.

The Jacobian of the algebraic SPYRO model must have a structure with pleasant properties for the solver. The mathematician working on this project creates a non-linear solver and this solver will obtain the solution of the collocation steam cracker models.

Chapter 2 contains the description of the ethane steam cracker model. As mentioned above we need some cracker models to test the collocation method on, it is important that this test case is not too big in order to sustain the overview of the model. This ethane model consists of 11 differential equations and a number of algebraic equations. This model is a so-called DAE system (Differential Algebraic Equation system). In the past the theory over DAE systems has increased (Brenan 96), we will apply the index determination of a DAE system to the ethane model. This index gives information on whether the DAE system can be solved.

The model we describe in this chapter has an initialization problem. Froment 79 solved this problem and we will give also an alternative solution. We used the concept of this index determination to prove also that the given model can indeed not be initialized. We solve the model first with standard mathematical packages like gPROMS and MATLAB before applying the collocation method. Therefor, we need some reference for the validation of the collocation method. During the integration of the ethane model we encountered some problems. These problems are explained in a mathematical way with the theory over the index and we could trace the equations that created the problems. Chapter 2 can be summarized as follows: it will show that we have tools and theory to understand possible problems and limits of the used test model.

The 3rd chapter will deal with the theory of the collocation method and the theory of continuation methods. In chapter 2 we used standard mathematical packages to solve the ethane cracker model and we were not concerned with the numerical solution method. With the general mathematical packages like gPROMS and MATLAB it is very difficult (maybe impossible) to handle open models in a convenient way. The open model demands the use of a generic program language like FORTRAN and the use of numerical techniques such as the collocation method to transform the cracker model into a numerical mathematical model. The collocation method transforms differential equations into algebraic equations. These algebraic equations must be solved to obtain the solution of the cracker model. A way to obtain a solution of a set of non-linear equations is with the continuation method. This method enables the engineer to use a physical insight to obtain the solution of the problem.

In chapter 4 we will improve the test model. The reason not to derive our own model is for the fact that the main target is to experiment with the collocation technique on steam cracker models. The model where collocation should be applied on is the SPYRO model and therefor it is not a priority to make our own model. This is not a justification, not to check the used test model. We will analyze the momentum and heat balances of the test model. Maybe the results obtained can be used to the SPYRO model. For some reasons we are not able to use SPYRO, so therefor no conclusions could be made over the usefulness of the results to the SPYRO model. We will use the general momentum and energy balance of Bird 60 and derive a one dimensional balance for the modeling of steam crackers. The relevant terms of the momentum balance were examined. We investigated the way the friction of the bends is accounted for. Two possible approaches were examined. The discussion of the momentum balance is based both on theory as well as on the numerical results. The general one dimensional macroscopic energy balance is derived and applied to tube flow. The energy balance in the test model is a very simplified energy balance. In the period of time that the test model was published, no high speed computers and advanced algorithms were available to solve DAE systems.

Therefor the equations had to be changed to transform the DAE model in an ODE model. Nowadays we have faster computers and are able to integrate DAE models directly. When using the collocation method it is very easy to add algebraic equations to the model which makes it possible to use a less simplified energy balance. In this paragraph we compare different energy balances with each other and we compare the produced results with data of a real steam cracker.

In the 5th chapter we deal with various topics. The first topic is the validation of the collocation method on the ethane steam cracker model. For this validation we used as reference the results obtained with gPROMS. For the readers who are not familiar with gPROMS package, we compared the results with the well-known GEAR routine (of MATLAB). We examined the influence of the increase of the number of collocation points per finite element and the increase of the number of finite elements in the domain of interest. The second topic deals with the large 'steam cracker' models. These large models are created to test the non-linear solver of the mathematician working on this project. For these large models it is very important to express the component continuity equations in the right variables. The third topic of this chapter consider the Jacobian structure and the continuity equations. The last topic concerns the path to obtain the solution of a collocation model. As mentioned above a mathematician is also working on this project and therefor it seems logic not to be concerned with how the models should be solved. A priori, we do not know how difficult the SPYRO problem is, so therefor we created large test models in which the steepness of the resulting curves can be altered. We expect that the large models with both steep and flat curves could be difficult problems. We will solve these difficult problems with the continuation method. This continuation method provides ways to obtain the solution of difficult problems. It is possible to use a physical insight to obtain the solution of the problem with the continuation methods, this is the reason why we use continuation techniques.

In chapter 6 conclusions and recommendations for continuing work are given.

2 Ethane Cracker Model

2.1 Introduction

We need some cracker models to test and validate the collocation method. The used cracker model is published by Froment and Bischoff 79 and is described in the next paragraph. Most models used by chemical engineers consists of Differential and Algebraic Equation (DAE) systems. In the past the theory over DAE systems has increased (Brenan 96), one subject is the index of a DAE system. This index gives information on the solvability of a model and provides ways to explain problems. We determined the index of the test model and used it to explain problems encountered during integration of the test model. The test model described in the next paragraph has an initialization problem. Froment 79 gives a solution to this initialization problem, we will give an alternative solution. The concept of the index determination is applied to prove that the given test model has an initialization problem. The index of the test model is obtained by a mathematical procedure, therefor it is interesting to see if the obtained index has a physical meaning, this will be looked at and described at the end of this chapter.

2.2 Ethane Cracker Model Description

The chemical process of ethane pyrolysis for the production of ethylene is modeled in a mathematical description for simulation purposes. More general information on the process of steam cracking is given in the previous chapter. This section denotes the mathematical description of the process in a radiant coil. The description of the process can be found in Froment and Bischoff 1979.

Figure 3 schematically represents an ethane cracker given by Froment 79. Appendix 1 gives a more detailed information on the geometry, feed and boundary conditions.

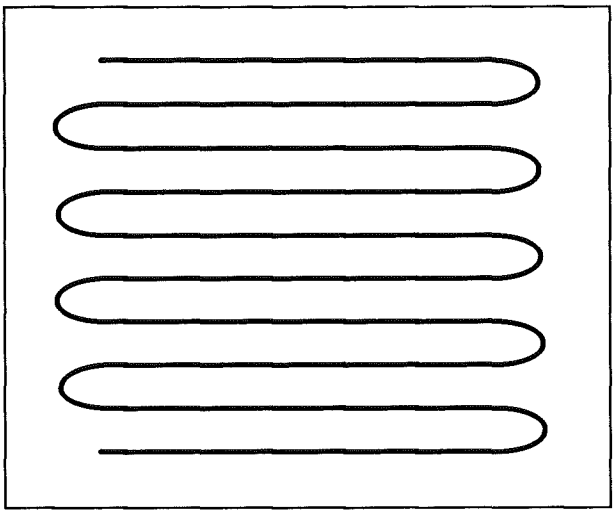


Figure 3: Schematically layout of the coil in the ethane cracker with horizontal tubes Froment 79.

The following set of continuity equations for the components for an infinitely small part of the coil with length dz have to be solved, together with the energy equation and the pressure drop equation:

$$\frac{dF_j}{dz} = A_{coil}RATE_j = A_{coil}\left(\sum_{i=1}^{7} \alpha_{ij} r_i\right)$$
(II-1)

for: components, j = 1 to 9 and reactions, i = 1 to 7

$$\frac{dT}{dz} = \frac{\left[q(z)\pi d + A_{coil}\sum_{i=1}^{7}(-\Delta H_i)r_i\right]}{\sum_{j=1}^{9}F_jCp_j}$$
(II-2)

$$-\frac{dP}{dz} = \left[2\frac{f}{d} + \frac{f_{bend}}{2\pi r_b}\right] \rho u^2 + \rho u \frac{du}{dz}$$
 (II-3)

with initial conditions: $F_j = F_{0,j}$, $T = T_0$ and $P = P_0$, all at z = 0. The components are: methane (CH_4) , acetylene (C_2H_2) , ethylene (C_2H_4) , ethane (C_2H_6) , propylene (C_3H_8) , propane (C_3H_6) , 1,3-butadiene (C_4H_6) , hydrogen (H_2) and steam (H_2O) . Appendix 1 contains more information on the boundary conditions. In equation (II-1) $RATE_j$ is the total rate of change of the amount of component j and r_i is the rate of the i-th reaction. We disagree with the expression, given by Froment 79, for the way the friction of the bends is accounted for. This difference in opinion is given in appendix 2. In formula (II-3) given above, the corrected friction term for the bends is shown.

The heat flux through the tube wall is given by q(z), d states the internal diameter of the tube, A_{coil} denotes the cross-sectional area of the tube and the radius of a bend is represented by r_b . The stoichiometric coefficient matrix is for the ethane cracker model defined as, α .

$$\alpha = \begin{pmatrix} 0 & 0 & 1 & -1 & 0 & 0 & 0 & 1 & 0 \\ 0 & 0 & -1 & 1 & 0 & 0 & 0 & -1 & 0 \\ 1 & 0 & 0 & -2 & 0 & 1 & 0 & 0 & 0 \\ 1 & 1 & 0 & 0 & -1 & 0 & 0 & 0 & 0 \\ -1 & -1 & 0 & 0 & 1 & 0 & 0 & 0 & 0 \\ 0 & -1 & -1 & 0 & 0 & 0 & 1 & 0 & 0 \\ 0 & 0 & -1 & -1 & 1 & 0 & 0 & 0 & 0 \end{pmatrix}$$

$$(II-4)$$

The rows of the stoichiometric coefficient matrix are denoted by i and the columns are denoted by j, the rows represent the reactions and the columns represent the components of the system.

The rate of the seven reactions are defined as follows:

$$r_i = k_i \prod C_j^{k_j} \tag{II-5}$$

with the following expression for the concentrations:

$$C_{j} = \frac{F_{j}}{\sum_{s=1}^{9} F_{s}} \frac{P}{RT}$$
(II-6)

and whereby the product given in formula (II-5) is taken over all the reactants of the *i*-th reaction. For reaction i, k_j is equal to 1 when in the stoichiometric matrix (II-4) the coefficient is negative and is equal to 0 in all other cases. The universal gas constant is given by R.

The heat of reaction is the sum of heats of formation of reactants and products:

$$\Delta H_i = \sum_{j=1}^9 \alpha_{i,j} \Delta H_{f,j} \quad \text{for : } i = 1 \text{ to } 7$$
 (II-7)

where $\alpha_{i,j}$ are the stoichiometric coefficients and

$$\Delta H_{f,j} = \Delta H_{f,j}^o + \int_{T_{tot}}^T Cp_j dT \quad \text{for } j = 1 \text{ to } 9$$
 (II-8)

where the specific heat is given by:

$$Cp_{j} = A_{j} + B_{j}T + C_{j}T^{2} + D_{j}T^{3}$$
 for : $j=1$ to 9 (II-9)

The friction factor for straight tubes is given by:

$$f = 0.046 \left(\frac{dG}{\mu}\right)^{-0.2} \tag{II-10}$$

The mass flux is denoted by G. For a bend the next expression is used:

$$f_{bend} = 0.0714 + 0.266 \frac{d}{r_b} \tag{II-11}$$

The viscosity is calculated from the viscosity of the individual components

$$\mu = \frac{\sum_{j=1}^{9} F_{j} \mu_{j}}{\sum_{j=1}^{9} F_{j}}$$
 (II-12)

How the viscosity of the individual components is calculated is given in appendix 1. The mean molecular mass is given by:

$$M_M = \frac{G A_{coil}}{\sum_{j=1}^{9} F_j}$$
 (II-13)

The velocity is denoted as:

$$u = \frac{G}{M_M} \frac{RT}{P} \tag{II-14}$$

The density of the fluid can be evaluated with:

$$\rho = \frac{M_M P}{RT} \tag{II-15}$$

The parameters required to solve this model are given in appendix 1.

The components profiles, the temperature and the pressure profile in the ethane cracker are given in the next figure. These profiles are obtained when the ethane model of Froment 79 is integrated.

The Molar Flowrates versus position in reactor

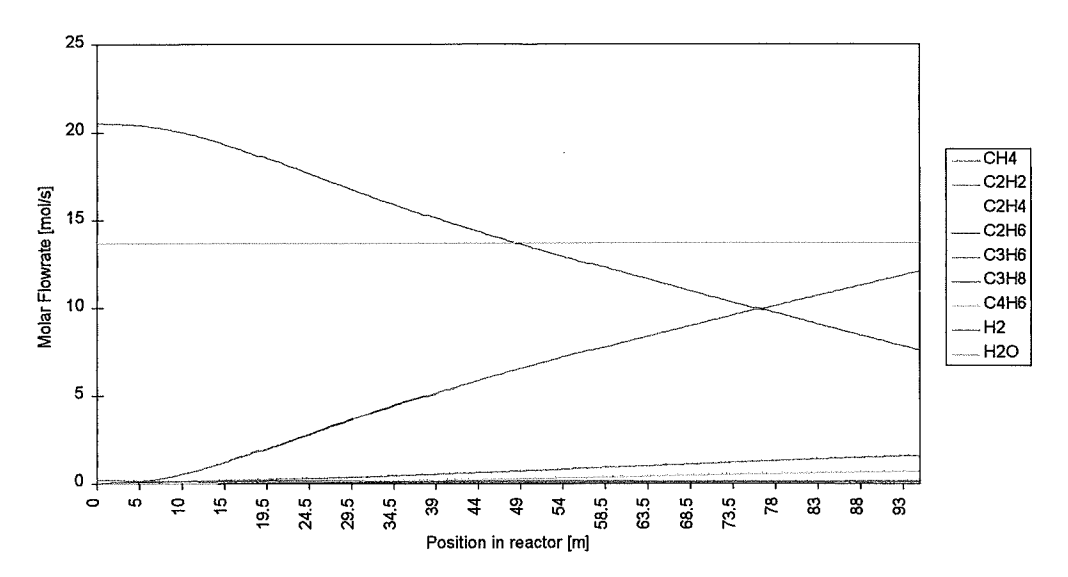


Figure 4: Component profiles in the ethane steam cracker described by the ethane model of Froment 79.

Temperature and pressure versus position in reactor

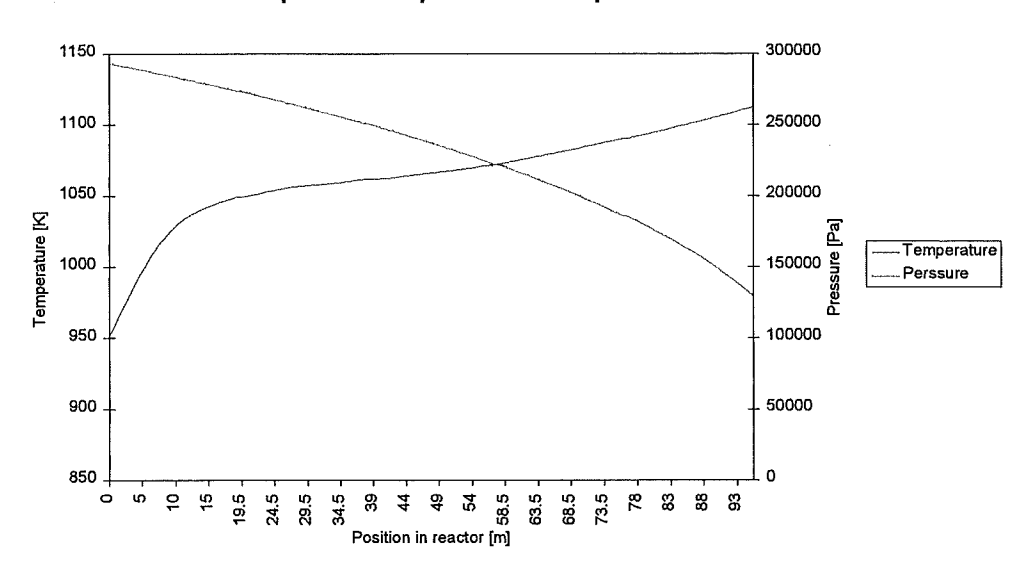


Figure 5: Temperature and pressure profile in the ethane steam cracker described by the ethane model of Froment 79.

2.3 The Index of Ethane Cracker Model

Most of the models developed by scientist and engineers consist of Differential and Algebraic Equations (DAE). Usually the DAE is converted into an ODE (Ordinary Differential Equations), nowadays we consider these DAE models directly, rather than to try to rewrite it as an ODE. In a DAE system, there are algebraic constraints on the variables. In general notation a DAE system can be written as:

$$\mathbf{x'} = \mathbf{f}(\mathbf{x}, \mathbf{y}, \mathbf{t}) \tag{II-16}\mathbf{A}$$

$$0 = \mathbf{g}(\mathbf{x}, \mathbf{y}, \mathbf{t}) \tag{II-16}\mathbf{B}$$

The x is a vector of variables given by a differential equation which are explicit given by equation (II-16)A. The y is a vector of algebraic variables which are given by the algebraic equations g. De derivative of x to t is specified by x'. Most of the numerical integration routines deal with explicit ODEs such as given by (II-16)A. If the problem given by (II-16) is to be solved then we try to get the system (II-16) in the form of an explicit ODE system. One way of doing this is to differentiate the constraint equation (II-16)B with respect to t. The result is:

$$\mathbf{x'} = \mathbf{f}(\mathbf{x}, \mathbf{y}, \mathbf{t}) \tag{II-17}\mathbf{A}$$

$$\mathbf{g}_{\mathbf{y}}(\mathbf{x},\mathbf{y},t)\cdot\mathbf{x}' + \mathbf{g}_{\mathbf{y}}(\mathbf{x},\mathbf{y},t)\cdot\mathbf{y}' + \mathbf{g}_{\mathbf{t}}(\mathbf{x},\mathbf{y},t) = 0$$
(II-17)B

Wherein \mathbf{g}_x is the partial derivative of \mathbf{g} to \mathbf{x} and \mathbf{g}_y is the partial derivative of \mathbf{g} to \mathbf{y} . The \mathbf{x}' and \mathbf{y}' are the partial derivatives of \mathbf{x} and \mathbf{y} to \mathbf{t} . The \mathbf{g}_t are the partial derivatives of \mathbf{g} to \mathbf{t} . The matrix \mathbf{g}_x , \mathbf{g}_y and vector \mathbf{g}_t can be evaluated. If \mathbf{g}_y is nonsingular we get the following explicit ODE system.

$$\mathbf{x'} = \mathbf{f}(\mathbf{x}, \mathbf{y}, \mathbf{t}) \tag{II-18}\mathbf{A}$$

$$y' = [g_y(x,y,t)]^{-1} \cdot (-g_t(x,y,t) - g_x(x,y,t) \cdot x')$$
 (II-18)B

System (II-16) is then an implicit ODE and we say that system (II-16) has index one (Brenan 96). If this is not the case, suppose that with algebraic manipulations we can rewrite (II-18) in the form of (II-16) but with different x, y. Again we differentiate the constraint equation (II-16)B. If an implicit ODE results, we say that the original problem has index two. If the new system is not an implicit ODE, we repeat the process. The number of differentiation steps required in this procedure is the index. For further information on the index, the reader is referred to reference (Brenan 96).

The DAE system described in the paragraph 2.2 can be represented for compactness with a vector notation. There is one equation which is different namely the momentum equation, this equation (II-20) will be discussed separately. The full set of equations which is used for the index determination is given in appendix 6. In analogy with the preceding index determination the following result is obtained:

$$\frac{d\mathbf{x}}{dz} = \mathbf{f}(\mathbf{x}, P, u, \mathbf{y}, z) \tag{II-19}$$

$$\frac{dP}{dz} + \rho u \frac{du}{dz} + f(u, \mathbf{y}) = 0 \tag{II-20}$$

$$\mathbf{g}(\mathbf{x}, P, u, \mathbf{y}, z) = 0 \tag{II-21}$$

Where x is the vector of explicit differential variables, with the corresponding ODE equations. The vector x represents:

$$\mathbf{x} = \begin{bmatrix} F_j & T \end{bmatrix}^T \tag{II-22}$$

with
$$j = 1, 2, 3, ..., 9$$

The pressure and the velocity (P, u) dependence on z is given by one ODE, equation (II-20).

The algebraic equations are reduced to zero and are given by the vector function \mathbf{g} (II-21). The algebraic variables \mathbf{y} are:

$$y = [\rho, M_m, f, r_i, \Delta H_i, \Delta H_{f,j}, Cp_j, \mu, sumF, \mu_j]^T$$
 with $j = 1, 2, 3 ... 9$ and $i = 1, 2, 3 ... 7$ (II-23)

All the algebraic equations of g (II-21) are given in appendix 6. In order to obtain the index we have to differentiate equation (II-21) with respect to z. In this case we also have to differentiate with respect to the implicit differential variables P and u, to get a complete explicit set of ODEs. The derivative of the algebraic equations is given by:

$$\frac{d\mathbf{g}}{d\mathbf{x}} \cdot \frac{d\mathbf{x}}{dz} + \frac{d\mathbf{g}}{dP} \cdot \frac{dP}{dz} + \frac{d\mathbf{g}}{du} \cdot \frac{du}{dz} + \frac{d\mathbf{g}}{dv} \cdot \frac{d\mathbf{y}}{dz} + \frac{d\mathbf{g}}{dz} = 0$$
 (II-24)

Just as in the example above we want to have y' in a explicit notation. In this case it is more complicated because the derivative of g with respect to y is not a square matrix, the reason is of course the derivatives of g with respect to P and g. To overcome this problem equation (II-20) and (II-24) can be put in the following vector notation.

$$\mathbf{A} \cdot \mathbf{X} = \mathbf{B} \tag{II-25}$$

$$\begin{pmatrix} 1 & \rho u & 0 \\ \frac{d\mathbf{g}}{dp} & \frac{d\mathbf{g}}{du} & \frac{d\mathbf{g}}{d\mathbf{y}} \end{pmatrix} \cdot \begin{pmatrix} \frac{dp}{dz} \\ \frac{du}{dz} \\ \frac{dy}{dz} \end{pmatrix} = \begin{pmatrix} -f(u, \mathbf{y}) \\ -\frac{d\mathbf{g}}{d\mathbf{x}} \cdot \mathbf{f}(\mathbf{x}, P, u, \mathbf{y}, z) \end{pmatrix}$$
(II-26)

The size of the matrix and vectors is:

$$\mathbf{A} = \begin{pmatrix} lxl & lxl & lx47 \\ 48xl & 48xl & 48x47 \end{pmatrix}, \quad \mathbf{X} = \begin{pmatrix} lxl \\ lxl \\ 47xl \end{pmatrix}, \quad \mathbf{B} = \begin{pmatrix} lxl \\ 48xl \end{pmatrix}$$
 (II-27)

The first row of the matrix A is the ODE equation (II-20) which gives the dependence of P and u on z. If the matrix A is nonsingular, i.e. $\det(A) \neq 0$, the DAE system (II-19), (II-20) and (II-21) is an implicit ODE and has index one.

In Froment 79 the problem of the momentum equation is solved by differentiating u with respect to z. The result is an explicit ODE system. The conclusion is that the system has index one. In a powerful tool like MAPLE V release 5 the matrix A can be constructed and the determinant can be calculated. The result is:

$$\det(\mathbf{A}) = \frac{M_m u G - RT \rho}{RT \rho} \tag{II-28}$$

The DAE system has indeed index one, if the numerator is not equal to zero. This could have some effects on the integration process.

Equation (II-28) can be written in a more useful form, to implement it in the simulation program gPROMS in order to check what is going to happen.

$$\det(\mathbf{A}) = \frac{RTG^2 - M_m P^2}{M_m P^2} \tag{II-29}$$

2.4 Initialization Problem

The same concept of determination of the index can be applied to answering the question: is there an initialization problem? An initial value problem defined in the previous paragraph (II-19), (II-20) and (II-21) with the corresponding set of initial conditions is given below.

$$\frac{d\mathbf{x}}{dz} = \mathbf{f}(\mathbf{x}, P, u, \mathbf{y}, z) \tag{II-19}$$

$$\frac{dP}{dz} + \rho u \frac{du}{dz} + f(u, y) = 0$$
 (II-20)

$$\mathbf{g}(\mathbf{x}, P, u, \mathbf{y}, z) = 0 \tag{II-21}$$

At
$$z = 0$$
, $x(0) = x_0$, $P(0) = P_0$, $u(0) = u_0$ (II-30)

The expressions above (II-19), (II-20) and (II-21) are represented by the following vector equation, for initialization purposes:

$$\xi(\mathbf{x}) = \begin{pmatrix} \frac{d\mathbf{x}}{dz} \Big|_{z=0} - \mathbf{f}(\mathbf{x}, P, u, \mathbf{y}, z) \\ \frac{dP}{dz} \Big|_{z=0} + \rho u \frac{du}{dz} \Big|_{z=0} + f(u, \mathbf{y}) \\ \mathbf{g}(\mathbf{x}, P, u, \mathbf{y}, z) \end{pmatrix} = 0$$
(II-31)

 χ is given in the next vector:

$$\chi = \left[\frac{d\mathbf{x}}{dz} \right|_{z=0}^{T} \frac{dP}{dz} \Big|_{z=0}^{z=0} \frac{du}{dz} \Big|_{z=0}^{T} \mathbf{y}^{T} \right]^{T}$$
(II-32)

with the vectors x and y defined by the expressions (II-22) & (II-23). In order to initialize the above given initial value problem (IVP), we have to solve equation (II-31). The unknowns are given in the vector defined by (II-32). The vector x and scalars P, u and z are substituted with (II-30). In order to solve the set (II-31) the determinant of the Jacobian of ξ must be nonsingular. In a tool like MAPLE V release 5 the Jacobian and the determinant of the Jacobian can be calculated symbolically. The result is:

$$\det(\xi) = 0 \tag{II-33}$$

The Jacobian of (II-31) is singular, so therefor no solution can be found to problem (II-31). This means that we have an initialization problem. If we run gPROMS with the set given in paragraph 2.2, it returns with an error message saying: that gPROMS is not able to initialize. In the next paragraph initialization problem is solved, according to Froment and an alternative solution is given.

2.5 Solution of Initialization Problem

2.5.1 Froment Solution

In the previous paragraph we concluded that the problem described in paragraph 2.2 can not be initialized. To overcome this problem Froment and Bischoff differentiated the equation for the velocity and substituted the result into the equation for the pressure profile, this resulted in an explicit model. It is also possible to substitute all the algebraic equations into the differential equations and solve the problem with an ordinary integration routine like for instance the GEAR routine. The velocity is given by:

$$u = \frac{G}{M_M} \frac{RT}{P}$$
 (II-34)

Differentiation of the velocity equation yields:

$$\frac{du}{dz} = \frac{GR}{P} \left[T \frac{d\left(\frac{1}{M_m}\right)}{dz} + \frac{1}{M_M} \frac{dT}{dz} \right] - \frac{G}{M_M} \frac{RT}{P^2} \frac{dP}{dz}$$
 (II-35)

Substitution of this result into the equation to prescribe the pressure profile gives:

$$\frac{dP}{dz} = \frac{\sum_{j=1}^{9} \frac{dF_{j}}{dz}}{\frac{GA_{coil}}{GA_{coil}}} + \frac{1}{M_{M}} \left[\frac{1}{T} \frac{dT}{dz} + \left(\frac{2f}{d} + \frac{f_{bend}}{2\pi r_{b}} \right) \right] - \frac{1}{M_{M}P} - \frac{P}{G^{2}RT}$$
(II-36)

When this momentum equation is used in gPROMS it is able to initialize and start with the integration process. The next sub-paragraph will describes a less 'complex' solution.

2.5.2 Alternative Solution to the Initialization Problem

The Froment method yields a somewhat 'complicated' solution, but is gives an explicit differential scheme which is a must for the integration routines available at the time Froment 79 published his work. Nowadays we have DAE integration routines which are able to integrate index one problems, such a program is gPROMS. In this section we will give a solution which is more elegant than the Froment solution.

The equation to prescribe the pressure profile is given by:

$$-\frac{dP}{dz} = \left[2\frac{f}{d} + \frac{f_{bend}}{2\pi r_b}\right] \rho u^2 + \rho u \frac{du}{dz}$$
 (II-37)

The expression for the velocity of the fluid in the radiant coil can be rewritten to:

$$u = \frac{G}{\rho} \tag{II-38}$$

Substitution of (II-38) into (II-37) results in:

$$-\frac{dP}{dz} = \left[2\frac{f}{d} + \frac{f_{bend}}{2\pi r_b} \right] \rho_u^2 + G\frac{du}{dz}$$
 (II-39)

Recall that G denotes the mass flux through the coil and is a constant. The equation above can be rewritten to:

$$-\frac{dPx}{dz} = \left[2\frac{f}{d} + \frac{f_{bend}}{2\pi r_b}\right] \rho u^2 \tag{II-40}$$

with:

$$Px = P + Gu ag{II-41}$$

This solution to the initialization problem yields an index one problem and can be solved with gPROMS. It is also possible, using the formula for the roots of a second degree polynomial, to obtain a system that can be solved with an explicit integration routine, like the GEAR method. To obtain an explicit system we need an expression for the pressure, the equations that must be solved are:

$$Px = P + Gu \qquad u = \frac{G}{\rho} \qquad \rho = \frac{M_M P}{RT}$$

These equations can be substituted into each other to obtain one equation, the result is:

$$P^2 - Px P + G^2 \frac{RT}{M_M} = 0$$

This expression can be solved analytically for P:

$$P = \frac{Px}{2} + \frac{1}{2}\sqrt{Px^2 - 4G^2 \frac{RT}{M_M}}$$
 (II-42)

2.6 Index Problem During Solving of Test Model

The test model described in paragraph 2.2 can not be solved due to the fact that we have an initialization problem. In the preceding paragraph the initialization problem is solved. Froment 79 denotes some simulation results, they showed simulation results of a 95 meter long cracking coil, smooth pressure and temperature curves. The reason to denote that there is a solution and the pressure profile is smooth, is when we integrate the Froment 79 model with gPROMS or with the GEAR routine of MATLAB, the programs crashes after 25 meters. When using the collocation techniques (more of this model later in the report), the model does not converge to a solution. Inspection of the curves (produced with results of gPROMS or MATLAB) led to the conclusion that the pressure is going to minus infinity at 25 meters.

Froment 79 denotes nothing on different momentum equations in a bend or straight part of the tube. If it was the case, that two equations were used, one for in the bends and one for the straight part of the tube, then there should be dents in the pressure curve. Recall the index of the test model, which is given by (II-29):

$$\det(\mathbf{A}) = \frac{RTG^2 - M_m P^2}{M_m P^2}$$

When this equation is implemented in for instance gPROMS, the value of $\det(A)$ goes from \approx -1 to $+\infty$ through zero at $z\approx25$ meters. So mathematical speaking we could say that there are problems at 25 meters. Appendix 2 shows some more information on the friction factor which accounts for the friction due to the bends. A possible solution to obtain a smooth pressure profile is to spread the friction of the bends over the whole pipe. When this is done the expression for the pressure is given by:

$$-\frac{dPx}{dz} = \left[2\frac{f}{d} + \frac{N_{bend}f_{bend}}{2L}\right]\rho u^2 \tag{II-43}$$

With:

$$Px = P + Gu ag{II-44}$$

The model with the preceding equation converges to a solution, we concluded that the model denoted in Froment 79 is not complete and/or the results do not belong to the model. In gPROMS or MATLAB it is rather simple to implement that two equations for the pressure profile are used, one for the bends and one for the straight part of the coil. The pressure curve obtained with such a model contains dents, as expected.

2.7 Physical Meaning of Index

At first sight we concluded that a physical reason, for the crashing of the model after 25 meters, could be that the pressure drop is too high for convective transport of the fluid in the pipe. With a given pressure at the entrance of a pipe an engineer can not take an infinite long pipe, at one point there is "no pressure" anymore. The pressure at the entrance is not enough to overcome the friction due to the tube wall. The system needs then to be described with another set of equations. This statement can not be connected to the index of the DAE system, because the friction does not occur in the index of the problem, which is given by:

$$\det(\mathbf{A}) = \frac{M_m u G - RT \rho}{RT \rho} \tag{II-45}$$

When det(A) is zero the index of the system changes from one to two or higher. This has as the effect that the integration process will crash at the point where det(A) is zero or in the case of the collocation model no solution will be found. The question arises what the physical explanation of the determinant could be. The determinant is obtained via a mathematical procedure and the question is can we find a physical meaning to this result, if there is one of course. It is possible to write (II-45) in the next form (det(A)=0):

$$u^2 = \frac{RT}{M_M} \tag{II-46}$$

This expression is similar to the expression of the velocity of sound in an ideal gas, see appendix 8. The conclusion could be drawn that the algebraic constraints on the differential variables imply that the velocity in the tube can not be greater then the speed of sound.

This could be an explanation. The det(A) is smaller then zero and greater then -1 before det(A)=0 is reached (-1 < det(A) < 0). The expression below states that the velocity before det(A)=0 is smaller the speed of sound.

$$u^2 = \left[1 + \det(\mathbf{A})\right] \frac{RT}{M_M} \tag{II-47}$$

A careful reader of appendix 8, has already concluded that the velocity of sound denoted by (II-46) is the velocity of sound in a tube at isothermal conditions and that the actual velocity of sound in a tube under non isothermal conditions is maximal:

$$u_{\text{max}} = \sqrt{\frac{Cp}{Cv} \frac{RT}{M}}$$
 (II-48)

The conclusion must be that until now we have no physical meaning for the obtained index, if a reason can be found at all.

3 Numerical Implementation

3.1 Computerized model

In the preceding chapter we used a standard mathematical package, such as gPROMS and MATLAB, to obtain a solution. These packages make use of various techniques to approximate the real solution of a DAE model, until now we were not interested in the way this was done. In engineering, most models are used to design or simulate a process unit, e.g. a steam cracker. It is then very desirable to have an open model (the equations are written in residual form). What we mean with an open model is that an engineer can easily decide what the variables should be and what the parameters are. A simple example: in the SPYRO simulation package for radiant steam cracker coils, it is not possible to calculate the required coil length, which results in a given yield. The engineer has to apply a trial and error method by changing the length of the coil in order to obtain the desired yield. In the open model the coil length could be a simulation result. In general mathematical packages, e.g. gPROMS, MATLAB, it is very difficult, maybe impossible to handle in a convenient way these sort of models. When using a generic program language, such as FORTRAN, it is possible to create such a model which can provide the open structure. The engineer has to translate the given model, such as given in the previous chapter 2.2, to a mathematical model. When using general mathematical software packages we don't need to be concerned about these things as numerical implementation. Due to the fact that it is interesting to make an open steam cracker model, these efforts have to be made, a numerical method that can be of some assistance is the method of weighted residuals, specially the collocation method. This collocation method transforms a differential equation into a number (more than one) of algebraic equations. When dealing with a set of algebraic equations it is easy to add, change or remove variables, the only thing that has to be done is: add change or remove algebraic equations. Since a lot of methods are available that solve a set of non-linear algebraic equations and the preceding properties of the collocation method it explains why the collocation method is interesting. An iterative method to solve a system of non-linear equations is the continuation method. The continuation method solves difficult problems. This is done by solving a series easy subproblems. With this method an engineer is able, depending on the category of continuation method used, to use a physical insight for obtaining the solution. This chapter will give all the relevant information to understand the numerical implementation of the steam cracker model. First we shall begin with the collocation method. Thereafter we explain the continuation method.

3.2 Orthogonal Collocation

Orthogonal collocation techniques belong to the group of methods of weighted residuals (Villadsen and Michelsen 78; Finlayson 80; Seferlis 95) that solve two point boundary value problems of the form:

$$y^{(m)} = f(y^{(m-1)} \ y^{(m-2)} \ ,..., \ y^{(1)} \ y \ x) \ x \in [a, b]$$
 (III-1)

with
$$y^{(j)}(a) = y_{a,j}$$
 and $y^{(j)}(b) = y_{b,j}$ $j = 0,..., m$ (III-2)

where x is the independent variable, y is the dependent variable, $y^{(m)}$ denotes the m-th order derivative of y and $y_{a,j}$, $y_{b,j}$ are the fixed boundary values for the derivatives of y.

An example of a two-point boundary value problem is:

$$\frac{d^2y}{dx^2} - \phi^2 y = 0 \tag{III-3}$$

With the boundary conditions:

$$x = 0 \qquad \frac{dy}{dx} = 0 \tag{III-4}$$

$$x = 1$$
 $y = 1$

For this problem the exact solution is also known:

$$y(x) = \frac{\cosh(\phi x)}{\cosh(\phi)}$$
 (III-5)

This example can be used to model a diffusion with chemical reaction in a catalyst particle. The parameter ϕ specifies the ratio between the reaction rate and the diffusion rate (fast reaction ϕ is large, slow reaction ϕ is small) (Rice 95).

The main aspect of the methods of weighted residuals is the approximation of the solution of (III-1) can be written as a polynomial (trail function). Below we will explain the method and explain when collocation can be called orthogonal collocation. For the explanation we use a polynomial given by Finlayson 72. An other polynomial that can be used is the Lagrange polynomial (see following sub-paragraph) this polynomial is used for collocation on the steam cracker models. We use Lagrange polynomials because the calculation of the derivatives does not fail even when matrix \mathbf{Q} (see (III-18)) is singular. We did not investigate if matrix \mathbf{Q} can become singular.

$$y(x) = a_0 + x(1-x)\sum_{j=1}^{N} a_j P_{j-1}$$
(III-6)

 $P_{\rm m}$ is some type of polynomial. N is the number of interior collocation points. In equation (III-6) the end points of the collocation interval are submitted to the process by multiplying the polynomial with x(1-x). The parameter a_0 is a constant, $a_{\rm j}$ are also parameters. These parameters have to be determined by the collocation method. The polynomial $P_{\rm m}$ can be given by (Finlayson 72):

$$P_m(x) = \sum_{j=1}^m \gamma_j x^j \tag{III-7}$$

The polynomials defined by equation (III-7) are called Jacobi polynomials when they satisfy the orthogonality condition (III-8) for j=0,1,2,...,(m-1), that is, all Jacobi polynomials are orthogonal to each other except to each other (i.e., when j=m) (Rice 95). If $\alpha=\beta=0$ they are called Legendre polynomials.

$$\int_{0}^{1} \left[x^{\beta} (1 - x)^{\alpha} \right] P_{j}^{(\alpha, \beta)}(x) P_{m}^{(\alpha, \beta)}(x) dx = 0$$
(III-8)

Substituting the trail function (III-6) in equation (III-1) we get:

Res
$$(x, \mathbf{a}) = L \left[a_0 + x(1-x) \sum_{j=1}^{N} a_j P_{j-1} \right]$$
 (III-9)

L is the differential operator defined by equation (III-1) or (III-3). The residual Res is in general non-zero over the whole domain of interest, so that it will be dependent on x and parameter vector \mathbf{a} .

Since the residual Res is a function of x and parameter vector a, we have to minimize it over the whole domain of interest to make the residual only dependent on the parameters of the polynomial. To do this, we need to define some form of averaging. The following integral over the whole domain may be used as a means of averaging.

$$\int_{V} \operatorname{Res}(x, \mathbf{a}) w_{k} \, dx = 0 \tag{III-10}$$

In the collocation method the test function $w_k(x)$ is the Dirac delta function at N interior collocation points.:

$$W_k = \delta(x - x_k) \tag{III-11}$$

Where x_k is the k-th collocation point. The useful property of the Dirac's delta function is:

$$\int_{x_{k}^{-}}^{x_{k}^{+}} \operatorname{Res}(x, \mathbf{a}) \, \delta(x - x_{k}) \, dx = \operatorname{Res}(x_{k}, \mathbf{a})$$
(III-12)

If the N collocation points are chosen as the roots of an orthogonal Jacobi polynomial of N -th degree, the method is called *orthogonal collocation* (Rice 95).

To solve the example defined by equation (III-3) we need the first and second derivative of function (III-6). The trail function (III-6) with the polynomials (III-7) can be rewritten as (Finlayson 72):

$$y(x) = \sum_{j=1}^{N+2} d_j x^{j-1}$$
 (III-13)

As a matter of fact all polynomials can be rewritten as expression (III-13).

Take the first derivative and the Laplacian of this expression and evaluate them at the collocation points:

$$y(x_i) = \sum_{j=1}^{N+2} x_i^{j-1} \cdot d_j$$
 (III-14)

$$\frac{dy}{dx}\Big|_{x_i} = y'(x_i) = \sum_{j=2}^{N+2} (j-1) \cdot x_i^{j-2} \cdot d_j \quad \text{if } j = 1, \ \frac{dy}{dx}\Big|_{x_i} = 0$$
 (III-15)

$$\frac{d^2y}{dx^2}\Big|_{x_i} = y''(x_i) = \sum_{j=3}^{N+2} (j-1)\cdot (j-2)\cdot x_i^{j-3}\cdot d_j \quad \text{if } j=1 \quad \text{or} \quad j=2, \quad \frac{d^2y}{dx^2}\Big|_{x_i} = 0 \quad (\text{III-16})$$

These can be written in matrix notation as follows. Note that there are N interior collocation points and two boundary values x = 0 and x = 1. The square matrices have $(N+2)\cdot(N+2)$ elements:

$$\mathbf{y} = \mathbf{Q} \cdot \mathbf{d} \qquad \mathbf{y'} = \mathbf{C} \cdot \mathbf{d} \qquad \mathbf{y''} = \mathbf{D} \cdot \mathbf{d}$$

$$Q_{ij=x^{j-1}} \qquad C_{ij} = (j-1) \cdot x_i^{j-2}; C_{i,1} = 0 \quad D_{ij} = (j-1) \cdot (j-2) \cdot x_i^{j-3}; D_{i,1} = D_{i,2} = 0$$
(III-17)

Solving for d, we are able to rewrite the first derivative and Laplacian as:

$$\mathbf{y'} = \mathbf{C} \cdot \mathbf{Q}^{-1} \mathbf{y} = \mathbf{A} \cdot \mathbf{y} \qquad \qquad \mathbf{y''} = \mathbf{D} \cdot \mathbf{Q}^{-1} \mathbf{y} = \mathbf{B} \cdot \mathbf{y}$$
 (III-18)

3.2.1 Lagrange Polynomial

The Lagrange interpolation polynomial is a special form of (III-13). If N interior collocation points are chosen, and we have two boundary values at x = 0 and x = 1, the following polynomial can be used (Rice 95).

$$y_{N+1}(x) = \sum_{j=1}^{N+2} l_j(x) y_j$$
 (III-19)

This polynomial passes through all (N+2) collocation points: (x_1,y_1) , (x_2,y_2) , ..., (x_{N+2},y_{N+2}) The order of the polynomial given by (III-19) is defined as N+2. The degree of Lagrange interpolation polynomial is N+1, y_j is the value of y at the point x_j and $l_j(x)$ is called the Lagrange interpolation polynomial. It is defined as:

$$l_j(x_i) = \begin{cases} 0 & j \neq i \\ 1 & j = i \end{cases}$$
 (III-20)

The Lagrange interpolation polynomial is a useful building block. There are (N+2) building blocks, which are (N+1)-th degree polynomials. The building blocks are given as

$$l_{j}(x) = \prod_{\substack{i=1\\i\neq j}}^{N+2} \frac{(x-x_{i})}{(x_{j}-x_{i})} = \frac{p_{N+2}(x)}{(x-x_{j}) \cdot \left[\frac{dp_{N+2}(x_{j})}{dx}\right]}$$
(III-21)

where $p_{N+2}(x)$ is called the node polynomial. It is a N+2 degree polynomial and is defined as

$$p_{N+2}(x) = (x - x_1) \cdot (x - x_1) \cdot \dots \cdot (x - x_{N+1}) \cdot (x - x_{N+2})$$
 (III-22)

where x_i (i = 1, 2, ..., N+1, N+2) are the collocation points. The $p_{N+2}(x)$ is called node polynomial because it passes through all the nodes x_i (i = 1, 2, ..., N+1, N+2). The value of y at any point including the collocation points, say x^* , is given by:

$$y_{N+1}(x^*) = \sum_{j=1}^{N+2} y_j l_j(x^*)$$
 (III-23)

The differentiating of a Lagrange interpolation polynomial is given in detail in appendix 3. The result is for the first derivative, at the i-the point:

$$\frac{dy}{dx}\bigg|_{i} = \sum_{j=1}^{N+2} \mathbf{A}_{i,j} y_{j} \tag{III-24}$$

for the second derivative:

$$\left. \frac{d^2 y}{dx^2} \right|_i = \sum_{j=1}^{N+2} \mathbf{B}_{i,j} y_j \tag{III-25}$$

The computation of the matrices A and B is different than the way given by expression (III-18), the results are the same.

Equation (III-3) is reduced from a differential equation to the following set of algebraic equations:

$$\sum_{\substack{j=1\\N+2}}^{N+2} \mathbf{A}_{1,j} \cdot y_j = 0 \qquad y' = 0 \text{ at } x = 0$$

$$\sum_{\substack{j=1\\N+2}}^{N+2} \mathbf{B}_{i,j} \cdot y_j - \phi^2 \cdot y_i = 0 \text{ for } i = 2, 3, ..., N+2$$

$$y_{N+2} - 1 = 0 \qquad y = 1 \text{ at } x = 1$$
(III-26)

The size of A and B is $(N + 2) \cdot (N + 2)$. The vector y has length N + 2. The algebraic equations (III-26) can be solved with an ordinary solver or optimizer. The result is a set of (x_i, y_i) which are a solution of the differential equation given by expression (III-3). To obtain the full polynomial we use the Lagrange interpolation formula. This way of collocation is called global collocation, because the collocation method is applied over the whole domain of interest.

3.2.2 Orthogonal Collocation on Finite Elements

It is also possible to split the domain [0,1], for equation (III-3), into many sub-domains and use collocation within each sub-domain. This is called Orthogonal Collocation on Finite Elements (OCFE) (Rice 95; Villadsen 78). The sub-domains are normalized to the range [0,1]. This is done by transforming the independent variable with:

$$x = \frac{z - a}{b - a} \tag{III-27}$$

In this way the domain [a, b] is transformed into [0,1]. An arbitrary domain, say [0, Γ] is divided into two sub-domains, this is sketched in Figure 6 below. In sub-domain 1 and 2, respectively N and M interior collocation points are chosen. The total number of unknowns is (N+2)+(M+2). The number of equations is N+M plus two boundary conditions, if example (III-3) is taken.

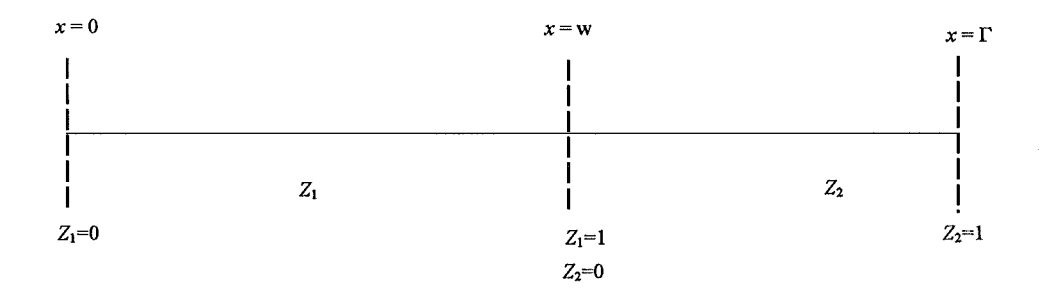


Figure 6: Two elements in the domain $[0, \Gamma]$

There are still two equations needed. These are obtained by invoking the continuity of y and y' at the junction of the two sub-domains, that is,

$$y_{1}(z_{1} = 1) = y_{2}(z_{2} = 0)$$

$$\frac{dy_{1}}{dz_{1}}\Big|_{z_{1}=1} = \frac{dy_{2}}{dz_{2}}\Big|_{z_{2}=0}$$
(III-28)

This results in the following set of algebraic equations:

$$\sum_{j=1}^{N+2} \mathbf{A}_{1}(1,j)y_{1}(j) = 0 y' = 0 \text{at } x = 0$$

$$\sum_{j=1}^{N+2} \mathbf{B}_{1}(i,j)y_{1}(j) - w^{2}\phi^{2}y_{1}(i) = 0 \text{for } i = 2, 3, ..., N+2$$

$$\sum_{j=1}^{N+2} \mathbf{A}_{1}(N+2) - y_{2}(1) = 0$$

$$\frac{1}{w} \sum_{j=1}^{N+2} \mathbf{A}_{1}(N+2,j)y_{1}(j) - \frac{1}{1-w} \sum_{j=1}^{M+2} \mathbf{A}_{2}(1,j)y_{2}(j) = 0$$

$$\sum_{j=1}^{M+2} \mathbf{B}_{2}(i,j)y_{2}(j) - (1-w)^{2}\phi^{2}y_{2}(i) = 0 \text{for } i = 2, 3, ..., M+2$$

$$y_{2}(M+2) - 1 = 0 y = 1 \text{ at } x = 1$$

The algebraic equations (III-29) can be written in matrix form. For N=M=2 the following set is obtained:

3.2.3 Collocation of Coupled Differential Equations

A set of coupled ordinary differential equations can be represented with the following vector notation:

$$\frac{d\mathbf{y}}{d\mathbf{r}} = \mathbf{g}(x, \mathbf{y}) \qquad \text{with: } \mathbf{y}(0) = \mathbf{y}_0 \tag{III-30}$$

where:

$$\mathbf{y} = [y_1, y_2, ..., y_E]^T$$
 (III-31)

$$\mathbf{y}_0 = [y_0(1), y_0(2), ..., y_0(E))]^T$$
 (III-32)

and:

$$\mathbf{g} = [g_1(x, \mathbf{y}), g_2(x, \mathbf{y}), ..., g_E(x, \mathbf{y})]^T$$
(III-33)

Using global collocation and discretization at properly chosen interior collocation points $x_1, x_2, ..., x_N$ yields the following $(N+1)\cdot E$ set of collocation equations:

$$\mathbf{Y}_{1,1...E} - \mathbf{y}_{0}^{T} = 0$$

$$\sum_{j=1}^{N+1} \mathbf{A}_{i,j} \mathbf{Y}_{j,k} - \mathbf{G}(\mathbf{Y}) = 0 \quad \text{for } i = 2, 3, ..., N+1 \text{ and } k = 1, 2, ..., E$$
(III-34)

Y is an $(N+1)\cdot E$ matrix, the i,j-th elements representing the value of the j-th component at the i-th collocation point, the columns give the y-values of the j-th equation and the rows represent the y-values of all the equations at the i-th collocation point. A is an $(N+1)\cdot (N+1)$ matrix, the right hand side end points is not included as a collocation point, if this point is submitted to the collocation process then the size of A is $(N+2)\cdot (N+2)$. G is an $(N\cdot E)$ matrix. The i,j-th element of matrix G is given by $G_{ij} = g_j(Y_{i,1}, Y_{i,2}, ..., Y_{i,E})$. Consider, e.g., the case of three equations (E=3) and two *interior* collocation points (N=2):

$$\mathbf{Y}_{1,1} - \mathbf{y}_{0}(1) = 0 \qquad \mathbf{Y}_{1,2} - \mathbf{y}_{0}(2) = 0 \qquad \mathbf{Y}_{1,3} - \mathbf{y}_{0}(3) = 0$$

$$\sum_{j=1}^{N+1} \mathbf{A}_{2,j} \mathbf{Y}_{j,1} - \mathbf{g}_{1}(\mathbf{Y}_{2,1..M}) = 0 \qquad \sum_{j=1}^{N+1} \mathbf{A}_{2,j} \mathbf{Y}_{j,2} - \mathbf{g}_{2}(\mathbf{Y}_{2,1..M}) = 0 \qquad \sum_{j=1}^{N+1} \mathbf{A}_{2,j} \mathbf{Y}_{j,3} - \mathbf{g}_{3}(\mathbf{Y}_{2,1..M}) = 0$$

$$\sum_{j=1}^{N+1} \mathbf{A}_{3,j} \mathbf{Y}_{j,1} - \mathbf{g}_{1}(\mathbf{Y}_{3,1..M}) = 0 \qquad \sum_{j=1}^{N+1} \mathbf{A}_{3,j} \mathbf{Y}_{j,2} - \mathbf{g}_{2}(\mathbf{Y}_{3,1..M}) = 0 \qquad \sum_{j=1}^{N+1} \mathbf{A}_{3,j} \mathbf{Y}_{j,3} - \mathbf{g}_{3}(\mathbf{Y}_{3,1..M}) = 0$$
(III-35)

This set of equations has to be solved with for instance an optimizer. The number of equations to be solved is $(N+1)\cdot E$.

This method of collocation can be used as a global collocation or as a collocation on finite elements. With collocation on finite elements the independent variable has to be transformed to the domain [0,1] within each element (see formula (III-27)).

3.2.4 Collocation of Coupled ODE's with Finite Element Method

When the solution of an ODE or DAE system has got steep gradients it is more advantageous to use trail functions that are defined only over part of the region. This is called Orthogonal Collocation on Finite Elements (OCFE). In the previous chapter the OCFE-method is explained by using only one equation. In normal situations an engineer has to solve more than one equation. How this is done for coupled ODE's is explained by an example. This is the same example as given by expression (III-30). The number of equations is three (E=3) and each element has two interior collocation points (N=2). The number of elements is 2 (NE=2) and the right hand side end point of each element is taken as a collocation point, the size of A is $(N+2)\cdot(N+2)$.

$$\begin{pmatrix} 1 & 0 & 0 & 0 & 0 & 0 & 0 & 0 \\ A(2,1) & A(2,2) & A(2,3) & A(2,4) & 0 & 0 & 0 & 0 \\ A(3,1) & A(3,2) & A(3,3) & A(3,4) & 0 & 0 & 0 & 0 \\ A(4,1) & A(4,2) & A(4,3) & A(4,4) & 0 & 0 & 0 & 0 \\ 0 & 0 & 0 & 1 & -1 & 0 & 0 & 0 \\ 0 & 0 & 0 & 0 & A(2,1) & A(2,2) & A(2,3) & A(2,4) \\ 0 & 0 & 0 & 0 & A(3,1) & A(3,2) & A(3,3) & A(3,4) \\ 0 & 0 & 0 & 0 & A(3,1) & A(3,2) & A(3,3) & A(3,4) \\ 0 & 0 & 0 & 0 & A(4,1) & A(4,2) & A(4,3) & A(4,4) \\ 0 & 0 & 0 & 0 & 0 & A(4,1) & A(4,2) & A(4,3) & A(4,4) \\ 0 & 0 & 0 & 0 & 0 & A(4,1) & A(4,2) & A(4,3) & A$$

The elements can be equally spaced over the domain of interest or placed in a region which contains steep profiles. Another way to place the elements is to use a criteria like the approximation error and distribute this error in such a way that each elements contains the same amount of error. This way of adaptive collocation on finite elements is described in appendix 4.

3.2.5 Form of the Residual Equations

In this section we will give some information what the form of the system of algebraic equations is, resulting from applying collocation on the ethane steam cracker model given in chapter 2.2. The model equations described in chapter 2.2, are transformed into algebraic residual equations, according to the preceding paragraph. When we are using MATLAB, it is more convenient to work with matrices instead of vector oriented residual equations. In MATLAB the ODEs are transformed to algebraic equations according to the matrices given above. In MATLAB it is easy to add more residuals if we want to solve more algebraic equations like for instance Px = P + Gu.

To solve the Froment problem in a generic program language, such as FORTRAN, all the residuals should be in a vector and not in a matrix. This makes it possible to get a global approach of the problem and translation to a much bigger problem then the Froment problem is done more easily. For the non-linear solver it is required that the Jacobian of the problem is diagonal or near diagonal. When collocation is applied the Jacobian has almost a perfect block diagonal form. The blocks contain all the equations defined in one finite element. This is illustrated in the Figure 7 below.

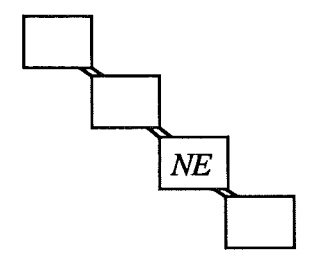


Figure 7: A schematic Jacobian structure with 4 finite elements

One finite element, for instance the one denoted with *NE* in Figure 7, has a block diagonal form with lines parallel to the diagonal. These lines are created through the derivatives of the approximating polynomial. The polynomial is a summation of all the y-values within a finite element, as a consequence the derivative is also a function of all the y-values in a finite element. The blocks are created by the *interior* collocation points and the right hand side end collocation point of an element, at these collocation points all the residuals are evaluated. The structure of one finite element is schematically given in Figure 8.

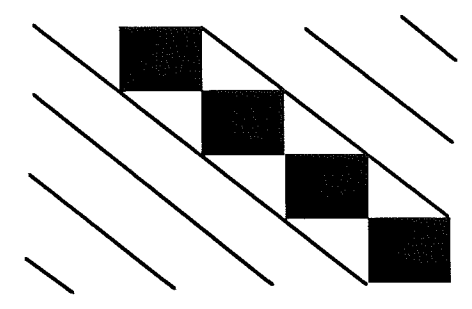


Figure 8: Finite element with 3 interior collocation point (schematically)

3.3 Continuation Methods

Many chemical engineering problems can be represented mathematically by a set of non-linear algebraic equations. A generalized set of such equations is given by:

$$f_{1}(x_{1}, x_{2}, ..., x_{n}) = 0$$

$$f_{2}(x_{1}, x_{2}, ..., x_{n}) = 0$$

$$\vdots$$

$$f_{n}(x_{1}, x_{2}, ..., x_{n}) = 0$$
(III-36)

Written in simplified form as f(x) = 0 (here 0 represents the zero vector).

The most common approach to this type of problem is to use Newton's method which can be written in the general form as:

$$\mathbf{x}^{k+1} = \mathbf{x}^k - \mathbf{J}^{-1}\mathbf{f}(\mathbf{x}) \tag{III-37}$$

where J is the Jacobian, defined as:

$$\mathbf{J} = \begin{pmatrix} \frac{\mathcal{J}_{1}}{\partial x_{1}} & \frac{\mathcal{J}_{1}}{\partial x_{2}} & \cdots & \frac{\mathcal{J}_{1}}{\partial x_{n}} \\ \frac{\mathcal{J}_{2}}{\partial x_{1}} & \frac{\mathcal{J}_{2}}{\partial x_{2}} & \cdots & \frac{\mathcal{J}_{2}}{\partial x_{n}} \\ \vdots & & & \vdots \\ \frac{\mathcal{J}_{n}}{\partial x_{1}} & \frac{\mathcal{J}_{n}}{\partial x_{2}} & \cdots & \frac{\mathcal{J}_{n}}{\partial x_{n}} \end{pmatrix}$$
(III-38)

With this method \mathbf{x}^k is the current (or initial, when k = 0) estimate of the solution vector which yields $\mathbf{f}(\mathbf{x}) = 0$. Equation (III-37) is applied with an updated Jacobian matrix (III-38) at each point until a criterion such as , $\|\mathbf{x}^{k+1} - \mathbf{x}^k\| < \varepsilon$, where ε represents the desired solution tolerance, is met.

The Newton method given above is a straightforward implementation and should converge at least 75% of all problems that have a physical origin with no particular difficulty provided that the appropriate physical insight was used in the generation of initial estimates of the unknown variables. Adding bells and whistles in the form of damping factors, line searches and the like will increase the probability of success to around 95%. However, an inherent disadvantage of Newton's method is that topological phenomena which generates singularity, or near-singularity, of the Jacobian matrix can prevent convergence. Continuation methods are one way to solve very difficult problems.

Paths to the solution of difficult problems are provided by what are known as homotopy or continuation methods (Ortega and Reinboldt, 1970); Garcia and Zangwill, 1981). In these methods, we start with a different problem, of the same dimension as the original problem, for which the solution is either known or easily obtainable. For example, if the equations to be solved is $\mathbf{f}(\mathbf{x}) = 0$ then a convenient function to start with would be $\mathbf{g}(\mathbf{x}) = \mathbf{f}(\mathbf{x}) - \mathbf{f}(\mathbf{x}_0) = 0$ where \mathbf{x}_0 is an arbitrary vector. A solution to this equation is obviously $\mathbf{x} = \mathbf{x}_0$. This new problem would then be gradually transformed or "bent", through some parameterization, into the original problem in such a way that as the parameter is varied from its initial value, paths are generated by the roots of the new problem as they are bent into the roots of the original problem. To continue the above example, one such parameterization is:

$$\mathbf{h}(\mathbf{x},t) = t\mathbf{f}(\mathbf{x}) + (1-t)\mathbf{g}(\mathbf{x}) = 0$$

$$t \in [0, 1]$$
(III-40)

At t = 0, $\mathbf{h}(\mathbf{x},0) = \mathbf{g}(\mathbf{x})$, and at t = 1, $\mathbf{h}(\mathbf{x},1) = \mathbf{f}(\mathbf{x})$. As t is varied from t = 0 to t = 1, the roots of $\mathbf{h}(\mathbf{x},t) = 0$ trace out paths that lead to the desired roots of $\mathbf{f}(\mathbf{x}) = 0$. This path-following approach is the key to what are termed as homotopy methods.

There are three categories of continuation methods that have been used for solving engineering problems:

- 1. Mathematical methods which place the model equations into a homotopy equation of purely mathematical origin. This type of homotopies are sometimes called "artificial-parameter generic homotopies," in contrast to natural-parameter homotopies. (see for example Watson, Billups and Morgan 1987)
- 2. Proprietary continuation methods which uses a physically meaningful homotopy parameter. This type as mentioned above is named natural-parameter homotopy. An example is we have obtained a solution of a model with a certain set of parameters and now we want to get a solution at a different set of parameters. The natural-parameter homotopies "bends" the first solution into the other solution. (see for example Seferlis and Hrymak 1996)
- 3. Physical continuation methods in which the nature of the equations being solved is exploited in some way. For instance by reactive distillation where the reactions are "brought in". Another example is when a solution of an extractive or azeotropic distillation is wanted. The distillation column is first solved with ideal thermodynamic behavior and the non-ideal properties are "bent" in during the continuation procedure, see for example Vickery and Taylor 1986.

3.3.1 Types of Homotopy

The number of possible homotopy functions is essentially unlimited. Linear homotopies based on equation (III-39) include the *Fixed Point Homotopy* (because of its relationship to the fixed-point problem) in which the "easy" problem is given by

$$\mathbf{g}(\mathbf{x}) = \mathbf{x} - \mathbf{x}_0 = 0 \tag{III-41}$$

Substitution of this expression into equation (III-39) gives:

$$\mathbf{h}(\mathbf{x},t) = t\mathbf{f}(\mathbf{x}) + (1-t)(\mathbf{x} - \mathbf{x}_0) = 0$$
 (III-42)

The homotopy which, so far, has been used often is the *Newton Homotopy* (so named because of its relationship to Newton's method). This homotopy has also been called the global homotopy. In the Newton homotopy the first problem is given by

$$\mathbf{g}(\mathbf{x}) = \mathbf{f}(\mathbf{x}) - \mathbf{f}(\mathbf{x}_0) = 0 \tag{III-43}$$

with x_0 an arbitrary vector. A solution of the set of equations (III-43) is obviously $x = x_0$. Equation (III-43) is incorporated into the linear homotopy, equation (III-39), so that:

$$\mathbf{h}(\mathbf{x},t) = t\mathbf{f}(\mathbf{x}) + (1-t)(\mathbf{f}(\mathbf{x}) - \mathbf{f}(\mathbf{x}_0)) = 0$$
(III-44)

or

$$\mathbf{h}(\mathbf{x},t) = \mathbf{f}(\mathbf{x}) - (1-t)\mathbf{f}(\mathbf{x}_0) = 0 \tag{III-45}$$

Advantages to the Newton homotopy include:

- The freedom to choose x_0 (or the way in which it is calculated) is useful if it is desired to restart the method.
- The homotopy equations are simple to calculate. Calculating $f(x_0)$ and storing it in a separate vector is no great burden since the function has to be evaluated at x_0 whether or not a homotopy is being used.
- No extra work is needed to obtain H_x and h_t (see next sub-paragraph); h_t is $f(x_0)$ and H_x is the Jacobian used in Newton's method, $H_x = J$.
- The Newton homotopy preserves the scale invariance of Newton's method in both the functions and the variables.

The Affine Homotopy, guarantees not only that the initial problem has a predetermined solution but that this solution is unique.

$$\mathbf{g}(\mathbf{x}) = \mathbf{J}(\mathbf{x}_0) \cdot (\mathbf{x} - \mathbf{x}_0) = 0 \tag{III-46}$$

where \mathbf{x}_0 is again the initial estimate of the solution vector to the equation $\mathbf{f}(\mathbf{x}) = 0$. The term $\mathbf{J}(\mathbf{x}_0)$ refers to the Jacobian of $\mathbf{f}(\mathbf{x})$ evaluated at the value \mathbf{x}_0 . This homotopy also preserves the scale invariance of Newton's method.

The derivative information for use in the homotopy differential equations is:

$$\mathbf{H}_{\mathbf{x}} = \mathbf{J} \qquad \mathbf{h}_{t} = \mathbf{f}(\mathbf{x}) - \mathbf{J}(\mathbf{x}_{0}) \cdot (\mathbf{x} - \mathbf{x}_{0}) \tag{III-47}$$

An advantage of this homotopy is that, by using an arclength parameterization and allowing the value of the homotopy parameter to exceed unity, all solutions to a given problem can be found in many cases. However, this points out a difficulty when using the homotopy differential equations for solving this problem; the solution to the homotopy equations can easily be multivalued for a given parameter value. This means that care must be taken in following the homotopy path in order to find all solutions.

3.3.2 Solution of the homotopy equations

In the classical homotopy method (Wayburn and Seader 1987), the interval [0, 1] is broken up into N parts with $t_{i+1} - t_i = 1/N$ for i = 0, 1, ..., N, $t_0 = 0$ and $t_N = 1$. Newton's method is applied to $\mathbf{h}(\mathbf{x}, t_{i+1}) = 0$, i = 0, 1, ..., N, with the solution of $\mathbf{h}(\mathbf{x}, t_i) = 0$ as a starting point. The solution of $\mathbf{h}(\mathbf{x}, t_0) = \mathbf{h}(\mathbf{x}, 0)$ is \mathbf{x}_0 , the known solution of $\mathbf{g}(\mathbf{x}) = 0$. This algorithm is schematically represented by:

- 1. Set t = 0.
- 2. Solve h(x,0) = 0. (Note: this is equivalent to solving g(x) = 0)
- 3. Increase t
- 4. Solve $h(x, t_{i+1}) = 0$ using, as initial estimates of x, the solution of $h(x, t_i) = 0$
- 5. If t < 1 return to step 3.

The classical homotopy could be improved by choosing the t_i 's so as to minimize the computational expense. Experience may be of some assistance if it is known that small steps in t can be used in one range of the parameter value whereas larger steps are possible elsewhere on the path. In this case, the size of all the homotopy steps may still be chosen in advance of solving the problem but now the steps will be of different sizes. If the homotopy equations are "well-behaved", these somewhat naïve methods for determining the step size may very well be sophisticated by a step size algorithm, if needed of course.

3.3.3 Homotopy Differential Equations

Strangely enough, in case of most realistic problems, the amount of computation can be reduced substantially by converting the nonlinear equations into an Initial Value Problem (IVP) for an ordinary differential equation as first shown by Davidenko 1953. Since the solution set of $\mathbf{h}(\mathbf{x}, t) = 0$ can be parameterized by t, the homotopy equation defines implicitly a function $\mathbf{x} = \mathbf{x}(t)$. Substituting this into equation (III-39) and taking total derivative with respect to t, we get:

$$\mathbf{H}_{x} \cdot \frac{d\mathbf{x}}{dt} + \mathbf{h}_{t} = 0 \tag{III-48}$$

which leads to the following initial value problem:

$$\frac{d\mathbf{x}}{dt} = -(\mathbf{H}_{\mathbf{x}})^{-1} \cdot \mathbf{h}_{t} \tag{III-49}$$

where

$$\mathbf{h} = [h_1, h_2, \dots, h_n]^T \tag{III-50}$$

$$\mathbf{x} = [x_1, x_2, ..., x_n]^T$$
 (III-51)

$$\mathbf{H}_{x} = \begin{pmatrix} \frac{\partial h_{1}}{\partial x_{1}} & \frac{\partial h_{1}}{\partial x_{2}} & \cdots & \frac{\partial h_{1}}{\partial x_{n}} \\ \frac{\partial h_{2}}{\partial x_{1}} & \frac{\partial h_{2}}{\partial x_{2}} & \cdots & \frac{\partial h_{2}}{\partial x_{n}} \\ \vdots & & & \vdots \\ \frac{\partial h_{n}}{\partial x_{1}} & \frac{\partial h_{n}}{\partial x_{2}} & \cdots & \frac{\partial h_{n}}{\partial x_{n}} \end{pmatrix}$$
(III-52)

$$\mathbf{h}_{t} = \left[\frac{\partial h_{1}}{\partial t}, \frac{\partial h_{2}}{\partial t}, \dots, \frac{\partial h_{n}}{\partial t} \right]^{T}$$
(III-53)

Equations (III-49) are known as the Homotopy Differential Equations (HDE's). If \mathbf{H}_{x}^{-1} exists for $\mathbf{x}(t)$ along the path, then the system (III-49), along with the initial conditions:

$$\mathbf{x}(0) = \mathbf{x}_0 \tag{III-54}$$

can be integrated to obtain x(t) directly.

We could use for instance Gear's method to integrate (III-49) with initial condition (III-54). This might be a good idea for some problems, since sharp turns in the homotopy path could be interpreted as stiffness. Alternatively, we could use Euler's method, but that would not take advantage of the fact that we have at our disposal the actual function that was differentiated to get the IVP. We can arrange matters so that the calculation does not depend on its history and eliminate all questions of stability by applying Newton's method to the homotopy equation with the point predicted by Euler's method as a starting "guess". We could use a higher-order predictor, but the experience of many workers (cf. Salgovic 1981), has indicated that the additional complexity is usually not justified. Some experts disagree with this conclusion and higher-order predictors should be studied.

Returning to the solution of the HDE's, we need to solve the matrix equation (III-48) for $\frac{d\mathbf{x}}{dt}$, which is the tangent line of the homotopy path parameterized by t at the solution $\mathbf{x}(t_i)$ of the homotopy equation $\mathbf{h}(\mathbf{x}(t_i), t_i) = 0$. The predicted value of $\mathbf{x}(t_{i+1})$, denoted by $\widetilde{\mathbf{x}}(t_{i+1})$, is obtained by an Euler step:

$$\widetilde{\mathbf{x}}(t_{i+1}) = \mathbf{x}(t_i) + \Delta t \left(\frac{d\mathbf{x}}{dt}\right)$$
 (III-55)

In general the Newton correction vector, $\mathbf{x}(t_{i+1})$, is obtained by solving the matrix equation:

$$\mathbf{H}_{x} \cdot (\mathbf{x}^{k+1}(t_{i+1}) - \mathbf{x}^{k}(t_{i+1})) = -\mathbf{h}(\mathbf{x}^{k}(t_{i+1}), t_{i+1})$$
(III-56)

With $\mathbf{x}^k(t_{i+1})$ as the solution of the expression given by (III-56) after the k-th iteration. The initial estimate is given by Euler's method, denoted by $\widetilde{\mathbf{x}}(t_{i+1})$. Equation (III-56) is applied with an updated Jacobian matrix (III-52) at each point until a criterion such as , $\|\mathbf{x}^{k+1} - \mathbf{x}^k\| < \varepsilon$, where ε represents the desired solution tolerance, is met. The path to obtain the solution is schematically given below:

- 1. Set t = 0.
- 2. If x(0) is not directly available solve h(x(0),0) = 0.
- 3. Calculate the tangent vector $\frac{d\mathbf{x}}{dt}$, by solving $\mathbf{H}_{\mathbf{x}} \cdot \frac{d\mathbf{x}}{dt} = -\mathbf{h}_{t}$, with the current $\mathbf{x}(t_{i})$.
- 4. Estimate the new x at t_{i+1} , represented by $\widetilde{\mathbf{x}}(t_{i+1})$, calculated by $\widetilde{\mathbf{x}}(t_{i+1}) = \mathbf{x}(t_i) + \Delta t \left(\frac{d\mathbf{x}}{dt}\right)$.
- 5. Solve $\mathbf{H}_{x} \cdot (\mathbf{x}^{k+1}(t_{i+1}) \mathbf{x}^{k}(t_{i+1})) = -\mathbf{h}(\mathbf{x}^{k}(t_{i+1}), t_{i+1})$ with $\widetilde{\mathbf{x}}(t_{i+1})$ as initial estimate.
- 6. If t < 1 then return to step 3.

This continuation method can be used to initialize a set of nonlinear equations. If we don't have a proper starting guess for a nonlinear solver, continuation can be of some assistance. The procedure to estimate the solution of a set nonlinear algebraic equations is as follows:

- 1. Set t = 0.
- 2. If x(0) is not directly available solve h(x(0),0) = 0.
- 3. Calculate the tangent vector $\frac{d\mathbf{x}}{dt}$, by solving $\mathbf{H}_{\mathbf{x}} \cdot \frac{d\mathbf{x}}{dt} = -\mathbf{h}_{t}$, with the current $\mathbf{x}(t_{i})$.
- 4. Calculate the new x at t_{i+1} , represented by $\mathbf{x}(t_{i+1})$, calculated by $\mathbf{x}(t_{i+1}) = \mathbf{x}(t_i) + \Delta t \left(\frac{d\mathbf{x}}{dt}\right)$.
- 5. If t < 1 then return to step 3.

A problem with these techniques may arise if the path doubles back on itself, in which case the homotopy equation does not have a unique solution for some values of t. These points where the path doubles back on itself, are called turning points or (regular) limit points. At these turning points the Jacobian \mathbf{H}_x is singular, we can either perturb \mathbf{x} slightly so that \mathbf{H}_x is nonsingular or we try recasting the differential equations in another form. This recasting can be accomplished by assuming that both \mathbf{x} and t can be written as functions of the arclength, \mathbf{s} , of the path (Klopfenstein 1961). More information on path paramerization by arclength can be found in appendix 5.

4 Improved Ethane Cracker Model

4.1 Balances

In this chapter we will improve the used test model. The reason why we did not derive a cracking model is because the main target is to experiment with the collocation method on steam cracking models. The model where collocation should be applied on is the SPYRO model and therefor it is not a priority to make our own model. This is not a justification, not to check the used test model. In general, we have three types of balances, namely: momentum, energy and mass balances. First we will study the momentum balance because this balance is modified in order to solve the initialization problem. Then we will continue with the energy balance. In the next chapter some considerations over the mass balances are given.

Froment 79 denotes a momentum balance that is named the 'usual Bernoulli equation'. We are not going to argue over this name, although we disagree with the name. We will start with the fundamental momentum balance given by Bird 60 and transform these vector-tensor equation to a one dimensional macroscopic momentum balance. By doing this we know the origin of the balance used. In specific we will look at the way the friction of the bends is accounted for and we compare the two momentum balances used to solve the initialization problem of the test model.

The energy balance in the test model is a very simplified energy balance. In the period of time that the test model was published, no high speed computers and advanced algorithms were available to solve DAE models. Therefor the equations had to be changed to transform the DAE model in an ODE model. Nowadays this is not needed any more and less simplified energy balances can be used. When using collocation it is easy to use a more sophisticated energy balance. We will compare different energy balances.

This derivation of the momentum and energy balances is given in appendix 7. In the paragraphs below we denote the results and show the difference between the different balances, starting with the results obtained with Froment balances. As mentioned, we shall start with the momentum balance.

4.2 Momentum Balance

For an infinitesimal volume with dimensions dx, dy and dz, the following differential momentum balance can be derived. The fluid is able to move through all six faces of the volume in any arbitrary direction. The equation below is a vector-tensor equation in rectangular coordinates (x, y, z) (Bird 60):

$$\frac{\partial}{\partial t} \rho \mathbf{v} = -[\nabla \cdot \rho \mathbf{v} \mathbf{v}] - \nabla P - [\nabla \cdot \tau] + \rho \mathbf{g}$$
 (IV-1)

An extraction of the equation of motion (IV-1) is given by Froment 79, namely:

$$-\frac{dP}{dz} = \left[2\frac{f}{d}\right]\rho u^2 + \rho u \frac{du}{dz} \tag{IV-2}$$

When we integrate the equation of motion over a volume and apply the result to a tube flow the equation below is obtained, for more information see appendix 7:

$$\frac{d}{dz}(PA + \Phi_m u) = -\frac{1}{2}f\rho u^2 S + \rho A g \tag{IV-3}$$

At first sight the result does not match, but when we divide equation (IV-3) by the cross-sectional area (A) (S is circumference) and recall that the mass flux is equal to the product of velocity (u) times density (ρ) , equation (IV-2) is almost obtained. The only difference is the influence of the gravity on the momentum. In appendix 7 we developed a criterion for neglecting effects of elevation changes. The criterion is:

$$C_{mb} = \frac{dg}{2fu^2}$$

where C_{mb} must be smaller than ε to neglect the influence of gravitation forces.

Were d and g are respectively the internal tube diameter and the acceleration of gravity. The friction factor is denoted by f and the velocity is given by u.

When we roughly calculate the criterion at the entrance and the end of the coil, the following results are obtained:

Entrance
$$C_{mb} \approx \frac{0.108 \times 10}{2 \times 0.004 \times 100^2} = 0.0135$$
 End of tube : $C_{mb} \approx \frac{0.108 \times 10}{2 \times 0.004 \times 350^2} = 0.0011$

Hence the gravitation forces have no significant contribution to the momentum equation and the momentum equation given by Froment can be used to model the pressure profile.

When checking the significance of the different terms in the momentum equation it is interesting to check if the kinetic term relative to the pressure term, has a significant meaning. The following criterion is developed (see equation (IV-3)):

$$C_{mb2} = \frac{\Phi_m u}{PA} = \frac{Gu}{P} \tag{IV-4}$$

where C_{mb2} must be smaller than ε to neglect the influence of the forces created by the velocity. The mass flux of the coil is denoted by G. Again an estimation is made at the entrance and exit of the coil:

Entrance:
$$C_{mb2} \approx \frac{100 \times 100}{3.10^5} = 0.033$$
 End of the tube: $C_{mb2} \approx \frac{100 \times 350}{1.5 \cdot 10^5} = 0.233$

It is clear that the kinetic contribution to the momentum balance cannot be eliminated.

4.2.1 Friction of the Bends

In chapter 2.6 we concluded that the friction term to account for the friction in the bends is not corrected, this is discussed in appendix 2. We also concluded that the results and the given formulas in the book of Froment 79 do not match. In this sub-paragraph we will give two different approaches to account for the pressure drop due to the bends.

The first approach is to use two sets of momentum equations namely one for the straight part of the tube and one for the bends. For instance, a general solver such as gPROMS it is no problem to define this and integrate over the whole length of the coil. When using collocation, coded in FORTRAN or MATLAB, it is no problem to use two sets of momentum equations. The bends are then defined as a finite element were collocation is applied on. The drawback of this method is that the number of equations to be solved expand rapidly, as the computation time. In a small model like the ethane model this is no problem, but when we use the SPYRO model, the size of the problem is much larger. At each collocation point all the residuals of the DAE system are computed, in the Froment case the size of the DAE system is 11 or larger, in SPYRO this is 125 or larger.

The second approach is to spread the friction due to the bends over the whole length of the coil this is accomplished by using the next equation (more information is given in appendix 2).

$$-\frac{dP}{dz} = \left[2\frac{f}{d} + \frac{N_{bend}f_{bend}}{2L}\right]\rho u^2 + \rho u \frac{du}{dz}$$
 (IV-5)

This equation makes it possible to choose the finite elements independent of the geometry of the coil. We will demonstrate the impact of this freedom with an example, we will look at the size of the resulting model and the numerical results at the end of the tube.

The total number of algebraic equations that have to be solved is given by:

$$NX = NE \cdot NT \cdot NY + NE \cdot (NT - 1) \cdot NU$$
 (IV-6)

Where the number of Finite Elements (=FE) is denoted by NE, the number of collocation points per FE is given by NT, the number of ODEs to be solved NY and the number of algebraic equations NU. We consider 5 finite elements with 5 collocation points per element and no algebraic equations NU = 0. The coil contains nine bends (see appendix 1) we consider the straight part of the tube (=10) as one element, the contents of Table 1 is:

Table 1: Considering the number of equations when comparing bends or no bends

	NX with no bends	NX with nine bends
Froment model (NY=11)	275	1045
SPYRO model (NY=125)	3125	11875

As can be seen, the size of the problem expands rapidly. This is in a production environment like an engineering agency not wanted. We can argue that the number of collocation points in the bends could be less, but even when we reduce the number of collocation points to the minimum of three per element the problem expands ≈ 2.3 times.

The numerical results at the end of the tube is for most purposes of modeling steam crackers important, therefor we check the different results of the two approaches. This is done by using the gPROMS. The model abbreviated by KR1 spreads the friction over the whole length of the coil. There are two equations to describe the pressure profile (one for the bends and one for the straight part of the coil) within the model named KR3. The numerical results are given in the two tables below.

Table 2: Numerical results on: Influence of the bend calculation on the molar flow rates

[mole·s ⁻¹]:	CH₄	C_2H_2	C ₂ H ₄	C_2H_6	C_3H_6	C_3H_8	C₄H ₆	H_2	H_2O
KR1	1.574150	0.100288	10.913700	7.529350	0.050957	0.115778	0.686901	12.063000	13.683900
KR3	1.569610	0.100458	10.915200	7.535020	0.050734	0.115643	0.684640	12.059900	13.683900
rel_diff	0.0029	-0.0017	-0.0001	-0.0008	0.0044	0.0012	0.0033	0.0003	0.0000

With:

$$rel_diff = \frac{KR1 - KR3}{KR1}$$

Table 3: Influence on T and P

	T [K]	P [Pa]
KR1	1112.42	129504.00
KR3	1112.51	130099.00
diff	-0.09	-595.00

with:

$$diff = KR1 - KR3$$

The conclusion is that the difference of the results obtained by the two approaches is smaller than one percent. This justifies the use of the momentum equation where the friction of the bends is spread over the whole length of the coil.

4.2.2 Comparison of Solution to Initialization Problem

In Chapter 2.4 two ways are given to circumvent the initialization problem. The solution of Froment yields a 'complex' equation that needs a lot of other equations, like the mass balances and energy balance. In this sub-paragraph we compare these two equations on there numerical results at the end of the cracking coil. A priori we expect the same results. In the preceding subparagraph we concluded that the momentum equation that spreads the friction of the bends over the whole length of the tube can be used. Recall the two momentum equations used to solve the initialization problem:

$$\frac{dPx}{dz} = -\left(\frac{2f}{d} + \frac{N_{bend}f_{bend}}{2L}\right)\rho u^2 \tag{IV-7}$$

with:

$$Px = P + Gu$$

$$\sum_{j=1}^{9} \frac{dF_j}{dz}$$

$$\frac{j=1}{dz} + \frac{1}{1} \left[\frac{1}{2} \frac{dT}{dz} + \left(\frac{2f}{2} + \frac{N_{bend} f_{bend}}{2} \right) \right]$$
(IV-8)

$$\frac{dP}{dz} = \frac{\sum_{j=1}^{9} \frac{dF_{j}}{dz}}{\frac{GA_{coil}}{GA_{coil}}} + \frac{1}{M_{M}} \left[\frac{1}{T} \frac{dT}{dz} + \left(\frac{2f}{d} + \frac{N_{bend}f_{bend}}{2L} \right) \right] - \frac{1}{M_{M}P} - \frac{P}{G^{2}RT}$$
(IV-9)

We define the model with momentum equation (IV-7) as KR4 and the model with expression (IV-9) is called KR1. Both models are solved with gPROMS. The results are:

Table 4: Results of different momentum equations .

[mole·s ⁻¹]:	CH_4	C_2H_2	C_2H_4	C_2H_6	C_3H_6	C_3H_8	C_4H_6	H_2	H_2O
KR1	1.574150	0.100288	10.913700	7.529350	0.050957	0.115778	0.686901	12.063000	13.683900
KR4	1.574130	0.100289	10.913700	7.529370	0.050956	0.115778	0.686894	12.063000	13.683900
rel_diff	0.0000	0.0000	0.0000	0.0000	0.0000	0.0000	0.0000	0.0000	0.0000

Where:

$$rel_diff = \frac{KR1 - KR4}{KR1}$$

Table 5: Results of T and P

	T [K]	P [Pa]
KR1	1112.42	129504.00
KR4	1112.42	129501.00
diff	0.00	3.00

Where:

diff= KR1 - KR4

The j stands for the number of elements (NE) and collocation points (NT), NE = NT.

We conclude that the difference between the results obtained with the two momentum balances is very small and recommend that equation (IV-7) should be used to model the pressure profile.

4.3 Energy Balance

In this section we will have a closer look at the energy balance that is used by Froment. We will show that the energy balance used in Froment is a very simplified energy balance. The reason is as mentioned in the first paragraph of this chapter, that in the past the solver required that all DAE models are rewritten to ODE models. This chapter will start with the derivation of the energy balance. This is followed by the inspection of the relevant terms of the energy balance. In two sub-paragraphs we compare different types of energy balances

For an infinitesimal volume with dimensions dx, dy and dz, the following finite difference energy balance can be given. The fluid is able to move through all six faces of the volume in any arbitrary direction. The equation below is a vector-tensor equation in rectangular coordinates (x, y, z) (Bird 60):

$$\frac{\partial}{\partial t} \rho \cdot \hat{E} = -(\nabla \cdot \rho \mathbf{v} \hat{E}) - (\nabla \cdot \mathbf{q}) - (\nabla \cdot P \mathbf{v}) - (\nabla \cdot [\mathbf{\tau} \cdot \mathbf{v}])$$
(IV-10)

An extraction of the energy balance given above is denoted in Froment 79:

$$\frac{dT}{dz} = \frac{\left[q(z)\pi d + A_{coil}\Delta H_r\right]}{\sum_{j=1}^{9} F_j C p_j}$$
(IV-11)

When the statement of the first law of thermodynamics for an open system (IV-10) is integrated over a volume and the result is applied to tube flow the next equation is derived (see appendix 7):

$$\frac{d}{dz}\left(\Phi_m\hat{H} + \Phi_m \frac{1}{2}u^2 + \Phi_m\hat{\Phi}\right) = q(z)S + \Delta H_r A_{coil}$$
 (IV-12)

The enthalpy is given by:

$$\hat{H}(T) = \int_{T_{ref}}^{T} Cp(T)dT + \hat{H}(T_{ref})$$
 (IV-13)

The potential energy is given through $\hat{\Phi}$, the total mass flow is denoted by Φ_m , the symbol \hat{H} stands for the enthalpy per unit of mass, the circumference is symbolized through S, the velocity, cross-sectional area of the coil are respectively given by u and A_{coil} .

If we want to neglect the potential energy contribution relative to the kinetic contribution, the next criterion can be used (appendix 7):

$$C_{hb} = \frac{2 \cdot h \cdot g}{u^2}$$

where C_{hb} must be smaller than ε to neglect the influence of the potential energy relative to the kinetic energy. Hereby is the potential energy $\hat{\Phi}$ approximated with $h \cdot g$, the term h is some measure for the height relative to the earth (h=0 at the lowest part of the system). The velocity is given through u. When the criterion is roughly evaluated at the entrance and the exit of the tube, the following results are obtained:

Entrance:
$$C_{hb} \approx \frac{2 \times 10 \times 10}{100^2} = 0.02$$
 End of the tube: $C_{hb} \approx \frac{2 \times 10 \times 10}{350^2} = 0.0016$

We conclude that the potential energy is relatively small to the kinetic contribution, so it may be neglected. In order to obtain equation (IV-11) Froment 79 made, the assumption that the kinetic energy can be neglected in contrast with the momentum balance where he added the kinetic term. Another assumption is made that the product of molar flow rate times the specific heat of is constant in a differential length of coil dz, in order to obtain equation (IV-11). When using more sophisticated techniques to solve DAE models, such as collocation it is possible to a use less simplified energy balance.

In the next two sub-paragraphs we will examine the kinetic energy term and the way to account for the heat of reaction.

4.3.1 Comparison of Energy Balances without Kinetic Energy

In this sub-paragraph we will give numerical results of models with different energy balances, and what they all have in common is that there are no kinetic energy contributions. As for the base case we use the Froment energy balance given by formula (IV-11), this model is denoted by KR4 as in sub-paragraph 4.2.2. Model KR5 contains the energy balance defined by:

$$\frac{d}{dz}(Hx) = q(z)S + A_{coil}\Delta H_r \tag{IV-14}$$

with:

$$Hx = \sum_{j=1}^{9} \left(F_j \int_{T_{nt}}^{T} Cp_j(T) dT \right)$$
 (IV-15)

Model KR7 contains the following energy balance:

$$\frac{d(Hx)}{dz} = q(z)S ag{IV-16}$$

were Hx is defined as:

$$Hx = \sum_{j=1}^{9} F_j \Delta H_{f,j}$$
 (IV-17)

The heat of formation at temperature, T, of component j, is denoted by $\Delta H_{f,j}$ (for the calculation see chapter 2.2 and for the parameters required for the models see appendix 1). The momentum equation used in all models is an equation defined by (IV-7) and (IV-8).

In this and the following paragraph we compare the results of different models approximated by the collocation technique. To validate the collocation technique we compare the results obtained with gPROMS and the results obtained with the collocation method (NE = NT = 6) of the KR4 model. We assume that the other models are within the same accuracy as the validated KR4 model. All the collocation models used in this and the next paragraph have the following collocation settings: NE = NT = 6.

Table 6: Validation of collocation model; molar flow rates.

[mole·s ⁻¹]:	CH ₄	C_2H_2	C_2H_4	C_2H_6	C_3H_6	C_3H_8	C_4H_6	H_2	H_2O
KR4(gPROMS)	1.57413	0.10029	10.91370	7.52937	0.05096	0.11578	0.68689	12.06300	13.68390
KR4(6/6)	1.56799	0.10038	10.89409	7.55836	0.05107	0.11545	0.68385	12.03755	13.68390
rel_diff	0.0039	-0.0009	0.0018	-0.0039	-0.0022	0.0029	0.0044	0.0021	0.0000

Where: rel_diff =
$$\frac{KR4(gPROMS) - KR(6/6)}{KR4(gPROMS)}$$

Table 7: results T and P.

	T [K]	P [Pa]
KR4(gPROMS)	1112.42	129501.00
KR4(6/6)	1112.16	129901.08
diff	0.26	-400.08

Where: diff = KR4(gPROMS) - KR4(6/6)

We conclude that the collocation model KR4(6/6) gives accurate results (all the answers are smaller than 1 percent).

The following numerical results are obtained with the collocation models, KR4, KR5 and KR7.

· · · · · · · · · · · · · · · · · · ·									
[mole·s ⁻¹]:	CH₄	C_2H_2	C_2H_4	C_2H_6	C_3H_6	C_3H_8	C_4H_6	H_2	H_2O
KR4	1.5680	0.1004	10.8941	7.5584	0.0511	0.1154	0.6838	12.0375	13.6839
KR5	1.4748	0.1011	10.4827	8.1128	0.0516	0.1097	0.6391	11.5380	13.6839
KR7	1.5680	0.1004	10.8941	7.5583	0.0511	0.1154	0.6838	12.0376	13.6839
rel_diff1	0.0594	-0.0071	0.0378	-0.0734	-0.0102	0.0494	0.0654	0.0415	0.0000
rel_diff2	0.0000	0.0000	0.0000	0.0000	0.0000	0.0000	0.0000	0.0000	0.0000

Table 8: Comparison energy balance without kinetic contribution

Where: rel_diff $i = \frac{KR4 - KRj}{KR4}$ with i = 1,2 and j = 5,7

Table 9: T and P results

	T [K]	P [Pa]
KR4	1112.16	129901.08
KR5	1106.23	133983.63
KR7	1112.16	129900.74
diff1	5.94	-4082.55
diff2	0.00	0.35

where: diffi = KR4 - KRj with i = 1,2 and j = 5,7

In the book of Froment 79 some industrial data is given, denoted by DATA in Table 10.

Table 10: Comparison of the yields with the literature data.

yields [kg \cdot (100 kg C_2H_6) ⁻¹]	KR4	KR5	KR7	DATA
C_2H_4	49.59	47.72	49.59	48.70
H_2	3.94	3.77	3.94	3.65
CH₄	4.08	3.84	4.08	3.40
conversion of C ₂ H ₆	0.63	0.60	0.63	0.62

The yield for ethylene is calculated as follows:

$$yield_{C_2H_4} = \frac{F_{C_2H_4}(z = L_{coil})}{F_{C_2H_6}(z = 0)} \frac{M_{C_2H_4}}{M_{C_2H_6}} 100$$
 (IV-18)

The yield for the components hydrogen and methane is calculated in the same way as for ethylene. The difference between the energy balances of KR4 and KR5 is the way the specific heat is used. We conclude that this has a significant effect on the component molar flow rates, temperature and pressure at the exit of the tube, see Table 8 and Table 9. Froment 79 shows in his book that the temperature and pressure at the end of the coil should be 1106 K and 1.33 bar, according to an industrial cracking coil. When the temperature, pressure and the yields are compared, model KR5 gives the best results but we want to calculate the enthalpy according to KR7 (equation (IV-17)). For a small kinetic scheme like the ethane model of Froment, it makes not a lot of difference if the heat of reaction is calculated or the enthalpy is evaluated differently.

When we have to deal with the SPYRO kinetic scheme that contains over 3000 reactions and 125 components, it makes a lot of difference if we calculate the heat of reactions for all the 3000 reactions or the enthalpy of 125 components, therefore we prefer not to calculate the heat of reaction, but calculate the enthalpy according to (IV-17).

The difference of the results between KR4 and KR7 is small. It seems that the effects of the specific heat and heat of reaction compensate each other, equation (IV-11) gives the same results as (IV-16). We do not yet understand this result.

The values generated by Froment 79 do not match the results obtained with KR4, two reasons for this can be given, namely: it is not clear how Froment calculated the pressure profile, and the heat of formation under standard conditions is calculated from group contributions.

In chapter 2 we determined the index of the model given in chapter 2.2. We also determined the index of the cracker model named KR5. The result is given by the following expression.

$$\det\left(\frac{d\mathbf{g}}{d\mathbf{y}}\right) = \frac{\left(\sum_{j=1}^{9} F_{j} C p_{j}\right) T \cdot \left[M_{M} G^{2} - T \rho^{2} R_{gas}\right]}{\rho^{2} R_{gas} T^{2}}$$

For the completeness of this report we added the index of model KR5.

4.3.2 Comparison of Energy Balances with Kinetic Energy

In this sub-paragraph we give numerical results of models that contain energy balances with a kinetic energy term, as the base case we use the Froment energy balance given by formula (IV-11). Model KR6 uses the energy balance defined by formula (IV-14). Were Hx is defined as:

$$Hx = \sum_{j=1}^{9} \left(F_j \int_{T_{ref}}^{T} Cp_j(T) dT \right) + A_{coil} G \frac{1}{2} u^2$$
 (IV-19)

Model KR8 does not use the heat of reaction to calculate the energy balance, but uses equation (IV-16). The kinetic energy is accounted for as follows:

$$Hx = \sum_{j=1}^{9} F_j \Delta H_{f,j} + A_{coil} G \frac{1}{2} u^2$$
 (IV-20)

The momentum equation used in all the models is defined by (IV-7) and (IV-8). The following numerical results are obtained for the models KR4, KR6 and KR8:

			•	-	•				
[mole·s ⁻¹]:	CH ₄	C_2H_2	C_2H_4	C_2H_6	C ₃ H ₆	C ₃ H ₈	C ₄ H ₆	H_2	H_2O
KR4	1.5680	0.1004	10.8941	7.5584	0.0511	0.1154	0.6838	12.0375	13.6839
KR6	1.4456	0.1008	10.3114	8.3290	0.0511	0.1077	0.6260	11.3397	13.6839
KR8	1.5350	0.1002	10.7023	7.8008	0.0507	0.1131	0.6689	11.8153	13.6839
rel_diff1	0.0781	-0.0046	0.0535	-0.1020	-0.0011	0.0672	0.0845	0.0580	0.0000
rel diff2	0.0211	0.0019	0.0176	-0.0321	0.0078	0.0202	0.0219	0.0185	0.0000

Table 11: Comparison energy balance, with kinetic contribution

Where: $rel_diffi = \frac{KR4 - KRj}{KR4}$ with i = 1,2 and j = 6,8

Table 12: T and P results

	T [K]	P [Pa]
KR4	1112.16	129901.08
KR6	1101.17	135217.99
KR8	1106.27	131373.35
diff1	10.99	-5316.91
diff2	5.90	-1472.27

Where: diffi = KR4 - KRj with i = 1,2 and j = 6,8

Table 13: Comparison of the yields with literature

yields	KR4	KR6	KR8	DATA
C_2H_4	49.59	46.94	48.72	48.70
H_2	3.94	3.71	3.87	3.65
CH ₄	4.08	3.76	4.00	3.40
conversion of C ₂ H ₆	0.63	0.59	0.62	0.62

The yields of ethylene, hydrogen and methane are evaluated according to (IV-18).

The Table 11 and Table 12 show that both energy balances with kinetic contribution give different answers than the energy balance used by Froment. Recall from the previous subparagraph that the temperature and pressure should be 1106 K and 1.33 bar.

When we look at the data (Table 13) supplied by Froment 79, gathered from a real cracking coil, we conclude that the energy equation given by (IV-16) and (IV-20), KR8, gave the best results, both numerically as well as theoretically (see equation (IV-12) and appendix 7). In the previous sub-paragraph the energy balance defined by and ,KR5 gives the best results. When KR5 and KR8 are compared, we conclude that KR8 gives numerically better results, the energy equation of KR8 is theoretically superior to the equation of KR5 because less information (kinetic term) is neglected.

The following criterion is developed to check if the kinetic energy term can be neglected relative to the enthalpy (see equation (IV-12)).

$$C_{hb2} = \frac{GA_{coil}u^2}{2H} \tag{IV-21}$$

Where C_{hb2} must be smaller then ε to neglect the influence of the kinetic energy relative to the enthalpy. The mass flux id given by G, the cross-sectional area is denoted by A_{coil} , the velocity is represented by u and the total enthalpy flow is denoted by H. The problem with this criterion is that the enthalpy can be calculated in different ways. If the enthalpy is calculated according to (IV-17) then the criterion (IV-21), is evaluated at the entrance and the end of the coil, that are respectively 0.1 % and 5%. When the enthalpy is calculated according to (IV-15) the criterion varies between 0.3% and 3%. This confirms the conclusion given above that an energy balance with a kinetic term should be used. The reason not to mention this in the beginning (as was done for the momentum balance in paragraph 4.2) of this paragraph, is that this criterion is not very clear due to the different definitions of the enthalpy.

In chapter 2 we determined the index of the model given in chapter 2.2. We also determined the index of the cracker model named KR8. The result is given by the following expression.

$$\det\left(\frac{d\mathbf{g}}{d\mathbf{y}}\right) = \frac{\left(\sum_{j=1}^{9} F_{j} C p_{j}\right) T \cdot \left[M_{M} G^{2} - T \rho^{2} R_{gas}\right] - u P A_{coil} M_{m} G^{2}}{\rho^{2} R_{gas} T^{2}}$$

For the completeness of this report we added the index of model KR8.

5 Model Scale-up

5.1 Introduction

This chapter deals with various topics. The first topic is about the validation of the collocation method on the ethane steam cracker model. For this validation we used as a reference the results obtained with gPROMS. For the readers who are not familiar with the gPROMS package, we compared the results with the well-known GEAR routine (of MATLAB). We examined the influence of the increase of the number of collocation points per finite element and the increase of the number of finite elements in the domain of interest. The second topic deals with how the 'large steam cracker' models are created. These large models are created to test the non-linear solver of the mathematician working on this project. For these large models it is very important to express the component continuity equations in the right variables. The third topic of this chapter consider the Jacobian structure and the continuity equations. The last topic discusses the path to obtain the solution of a collocation model. As mentioned above, a mathematician is also working on this project and therefor it seems logic not to be concerned with how the models should be solved. A priori, that we do not know how difficult the SPYRO problem is, so therefor we created large test models in which the steepness of the resulting curves can be altered. We expect that the large models with both steep and flat curves could be difficult problems. We will solve these difficult problems with the continuation method. This continuation method provides ways to obtain the solution of difficult problems. It is possible to use a physical insight to obtain the solution of the problem with the continuation methods, this is the reason why we use continuation techniques. When a set of algebraic equations must be solved we should provide the solver with an initial estimate of the solution. The problem is that not always a realistic estimate can be given, the continuation method can be of some assistance. We will investigate the use of a mathematical continuation method to improve a bad initial estimate by pre-solving of the collocation model. As mentioned we shall begin with the validation of the collocation method.

5.2 Validation of Collocation on Ethane Cracker Model

When we want to create a model with an open structure, a generic program language like FORTRAN must be used. We need to implement numerical procedures, such as collocation (see chapter 3), when using generic program languages to solve the models. In this paragraph we compare the results obtained with gPROMS, with the results obtained with the collocation model as a function of the number of finite elements (NE) and number of collocation per element (NT). We examined the influence of increasing the number of collocation points in one element on the difference between the collocation result and the gPROMS result. The influence of the number finite elements on the difference between gPROMS and the collocation model is also examined. The elements contained the smallest amount of collocation points per section namely three. In a, b and c of Figure 9, the effect of the number of collocation points on the results are shown. In a, b and c of Figure 10, the effect the number of finite elements are given.

For most engineering purposes the results at the end of the coil are important, z=L, therefor we compare the results of ethylene, ethane, temperature and pressure with the gPROMS results at this point. The comparison of the molar flow rates of the components ethylene and ethane is done relative and the comparison of the temperature and pressure is not done relative.

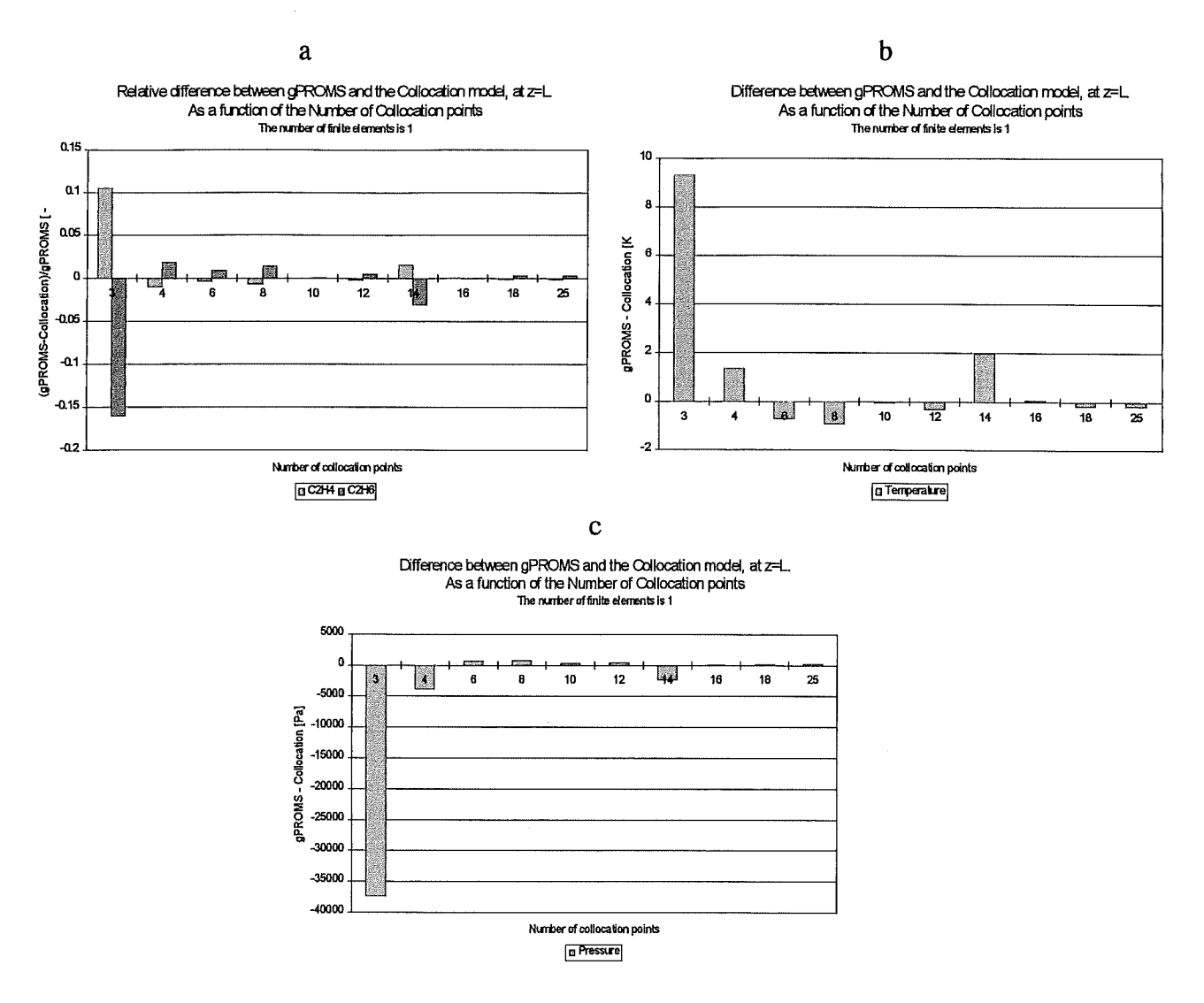


Figure 9: Validation collocation method; variation of collocation points per section.

The results show in Figure 9 that the difference between the collocation solution and the gPROMS solution decreases when the number of collocation points per section increases. When 14 collocation points are used the error increases. This sudden increase is an indication that the polynomial approximation is not inherently better when the order of the polynomial is increased. The theorem of Runge 1901 denotes that interpolation with higher order polynomials does not guarantee an increase of accuracy (the error goes to infinity), the theorem is explained below.

The theorem of Runge 1901, explained in Boor 78, denotes (for interpolation):

$$\lim_{n\to\infty} |p_n - f|_{\infty} = \infty$$

Where p_n is the approximating polynomial (order is n) of the function f. This theorem states that limit of the maximal absolute difference between the approximating polynomial of infinite order and function f is infinite.

On the following page the results of the investigation to the use of more elements is given.

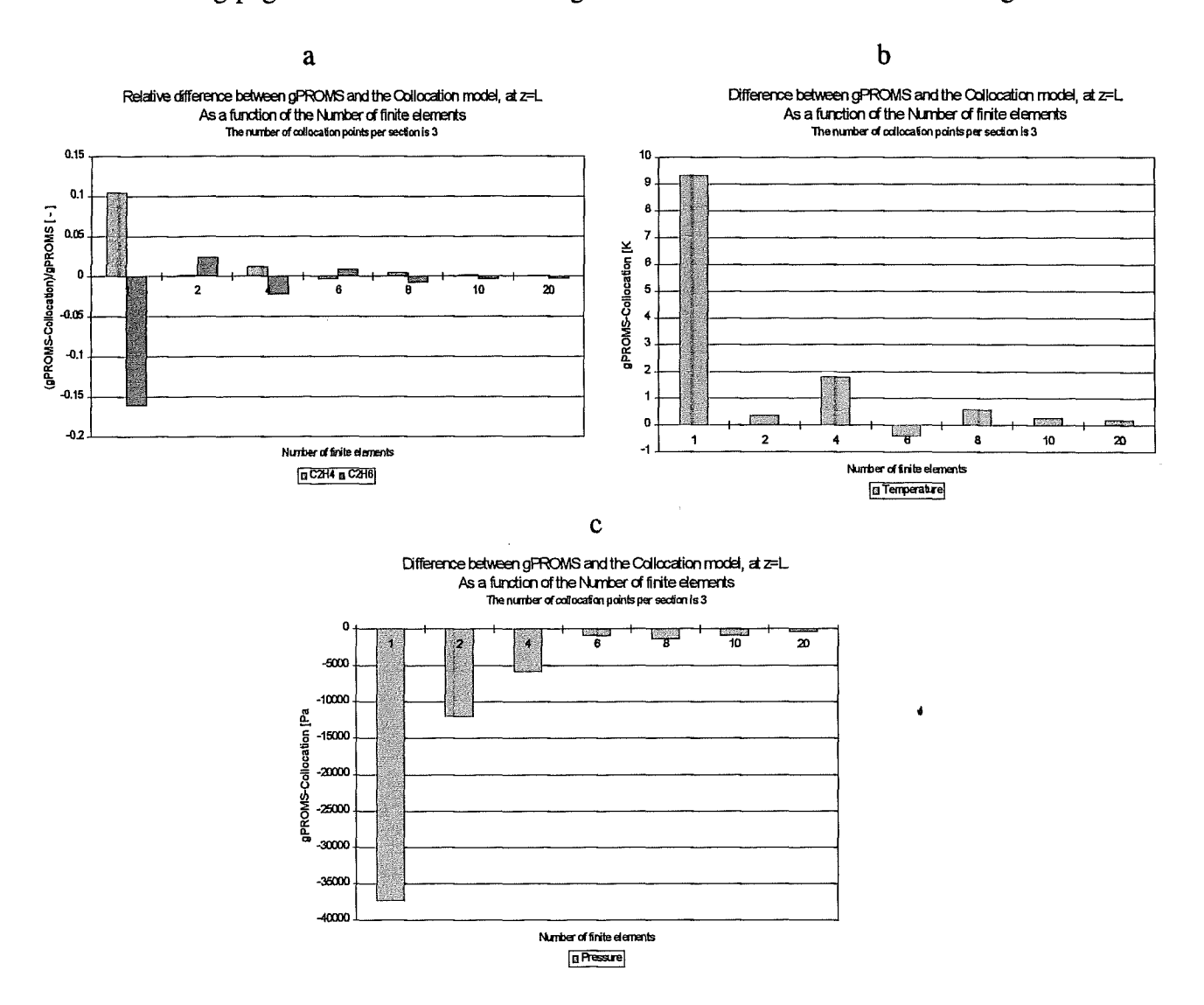


Figure 10: Validation collocation method; variation of the number of finite elements.

Figure 9 gives the results of an increasing number of collocation points, we conclude that more collocation points per section does not guarantee a better approximation. Figure 10 gives the results of the influence on the accuracy of the collocation method when the number of collocation finite elements are increased. We can conclude from these figures that more finite elements give a better approximation. Therefor we recommend to use more finite elements and not more collocation points per section to increase the accuracy of the collocation technique.

Collocation points

Another feature of the collocation method is the generation of the collocation points with the roots of an orthogonal polynomial. In all the collocation models, we use the roots of the Legendre polynomials ($\alpha = \beta = 0$) to generate the collocation points. In the literature, no indications are given as to which polynomials should be used. We experimented with different polynomials on the two point boundary value problem given in chapter 3.2. The reason for this is that an analytical solution is available and therefor comparison with the real solution is possible. The conclusion is that the accuracy of the estimated y-values at the collocation points is dependent on the number of collocation points and number of elements, for one polynomial used to generate the collocation points.

The results also depend on the problem whereon the collocation method is used. Therefor there is no clear preference for orthogonal polynomial to generate the collocation points. Based on the experiments with the two point boundary value problem (chapter 3.2) and the cracker model, we think that Legendre polynomials are good polynomials for collocation of the ethane cracker model. We did not show results because no general conclusion can be made.

Validation of implementation collocation

In the section above we examined the difference between the collocation solution and the gPROMS results, as a function of the collocation parameters *NE* and *NT*. In order to check if no implementation errors are made, we compare the MATLAB and the FORTRAN collocation models with each other. In MATLAB it is not possible to solve large models within an acceptable time, therefor relatively small models are compared. The results are given below.

 $[mole \cdot s^{-1}]$: CH₄ C_2H_2 C_2H_4 C_2H_6 C_3H_6 C_3H_8 C₄H₆ H_2 H_2O gPROMS 1.574150 | 0.100288 | 10.913700 | 7.529350 | 0.050957 | 0.115778 | 0.686901 12.063000 13.683900 MATLAB(4/6) 1.573929 0.100307 10.909327 7.534065 | 0.050931 | 0.115745 0.686802 12.058495 13.683894 KR1(4/6) 1.573929 0.100307 10,909327 7.534065 0.050931 0.115745 0.686802 12.058495 13.683895 MATLAB(4/7) 1.564106 0.100448 10.878809 7.579632 0.051107 0.115221 0.681924 12.018538 13.683894 KR1(4/7) 1.564106 0.100448 10.878810 7.579632 0.051107 0.115221 0.681924 12.018538 13.683895 0.118177 0.707995 MATLAB(5/5) 1.616701 0.099586 11.066635 7.310963 0.050328 12.256865 13.683894 1.616701 | 0.099586 | 11.066636 | 7.310963 | 0.050328 0.118177 0.707995 12.256865 KR1(5/5) 13.683895

Table 14: Validation of implementation collocation method

(4/6) means NE = 4 and NT = 6 or shorted by: (NE/NT)

Table 15: Validation of implementation collocation method

	T [K]	P [Pa]
gPROMS	1112.4200	129504.0000
MATLAB(4/6)	1112.3946	129406.3139
KR1(4/6)	1112.3946	129406.3045
MATLAB(4/7)	1111.9912	130037.6073
KR1(4/7)	1111.9912	130037.5980
MATLAB(5/5)	1114.2907	127371.7186
KR1(5/5)	1114.2908	127371.7089

It is very clear that the results obtained with MATLAB and FORTRAN collocation models are the same. We conclude that the collocation models are correctly implemented.

Comparison of gPROMS with GEAR

In the previous section we compared all the results obtained with the collocation models with the gPROMS results. Because not every reader is familiar with the gPROMS package, we compare the gPROMS results with GEAR integration routine at the end of the coil, z = L. The GEAR integration routine is available in the SIMULINK toolbox of MATLAB.

When using MATLAB we are able to use the GEAR routine via the MATLAB command ODESL. The default settings are used of both mathematical packages. In the following tables the results are presented.

Table 16: Comparison of gPROMS with GEAR

	CH₄	C_2H_2	C_2H_4	C_2H_6	C₃H ₆	C ₃ H ₈	C_4H_6	H_2	H_2O
GEAR	1.574185	0.100287	10.913760	7.529197	0.050957	0.115780	0.686920	12.063170	13.683894
gPROMS	1.574150	0.100288	10.913700	7.529350	0.050957	0.115778	0.686901	12.063000	13.683900
rel_diff	0.000022	-0.000012	0.000005	-0.000020	0.000006	0.000018	0.000028	0.000014	0.000000

$$rel_diff = \frac{GEAR - gPROMS}{GEAR}$$

Table 17: Comparison of gPROMS with GEAR

	T [K]	P [Pa]
GEAR	1112.4213	129506.4952
gPROMS	1112.4200	129504.0000
diff	0.0013	2.4952

diff = GEAR - gPROMS

The conclusion can be made that gPROMS and the GEAR routine gives the same results and it is justified that we compare all the collocation results with gPROMS.

5.3 Enlarged Ethane Cracker Model

In the previous paragraph we used the Ethane Cracker Model of Froment 79, to validate the collocation technique. What we want to use is a steam cracker model which has the size and properties of for instance SPYRO. For reasons we are not able to use the SPYRO model as a test case, we developed two collocation models which have the size of the SPYRO model. In this paragraph we will describe how the models are created.

The first model is called PER and solves a given number of ethane cracker models, of Froment, simultaneously. To test the solver we increased the steepness of the component curves. This is done by multiplying the mass balances with a value OMEGA(tel), where OMEGA is a vector with contains NUM_OF_BLOKS elements where NUM_OF_BLOKS is a scalar indicating how many ethane models are solved simultaneously.

$$\frac{dF_j}{dz} = A_{coil} \left(\sum_{i=1}^{7} \alpha_{ij} r_i \right) \text{OMEGA(tel)}$$
 (V-1)

The main reason to create a model which contains steep and or flat curves, is as mentioned to test the solver. In a large model like SPYRO different curves with steep and flat slopes have to solved simultaneously, the PER model is therefor created to have a model where the slope of the curves can be altered.

For the second model we created a 'new' kinetic scheme and defined this model as PR2. This scheme is a modified scheme given by Froment 79. The rate of reaction is the same as shown in chapter 2.2. This kinetic scheme is used NUM_OF_BLOKS times. The initial flow rates at the entrance of the cracker tube, used in the ethane cracker model, are divided by the scalar NUM_OF_BLOKS. The total mass flux, G, is kept the same as in the ethane model of chapter 2.2.

By doing this we imagine that there are NUM_OF_BLOKS times nine new components, and they react all with the same speed (the sets of nine of course). This can be altered with the vector OMEGA, just as in the PER model. So we have introduced more components which react in blocks of nine components. The reason to create PR2 is to have a model that has a Jacobian with full blocks on the diagonal like in Figure 11a, the PER model has a Jacobian with small block in the diagonal, like schematically given in Figure 13a.

Both models PER and PR2 are used to experiment and gather knowledge on modeling of large steam cracker models. In paragraph 5.4 we give some results of the simulation of the large model PR2. For cracker models which are hard to solve, we experimented with continuation methods to obtain a solution of the problem. The experiments are done with the PER model and homotopy of the physical category is used to solve the problem. All the results obtained with the continuation methods are given in paragraph 5.5.

5.4 Considerations over Mass Balance

At first sight the choice of the mass balance seems rather trivial. The set of continuity equations for the components given by Froment are:

$$\frac{dF_j}{dz} = A_{coil}RATE_j = A_{coil}\left(\sum_{i=1}^{7} \alpha_{ij}r_i\right)$$
 (V-2)

No spectacular change can be made to these equations. The rate of the reactions is defined as follows:

$$r_i = k_i \prod C_j^{k_j} \tag{V-3}$$

With the next expression for the concentration:

$$C_j = \frac{F_j}{\sum_{s=1}^9 F_s} \frac{P}{RT}$$
 (V-4)

The reason to show these equations is not from the point of view of a chemical engineer but from a mathematician. In chapter 3.2 we displayed figures with the structure of the Jacobian obtained with a vector oriented notation of the collocation residuals. In Figure 11a below the blocks are shown which are created by the residuals at the *interior* collocation point and the Right Hand Side (RHS) end point of a finite element, the black color denotes that the blocks are full with values which have to be stored. For the Froment ethane model the size of the block is 11x11, in SPYRO these blocks are 125x125. The reason why the blocks are completely full is that in equation (V-4), the sum of all the components is taken and as a consequence the mass balance at a *interior* collocation points and RHS endpoint has derivatives to all the components. Therefore it is better to reduce the number of derivatives by adding one equation and change the expression for the concentration. The concentration is given by:

$$C_j = F_j inv Qv (V-5)$$

With the inverse of the volumetric flow rate given by:

$$invQv = \frac{P}{RT\sum_{s=1}^{9} F_s}$$
 (V-6)

The result of this modification is best explained by the following Figure 11.

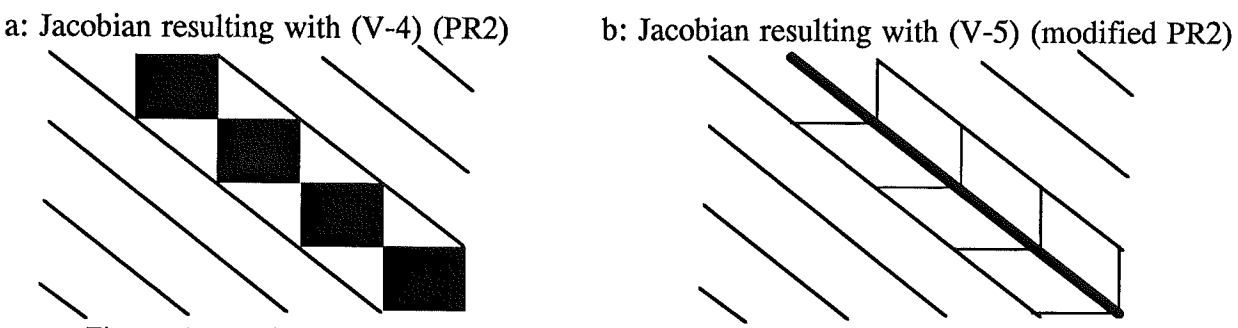


Figure 11: One finite element where the needed storage capacity is reduced (schematically).

From the preceding figure it is clear the storage requirements for the Jacobian reduces drastically when equation (V-5) is applied. When we solve the model with the concentrations calculated according to (V-5), no reduction of computation time is detected. At first sight this is not logical. To understand the reason we have to look at what the solver does with the Jacobian. The solver computes a LU-decomposition of the Jacobian. For a system with three finite elements (NE=3) and five collocation points per section (NT=5), the following LU-decomposition is obtained.

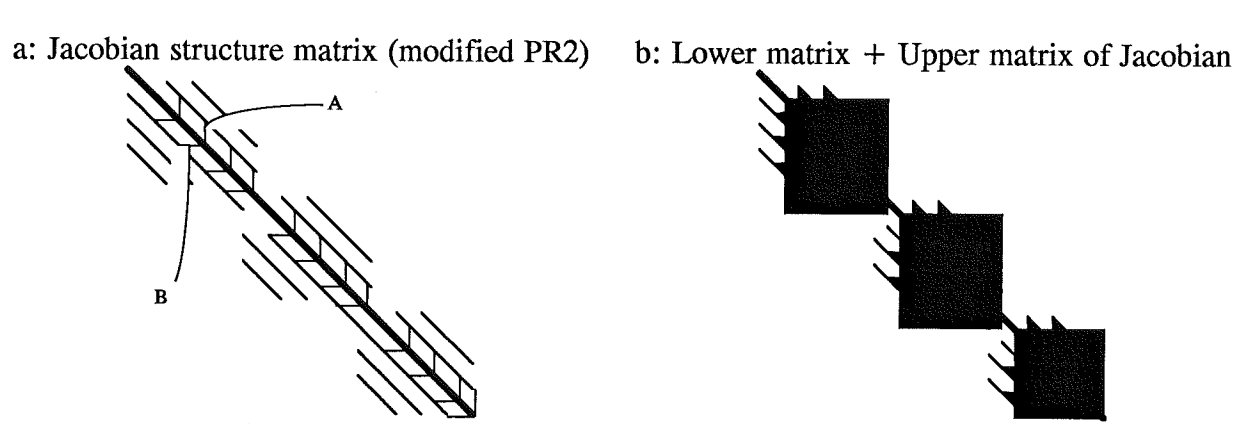


Figure 12: Structure Jacobian and its LU-decomposition (schematically)

As can be seen, the size of LU-decomposition explodes rapidly, so it makes no difference for the solver if the size of the Jacobian is smaller. This problem can be overcome when the values of the lines symbolized by A and B in Figure 12 are put to the right (lines A) and below (lines B) the finite elements, as shown in Figure 13. The LU-decomposition of the Jacobian has than less fill-in, as can be seen in Figure 13.

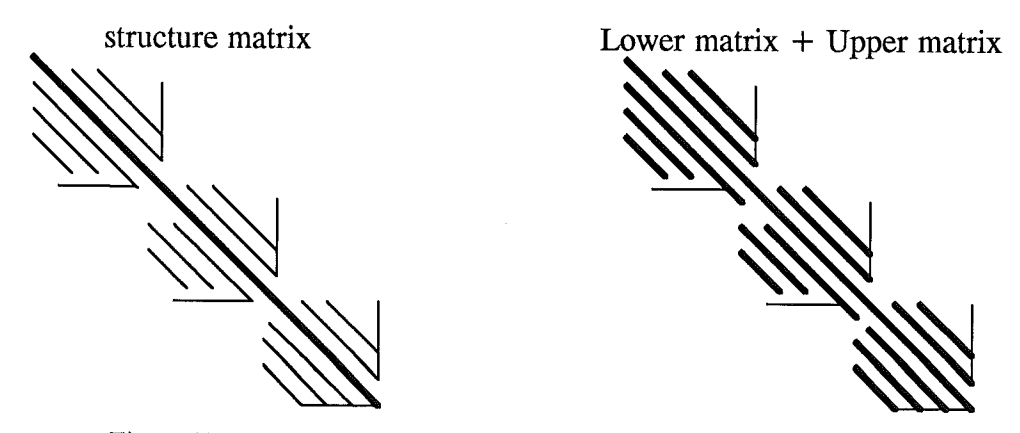


Figure 13: Structure Jacobian and its LU-decomposition (schematically)

5.5 Solution of Collocation Model with Homotopy

The collocation models used in chapter two to four can be solved with a Newton solver with damping. In paragraph 5.3 we presented two large 'steam cracker models' with the feature that the slope of the curves can be altered. When these two models are solved with increased steepness (OMEGA(tel) > 1) no solution is obtained with the Newton solver with damping. In this paragraph we will show that continuation techniques provides ways to obtain solutions of difficult problems, such as PER with OMEGA(tel) greater than 1. In chapter 3.3 three categories of homotopy methods are given, namely: mathematical, proprietary and physical continuation methods. The third method exploits the nature of the equations in some way. For example, in a reactive distillation column where the reactions are 'brought in'. This category of homotopy can also be applied to steam cracker models. For instance we could start with an isothermal and isobaric radiant coil and 'bend' the energy and momentum balances into the model. Another possibility is to start with a radiant coil wherein no reactions occur, the reactions are added to the model during the simulation. Of course there are more possible scenarios for a physical continuation method to solve steam cracker models.

In this paragraph we solved the PER model with NUM_OF_BLOKS is 2 and OMEGA = [p, 1], with p = 1, 10, 100, 1000, 10000. When we use homotopy where the reactions are 'brought in' no solution is found, for p-values of 10 and bigger. If we start the continuation method with isothermal and isobaric conditions, solutions are obtained for all the p-values mentioned. In this paragraph we will show the results obtained with p = 100 (profiles for the set of equations with OMEGA(2) = 1 are not shown), the reason for this is when using p = 1000 or bigger, the resulting profiles are very steep in the first part of the radiant coil (\pm 1 meter) and afterwards the component profiles are straight lines (nothing can be seen). The isothermal and isobaric conditions are implemented as follows, the energy and momentum balance are multiplied with the homotopy parameter, t:

$$\frac{dT}{dz} = t \frac{\left[q(z)\pi d + A_{coil}\sum_{i=1}^{7}(-\Delta H_i)r_i\right]}{\sum_{j=1}^{9}F_jCp_j}$$
(V-7)

$$\frac{dP}{dz} = t \frac{\sum_{j=1}^{9} \frac{dF_j}{dz}}{\frac{GA_{coil}}{GA_{coil}}} + \frac{1}{M_M} \left[\frac{1}{T} \frac{dT}{dz} + \left(\frac{2f}{d} + \frac{N_{bend}f_{bend}}{2L} \right) \right]}{\frac{1}{M_M P} - \frac{P}{G^2 RT}}$$
(V-8)

The path to the solution is schematically given below:

- 1. Set t = 0.
- 2. Solve the model, h(x(0),0) = 0, to obtain x(0).
- 3. Determine vector \mathbf{h}_t through perturbation of t and matrix \mathbf{H}_x through perturbation of x.
- 4. Calculate the tangent vector $\frac{d\mathbf{x}}{dt}$, by solving $\mathbf{H}_x \cdot \frac{d\mathbf{x}}{dt} = -\mathbf{h}_t$, with the current $\mathbf{x}(t_i)$.
- 5. Estimate the new \mathbf{x} at t_{i+1} , represented by $\widetilde{\mathbf{x}}(t_{i+1})$, calculated by $\widetilde{\mathbf{x}}(t_{i+1}) = \mathbf{x}(t_i) + \Delta t \left(\frac{d\mathbf{x}}{dt}\right)$.
- 6. Solve $\mathbf{H}_{x} \cdot (\mathbf{x}^{k+1}(t_{i+1}) \mathbf{x}^{k}(t_{i+1})) = -\mathbf{h}(\mathbf{x}^{k}(t_{i+1}), t_{i+1})$ with $\widetilde{\mathbf{x}}(t_{i+1})$ as initial estimate.
- 7. If t < 1 then return to step 3.
- 8. If t = 1 than the solution is found.

The reason why the Newton solver crashes is best illustrated with the next two graphs, Figure 14a & b.

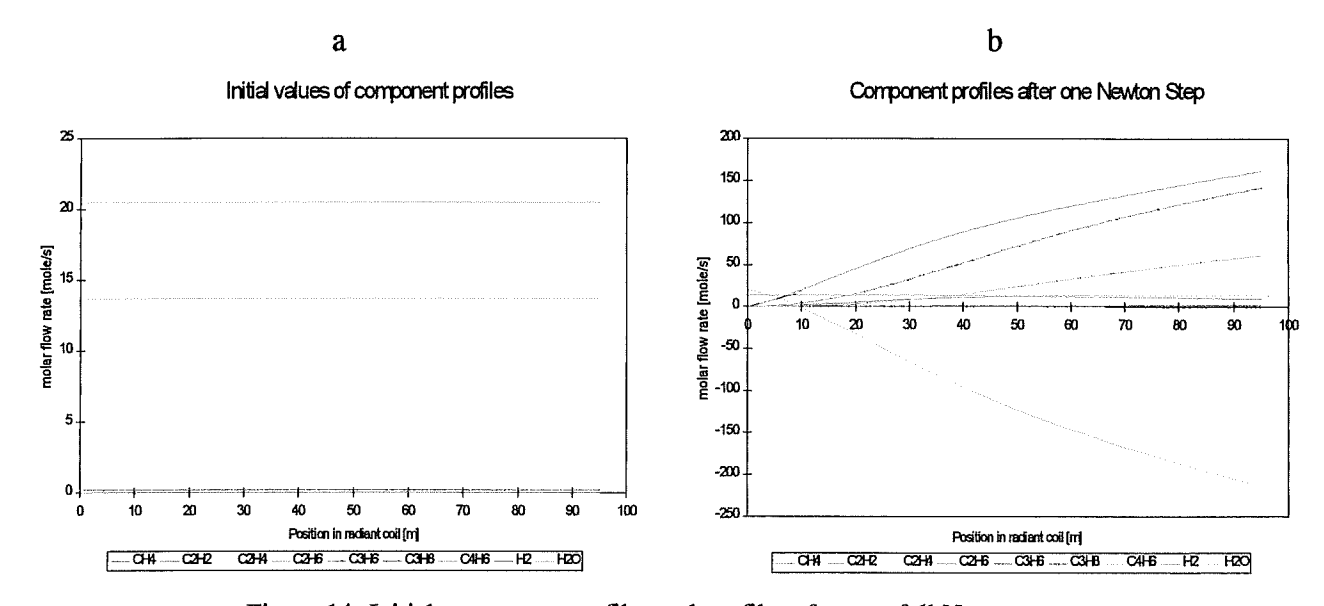


Figure 14: Initial component profiles and profiles after one full Newton step.

All the initial conditions for the nine components, temperature and pressure profiles are straight lines, as given in Figure 14a (only components profiles). After the first full Newton step, the curves in Figure 14b are obtained and followed through a run-time error of the program. The source of this error is a root of a negative value during calculation of the friction factor for the straight part of the tube. The negative value is obtained when the viscosity of the fluid is calculated with the molar flow rates as given in Figure 14b.

The obvious conclusion is: the full Newton step is too much, so damping should be applied. As a matter of fact with damping the program crashes to. The reason is that most damping routines check some kind of norm of the residuals, if these residuals are decreasing a full Newton step is executed. A better damping strategy is to check if the variables are within there definition domain. This kind of damping strategy does not belong to the scope of this project, it belongs to the mathematician also working on this project.

A chemical engineer uses the knowledge of the process to obtain the solution. An excellent method to do this is homotopy, which is explained above (equations (V-7) & (V-8) and the schematic algorithm). In the figure below the gradual added energy balance and momentum balance is demonstrated.

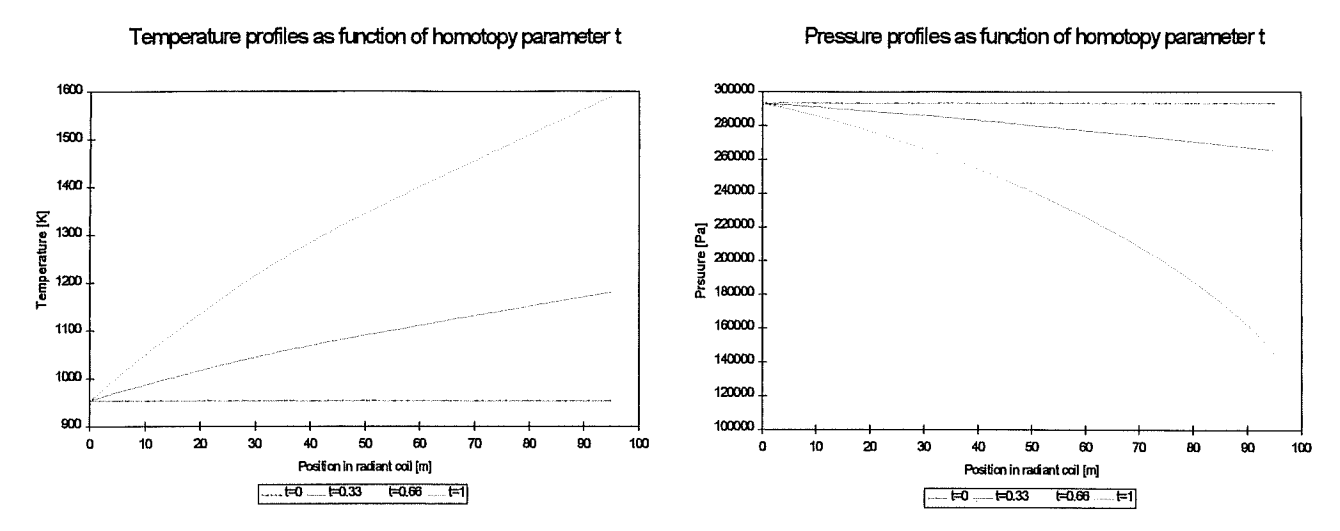


Figure 15: 'Switched on' energy and momentum balances,

The effects of the physical continuation method on the component profiles is presented in Figure 16 below (for the component profiles where the continuity equations are multiplied by p = 100). The profiles do not jump to extreme values as shown in Figure 14b.

In Figure 16a the components curves are given at isothermal and isobaric conditions, in Figure 16b & c they gradually develop to the end result, shown in Figure 16d. With the increase in steepness (bigger p-value) it is clear that the profiles are getting closer to the y-axis. When the p-value is 10,000 a lot of steps are needed (small Δt) to obtain the solution. When the slope of the profiles increases further, the placement and the number of finite elements is becoming important. In order to get an optimal placement of the elements an adaptive collocation technique can be used, such as given in appendix 4. This technique is tested on one equation which resulted in a better approximation than with equal placed elements (see appendix 4). The adaptive collocation technique gives an optimal placement of a given number of elements. Of course more elements can be placed in the beginning of the tube and less at the end of the tube, without using the adaptive collocation technique. The number of elements needed is depending strongly on the problem that is being solved.

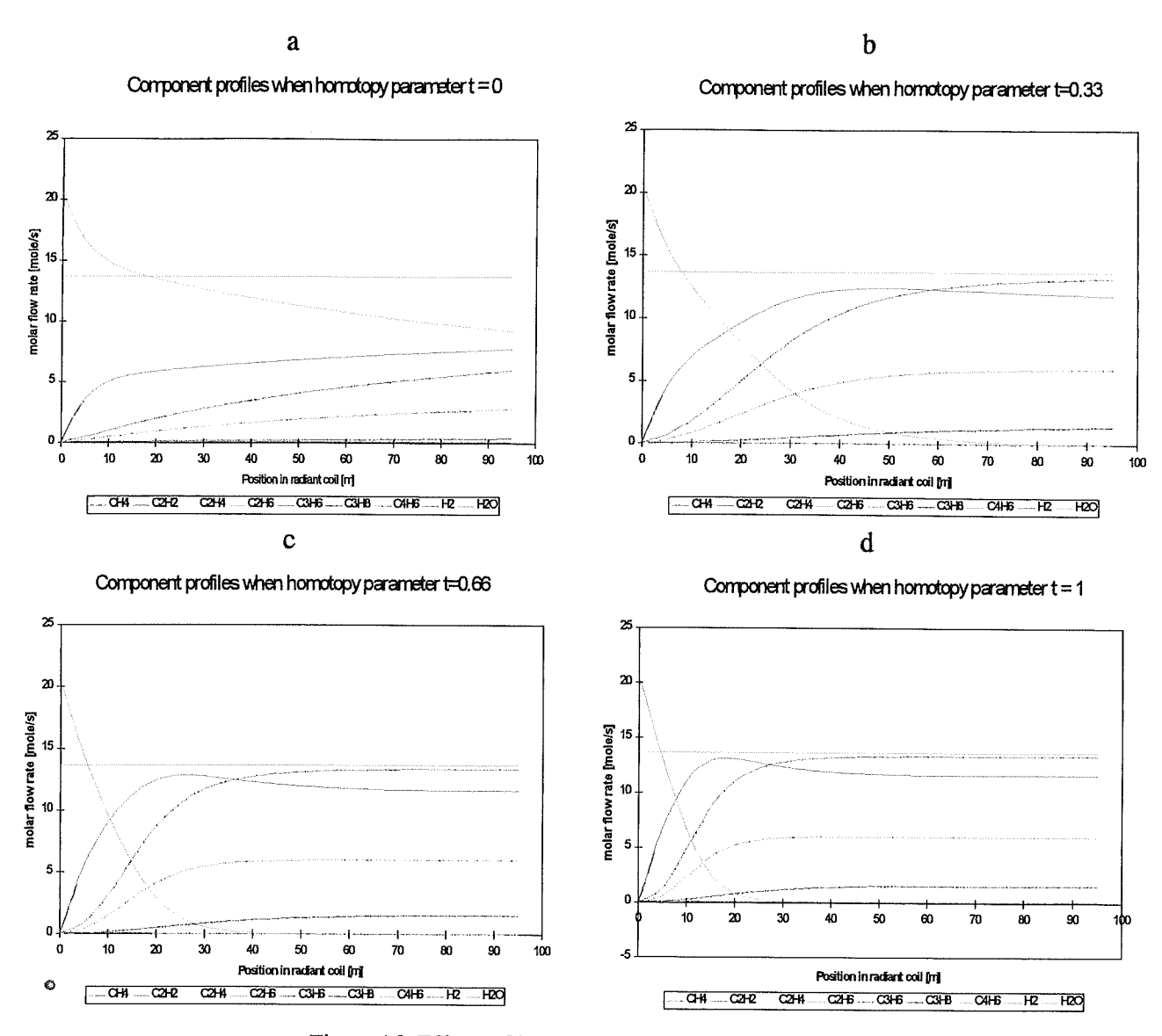


Figure 16: Effects of homotopy on component profiles.

5.5.1 Initialization of Collocation Model

In the preceding paragraph we used the continuation method to obtain the solution of difficult problems. The same continuation technique can be used to improve the initial estimation of a solution. This can yield a more efficient solution procedure. When using the initialization technique described in this sub-paragraph an arbitrary initial estimation can be supplied to solve the problem. The arbitrary initial estimation must of course be in the domain of definition of the variable, for example a negative temperature (Kelvin) or negative flow rates give problems. A mathematical continuation method is used, in contradiction to the preceding paragraph. This mathematical continuation initialization procedure reduces the computation requirements, as shown below. The reason to use a mathematical instead of a physical continuation method, is the computation time to obtain the final solution, this time must not increase. When using the physical continuation method a solution at homotopy parameter, t=0, must be available, for physical continuation this is not the case and a complete system must be solved first before the initialization can take place. The so called Newton homotopy is used for initialization, see chapter 3.3.

The next algorithm is used to initialize a set of collocation equations:

- 1. Set t = 0.
- 2. Solution of $\mathbf{h}(\mathbf{x}(0), 0) = 0$ is the arbitrary vector $\mathbf{x}(0) = \mathbf{x}_0$, recall $\mathbf{h}(\mathbf{x}, t) = \mathbf{f}(\mathbf{x}) (1 t)\mathbf{f}(\mathbf{x}_0) = 0$
- 3. Calculate the tangent vector $\frac{d\mathbf{x}}{dt}$, by solving $\mathbf{H}_{\mathbf{x}} \cdot \frac{d\mathbf{x}}{dt} = -\mathbf{h}_{t}$, with the current $\mathbf{x}(t_{i})$.
- 4. Calculate the new x at t_{i+1} , represented by $\mathbf{x}(t_{i+1})$, calculated by $\mathbf{x}(t_{i+1}) = \mathbf{x}(t_i) + \Delta t \left(\frac{d\mathbf{x}}{dt}\right)$.
- 5. If t < 1 then return to step 3.
- 6. If t = 1 then initialization is finished, initial estimation for model is obtained.

The criteria to check the computation requirements is the number of Jacobian and linear solver calls. The collocation model KR4 is used, this model is described in chapter 4.2.2. The following results are obtained. With the number of initialization steps (N) we denote the number of steps wherein the homotopy parameter t is varied equidistant from 0 to 1, so Δt is 1 divided N (except for 0 of course, then no initialization is applied).

Number of (N) Initialization steps	Step-size homotopy parameter Δt	Number of Newton steps	Number of Jacobian evaluations and linear solver calls.
0		9	9
1	1	8	9
2	1/2	5	7
3	1/3	4	7
4	1/4	4	8
5	1/5	4	9

Table 18: Effects of initialization of Jacobian and linear solver calls

The performance of the initialization method can be evaluated with the following criteria. This criteria is a measure of the difference between the profiles obtained with the initialization procedure and the final solution.

$$\sigma_{j} = \sqrt{\frac{\sum_{i=1}^{NS \cdot NT} \left(y_{i,j}^{final} - y_{i,j}^{Ini} \right)^{2}}{NS \cdot NT}}$$
(V-9)

Where σ_j is the 'mean' deviation of profile j, for instance the pressure profile, with the final result. This value σ_j gives an indication what the Newton solver has to do. The total number of collocation points is denoted by the product of *NS* and *NT*, respectively the number of finite elements and the number of collocation points per element. The index i indicates the value of the j-th (example j=12 is the pressure, see Table 20) variable y at the i-th collocation point. The following tables contain the numerical results obtained with equation (V-9).

Number of (N)	CH ₄	C_2H_2	C_2H_4	C_2H_6	C_3H_6	C_3H_8
Initialization steps	[mole·s ⁻¹]					
0	0.8766	0.1066	6.4985	7.7038	0.1067	0.0664
1	0.2393	0.4797	2.6823	3.6956	0.4553	0.0345
2	0.3500	0.0309	0.9001	0.5620	0.1121	0.0079
3	0.0746	0.0180	0.3321	0.3119	0.0476	0.0044
4	0.0227	0.0134	0.1875	0.2156	0.0276	0.0031
5	0.0147	0.0108	0.1298	0.1642	0.0194	0.0024

Table 19: Numerical results obtained with equation (V-9).

Table 20: Numerical results obtained with equation (V-9).

Number of (N)	C_4H_6	H_2	H ₂ O	T	Px	P
Initialization steps	[mole·s ⁻¹]	[mole·s ⁻¹]	[mole·s ⁻¹]	[K]	[Pa]	[Pa]
0	0.3644	7.2137	0.0000	116.14	68795.65	75585.79
1	0.3472	3.3168	0.0000	99.61	7681.45	12649.27
2	0.2395	0.6120	0.0000	25.27	4801.87	8254.23
3	0.0572	0.2993	0.0000	10.39	3760.55	6568.07
4	0.0178	0.1970	0.0000	6.35	3058.35	5427.95
5	0.0087	0.1468	0.0000	4.59	2570.46	4621.60

Table 18 shows when the number of initialization steps is 2, 3 or 4 then the initialization method reduces the computation time. The results given in Table 18 also show that more initialization steps do not result in a faster initialization. From Table 19 & Table 20 we can conclude that the difference between the final result and the result of the initialization method decreases as the number of initialization steps increase. The effect of the initialization on the profiles is shown in Figure 17. After visual inspection of the profiles we conclude that the shape of final curves is sufficiently approximated after three initialization steps for initialization purposes. This is in agreement with the results given in Table 18 (number of Newton steps).

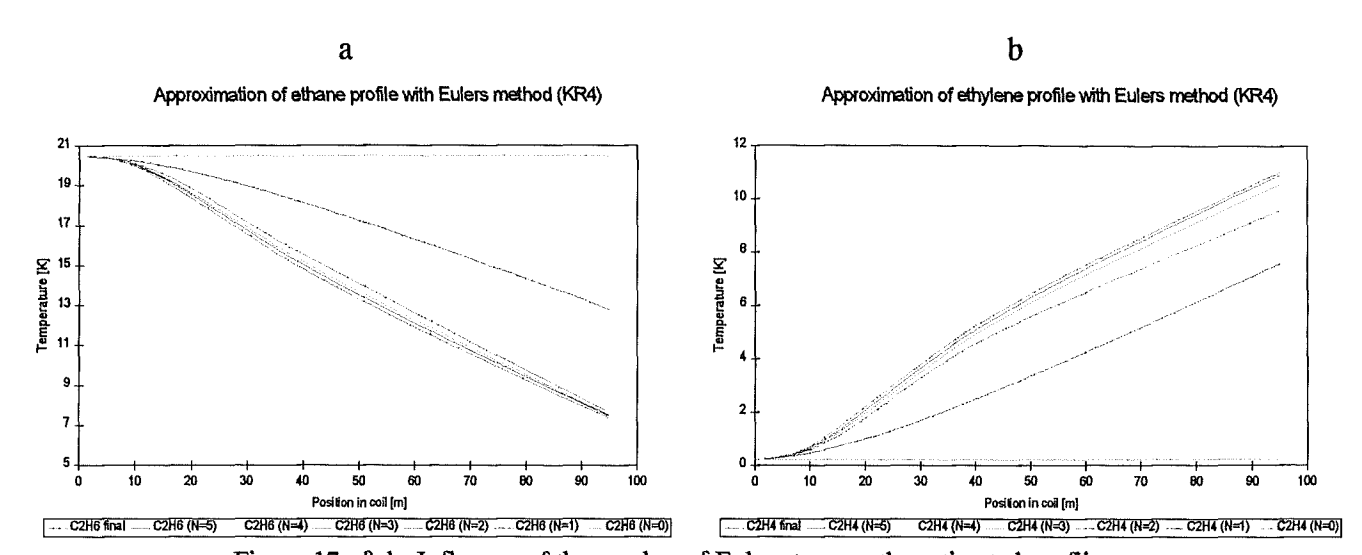


Figure 17a & b: Influence of the number of Euler steps on the estimated profiles.

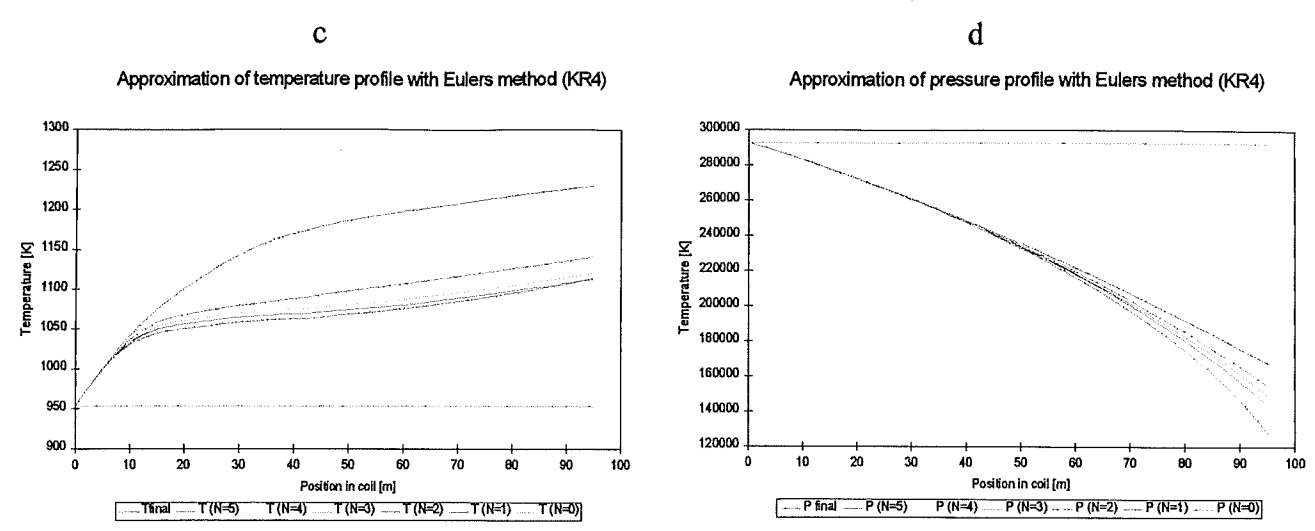


Figure 17c & d: Influence of the number of Euler steps on the estimated profiles.

6 Conclusions and Recommendations

The treatment of the conclusions and the recommendations will be spread over five sections. The first three sections deal with the answering of the problem statement (investigate if the collocation method can be used for the open SPYRO model) while the fourth and fifth section are concerned with the different momentum and energy balance that can be used for the modeling of steam crackers.

6.1 Collocation

The target of this report is to investigate the feasibility to create an open SPYRO model with the collocation method. We used a small ethane cracker model to gain knowledge and experience with collocation. We need to validate how accurate the collocation model is, therefor we integrated the model with the mathematical program gPROMS and assume that the gPROMS result is the correct solution. For readers that are not familiar with gPROMS, the results obtained with this program are compared with the results obtained with the well-know GEAR routine. The difference between the two results is smaller than 0.001%, so we conclude that the results are the same and gPROMS can be used as a reference.

To be certain that the collocation method was implemented in the right way, we compared the results of the models coded in MATLAB and FORTRAN. We concluded that we did not make any mistake because the results are exactly the same.

In this report two experiments are presented to make clear that the accuracy of the collocation method is better when the number of collocation points is increased. This increase in collocation points can be accomplished by increasing the number of finite elements and/or the number of collocation points per finite element. In this report we showed two tests, one with increasing number of finite elements and three collocation points per finite element. In the second test we used one finite element with increasing the number of collocation points. The first test showed a decreasing error as the number of finite elements was enlarged. This is confirm the expected properties of the collocation method. The second test showed that with increasing the number of collocation points the error decreased, but with 14 collocation points the error increased. When the number of collocation points was increased further, the error decreased again. This sudden increase is an indication that the polynomial approximation is not inherently better when the order of the polynomial is increased. The theorem of Runge 1901 denotes that interpolation with higher order polynomials does not guarantee an increase of accuracy. We conclude that it is better to use more finite elements with a small order of polynomial. This has another advantage which is explained in the next section. The approximation error for a given collocation scheme depends on the shape and the characteristics of the approximated component, temperature and pressure profiles and is therefor model dependent. We cannot conclude that for the SPYRO model a certain number of finite elements should be used but we can conclude, as mentioned above, that it is better to use more finite elements instead of using high order polynomials. The number of collocation points and finite elements is problem dependent.

Another feature of the collocation technique is the generation of the collocation points with the roots of an orthogonal polynomial. We investigated what polynomial gave the best result and conclude that we could not prove that a certain polynomial is the best. Although our opinion is that the Legendre polynomial generates the best collocation points we could not prove this.

The test model used to validate the collocation method is a DAE system. The index of a DAE system is a tool to check whether the solution of this model would pose any problems. It was found that the index might become more than 1 during integration. As yet no sound physical explanation has been found for this phenomena.

6.2 Mass balances

At first sight the choice of the mass balances seems rather trivial. When the mass balances is written in the most compact form, the resulting differential equations are a function of almost all the variables. We have seen that this affects the structure of the Jacobian because the continuity equations for the components have derivatives to all the components. When solving the steam cracker model with the collocation method, the resulting Jacobian is a finger print of the process. We gave a simple option to reduce the number of non-zeros in the Jacobian by defining one extra equation for the inverse of the volumetric flow rate. We expected that the computation time would decrease drastically with this small Jacobian but this is not the case. The reason for this is found in the algorithm of the solver. The Jacobian is transformed to a Lower and an Upper diagonal matrix via a LU-factorization. When the structure of the Jacobian is not correct the size of the LU-decomposition, increases drastically thus slowing the solver down. The proper Jacobian structure with the smallest computation time is problem dependent. What the proper Jacobian is, is defined by the mathematician also working on this project. The Jacobian is a block diagonal matrix where the blocks are created by the equations in a finite element. Generally we can say that these blocks should be as small as possible and/or consist of lines parallel to the diagonal. These blocks may not contain horizontal and vertical lines, if such lines exist they should be on the right and below the blocks.

There are two scenarios possible for the Jacobian structure. The first is to define smart equations that alter the Jacobian in such a way that the fill-in of the LU-decomposition is moderate. The second is the worst case scenario, when this is the case the equations cannot be changed to obtain the desired Jacobian structure. We have to exploit the properties of the collocation method used. The size of the LU-factorization depends on the thickness of the finite elements, that is, how many variables are defined per finite element. The number of variables per finite element is minimal when three collocation points per finite element is used. It is obvious that the number of elements has to be increased to obtain the desired accuracy as mentioned above.

6.3 Solving the collocation model

The mathematician is responsible to get the open SPYRO model solved. The reason why we created large 'steam cracker' models is to test the non-linear solver. We expect the SPYRO problem to be difficult due to the different equations. When the profiles generated with SPYRO are investigated, a variety of slopes are observed and we expect that the difficulty of SPYRO is created by the difference in slopes of the profiles. The created large models have the feature that the slope of the curves can be altered. So therefor we expect to make the conclusion when the large models are solved by the created solver, it can also solve the open SPYRO model. Path ways to provide a solution to difficult problems is given by the continuation method. This method enables the engineer to use a physical insight in obtaining the solution. We solved the large model with a slope that varies from 1 to 10,000 with a physical homotopy method. This method considers the steam cracker an isothermal and an isobaric system and during the solution the momentum and heat balances are added to the model.

When the large models with a difference in slope of $\pm 10,000$ are solved, the placement of the finite elements is becoming important. In the region were the slopes are very steep a lot of elements are needed to obtain an accurate solution. We conclude that the slope of the curves is not a problem for a solver that uses the physical continuation method. This report proposes a possible method to solve very difficult problems with a physical insight.

The continuation method can also be used to pre-solve the collocation models. The used initialization technique described in this report improves an arbitrary initial estimation of the solution. The continuation method does not use a physical insight to improve the initial estimation. A pre-solver must fulfill the demand that the total computation time does not increase. When using the physical continuation technique a lot of time is needed for the start-up of the method. A mathematical continuation method is therefor used to pre-solve the collocation models. We conclude that this method makes it possible to reduce the computation time. For the test model used to validate the collocation technique a reduction of 2 Jacobian and linear solver calls is observed on a total of 9 calls. This initialization technique can be used in the open SPYRO model when a user is not able to supply good initial estimates for the problem.

The general conclusion based on the three sections above is that the open SPYRO model can be created with the collocation technique. We must conclude that the collocation method should be tested on the SPYRO model itself to make a definite conclusion on the feasibility of open SPYRO with the collocation technique. The next two sections will give some recommendations concerning the momentum and energy balances.

6.4 Momentum Balance

The momentum balance contains different terms: pressure, kinetic, friction and a gravity term. We showed that the it is not justified to neglect the kinetic contribution to the momentum balance when modeling a steam cracker. In contradiction with the kinetic term, the forces of gravity can be safely neglected in the momentum balance.

Froment 79 denotes a momentum balance that also accounts for the pressure drop by the bends. We concluded that this equation is not correct, the term for the friction due to the bend should be divided by 2 and is only applicable in the bends.

A cracking coil consists of straight tubes connected to each other with bends. It is natural to consider two different momentum balances, one for the straight part of the tube and one for the bends in the tube. When using the collocation method to solve cracker models, it is no problem to do this, one bend is considered as one finite element. This ease of implementation is also the major drawback, because of the extra finite elements the size of the problem (used test model) increases at least 2 times. For a small model like the examined ethane cracker (11 equations) this is no problem but for a large model like SPYRO (125 equations) this is a problem when computation time is important. We developed a friction term for the bends in a coil that spreads the friction of the bends over the whole tube length. The major advantage of this calculation procedure of the friction is that the momentum balance is independent of the geometry of the cracking coil. In most practical applications the results at the end of the cracking coil are important. We compared the results of the model with two momentum balances and the model with one momentum balance. The results obtained with the two approaches for the friction of the bends are within one per cent the same. This justifies the use of the geometry independent momentum balance, especially for a large model such as SPYRO.

Froment 79 states a differential macroscopic momentum balance, this report gives the derivation of this macroscopic balance. The macroscopic momentum balance cannot be used because the resulting cracker model cannot be initialized. Froment 79 solved this problem by eliminating the velocity out of the momentum balance. The resulting expression for the pressure profile, is a function of all the derivatives of the molar flow rate and the derivative of the temperature. We showed that this elimination is not necessary and concluded that the alternative solution is more elegant.

Form the investigation of the index it also follows that a start-up problem of the numerical integration exists. The theory of the determination of the index does not only provide ways to investigate the solvability of a model but is also provides tools to check whether the problem can be initialized.

6.5 Energy Balance

Just as for the momentum balance, we derived the macroscopic energy balance. We conclude that the potential energy contribution can be safely neglected. The energy balance given by Froment 79 is a very simplified extraction of the derived macroscopic energy balance. Therefor we recommend not to use this balance because the collocation method enables the use of a more advanced energy balance.

Two possible methods can be used to account for the heat of the reaction. The first is to calculate the heat of every reaction separately and calculate the total produced heat of reaction with these heats and the net rates of the reactions. The second method is to use the heat of formation in the gaseous phase as a reference in contradiction with the first method where this reference enthalpy at the reference temperature is zero. In a small model like the test model, it makes no significant difference if the heats of the reactions are calculated or the enthalpy is calculated differently. When dealing with the SPYRO model with over 3000 reactions and 125 components, it makes a lot of difference if all the heats of reactions are calculated or the enthalpy is calculated differently. Therefor we recommend the second approach to account for the chemical contribution to the energy balance.

We showed that the potential energy contribution can be safely neglected. The velocity forces cannot be neglected at the momentum balance. This suggests that the kinetic contribution to the energy balance should also not be neglected. We showed that the energy contribution does not have such an impact on the results as the velocity forces on the momentum balance (maximal 5% for energy balance and 23 % for momentum balance). Simulation results indicated that the energy balance with kinetic energy gave results closer to plant data. Therefor we recommend the energy balance with a kinetic contribution.

7 References

Akker, H.E.A. v. d., Mudde, R.F., Fysische Transport Verschijnselen I, Delftse Universitaire Pers, 1996, ISBN 90-407-1204-2 cip

Allgower, E. L. and Georg, K., Numerical Continuation Methods, An Introduction, *Springer* - *Verlag Berlin Heidelberg New York*, 1990,

Bird, R.B., Stewart, W.E. and Lightfoot, E.N., Transport Phenomena, John Wiley & Sons, Inc. 1960.

Boor, Carl de, A Practical Guide to Splines, Applied Mathematical Sciences 27, Springer-Verlag, 1978.

Boor, C.de, Good Approximation by Splines with Variable Knots II, Dundee Conf. on Numerical Solutions of Differential Equations, Lecture Notes in Mathematics No 363, p. 12-19, *Springer-Verlag*, New York, 1978.

Brenan, K.E., Campbell, S.L. and Petzold L.R., Numerical Solutions of Initial-Value Problems in Differential-Algebraic Equations, SIAM, 1996.

Corvalán, C.M. and Saita, F.A., Automatic Step-size Control in Continuation Procedures, Comp. Chem. Engng, 15(10), 1991, pp. 729-739.

Davidenko, D.F., On a New Method of Numerical Solution of Systems of Nonlinear Equations., Dokl. Akad. Nauk SSSR, 88, 1953, pp.601.

Den Heijer, C. and Rheinboldt, W.C., On Steplength Algorithms for a Class of Continuation Methods, SIAM J. Anal., 18(5), 1981, pp. 925-948.

Finlayson, Bruce A., Non-Linear Analysis in Chemical Engineering, McGraw-Hill Inc., 1980, ISBN 0-07-020915-4

Finlayson, Bruce A., The Method of Weighted Residuals and Variational Principles, *Academic Press, Inc.*, 1972.

Franz, R.W. and Van Brunt, V. A Differential Homotopy Continuation Method For Interlinked Solvent Extraction Cascades., *Separat. Sci. Technol.*, 22(2/3), 1987, pp. 243-267.

Froment G.F. and Bischoff, K.B., Chemical Reactor Analysis and Design, John Wiley & Sons, Inc., 1979, ISBN 0-471-02447-3.

Garcia, C.B. and Zangwill, W.I., Pathways to Solutions, Fixed Points, and Equilibria, *Prentice-Hall*, Englewood, NJ, 1981.

Klopfenstein, R.W., Zeros of Nonlinear Functions, J. Ass. Comput. Mach., 8, 1961, pp. 366.

Koster, L.G., Gazi, E. and Seider, W.D. Finite Elements for Near-Singular Systems: Application to Bacterial Chemotaxis, *Computers Chem. Engng.*, 1993, 17 (5/6), pp. 485-503.

Kovach III, J.W. and Seider, W.D., Heterogeneous Azeotropic Distillation-Homotopy-Continuation Methods, *Comput. Chem. Engng*, 11(6), 1987, pp.593-605.

Nekrasov, B. Hydraulics For Aeronautical Engineers, MIR Publishers, Moscow, 1969

Ortega, J.M. and Rheinboldt W.C., Iterative Solution of Nonlinear Equations in Several Variables, *Academic Press*, New York, 1970.

Paloschi, J.R. Bounded Homotopies to Solve Systems of Algebraic Nonlinear Equations, *Comp. Chem. Engng.*, 19(12), **1995**, pp. 1243-1254.

Paloschi, J.R. Bounded Homotopies to Solve Systems of Sparse Algebraic Nonlinear Equations, Comp. Chem. Engng., 21(5), 1997, pp. 1531-541.

Reid, R.C., Prausnitz, J.M. and Poling, B.E. The Properties of Gases and Liquids, Fourth Edition, McGraw-Hill, Inc., 1987, ISBN 0-07-051799-1

Rheinboldt, W.C. and Burkardt, J.V. A Locally Parameterized Continuation Process, ACM Trans. Math. Software, 9(2), 1983, pp. 215-235.

Rheinboldt, W.C., Solution Fields of Nonlinear Equations and Continuation Methods, SIAM J. Numer. Analysis, 17(2), 1980, pp. 221-237.

Rice, Richard G., Do, Duong D. Applied Mathematics and Modeling for Chemical Engineers, *John Wiley & Sons, Inc.*, **1995**, ISBN 0-471-30377-1

Salgovic, A., Hlavacek, V. and Ilavasky, J. Global Simulation of Counter current Separation processes via One-Parameter Imbedding Techniques, *Chem Engng Sci.*, 36, **1981**, pp. 1599.

Seader, J.D., Kuno, M., Lin, W.J., et al., Mapped Continuation Methods for Computing All Solutions to General Systems of Nonlinear Equations., *Comp. Chem. Engng.*, 14(1), 1990, pp.71-85.

Seferlis, P. and Hrymak, A.N., Sensitivity Analysis for Chemical Process Optimization, *Comp. Chem. Engng.*, 20(10), **1996**, pp. 1177-1200.

Seferlis, P., Collocation models for destillation units and sensitivity analysis studies in proces optimization, thesis McMaster University, Hamilton, Ontario, April 1995

Seider, W.D. and Brengel, D.D., Nonlinear Analysis in Process Design, AICHE J., Journal Review, 37(1), 1991, pp.1-38.

Smith, J.B., Van Ness, H.C., Introduction to Chemical Engineering Thermodynamics, McGraw-Hill International Editions, Fourth Edition, 1987.

Sun, A.C. and Seider, W.D. Homotopy Continuation Algorithm for Global Optimization, in *Recent Advances in Optimization*, Floudas, C.A. and Pardalos, P.M., Princeton University Press, 1991, pp. 561-592.

Sundaram, K.M. and Froment, G.F. Modeling of Thermal Cracking Kinetics_I, Thermal Cracking of Ethane, Propane and Their Mixtures, *Chem. Eng. Science*, 1977, 32, p. 601-8

Vickery, D.J. and Taylor, R., Path-Following Approaches to the Solution of Multicomponent, Multistage Separation Process Problems, *AICHE J.*, 32(4), 1986, pp.547-556.

Villadsen, John; Michelsen, Michael L. Solution of Differential Equation Models by Polynomial Approximation, *Printice-Hall, Inc.*, **1978**, ISBN 0-13-822205-3.

Wayburn, T.L. and Seader, J.D., Homotopy Continuation Methods for Computer-Aided Process Design, *Comput. Chem. Engng.*. 11(1), 1987, pp. 7-25.

Wayburn, T.L. and Seader, J.D., Solution of Systems of Interlinked Distillation Columns by Differential Homotopy-Continuation Methods, *Proc. Conf. On Found. Computer-Aided Process Design*, ed., Westerberg, A.W. and Chien, H.H., Cache, 1984, pp. 765

8 Nomenclature

$A_{ m coil}$	Cross-sectional area	$[m^2]$
Cp	Specific heat	[J·mole ⁻¹ ·K ⁻¹]
d	Internal tube diameter	[m]
ΔH	Heat of reaction	[J·mole ⁻¹]
ΔH_{r}	Total heat of reaction	[J·mole ⁻¹]
$\Delta H_{ m f}$	Heat of formation	$[J \cdot m^{-3} \cdot s^{-1}]$
E .	Activation energy	[J·mole ⁻¹]
f	Friction factor due to the friction of the tube wall	[-]
F	Molar flow rate	[mole·s ⁻¹]
$f_{ m bend}$	Friction factor due to the friction of the bends	[-]
g	Acceleration of gravity	[m·s ⁻²]
$\overset{\circ}{G}$	Superficial mass flow velocity	$[kg \cdot m^2 \cdot s^{-1}]$
H	Enthalpy	[1]
\hat{H}	enthalpy of ideal gas	[J·mole ⁻¹]
Нх	enthalpy plus kinetic energy	[W]
K	Kinetic energy	in [*]
ko	Frequency factor	$[s^{-1} \text{ or } m^3 \cdot \text{mole}^{-1} \cdot s^{-1}]$
L	Length of coil	[m]
M	molecular weight	[kg·mole ⁻¹]
$M_{ m m}$	Mean molecular weight	[kg·mole ⁻¹]
P	Momentum	$[kg \cdot m \cdot s^{-1}]$
P	Pressure	[Pa]
Pc	Critical pressure	[Pa]
Px	dynamic momentum flow	[kg·m·s ⁻²]
$Q_{ m wall}$	heat flux through tube wall	$[J \cdot m^2 \cdot s^{-1}]$
\boldsymbol{R}	Gas constant	[J·mole-1·K-1]
r	rate of reaction per unit volume	[mole·m ³ ·s ⁻¹]
$r_{\rm b}$	Radius of bend of coil	[m]
S	circumference $(2\pi R)$	[m]
T	Temperature	[K]
t	time or homotopy parameter	[s] or [-]
Tc	Critical temperature	[K]
$oldsymbol{U}$	Internal energy	[J]
u	linear velocity	$[\mathbf{m} \cdot \mathbf{s}^{-1}]$
V	Volume	$[m^3]$
W	Mechanical work out	[W]
Z	Position in the reactor (length)	[m]
Zc	Critical compressibility factor	[-]

Greek Symbols

α	Stoichiometric coefficient	[-]
μ	Dynamic viscosity	[Pa·s ⁻¹]
ρ	density of the fluid	[kg·m3]
Φ_m	mass flow	$[kg \cdot s^{-1}]$
θ	Angle in cylindrical coordinates	[radians]
Φ	Potential energy	[7]
τ	viscous stress tensor	[Pa]

Subscript

f	fluid
i	i-th reaction
j	with respect to j-th component
w	wall

Brackets

 $\langle a \rangle$ average value of (a) over a flow cross section

Overlines

- time-smoothed
- ^ per unit of mass

APPENDICES

APPENDIX 1: Data of Froment Ethane cracker model.

The coil length (*L*) in the radiation section is 95 m. The length of the straight portions of the coil is 8.85 m, the length of the bends is 0.55 m. The radius of the latter (r_b) is 0.178 m. The internal diameter (*d*) of the tube is 0.108m. The ethane feed is 68.68 kg·m⁻²·s⁻¹. The ethane is 98.2 mole percent pure, the impurities being C_2H_4 (1 mole percent) and C_3H_6 (0.8 mole percent). The steam dilution amounts to 0.4 kg of steam per kilogram of ethane (=100 mole percent). The inlet pressure is 2.93 bar, the inlet temperature is 680°C. The following heat flux profile is used according to Froment 79 to simulate the firebox. First tube: 96 kJ·m⁻²·s⁻¹; second tube: 84; third tube: 80; fourth tube: 71; fifth tube 63; sixth, seventh, eight, ninth, and tenth tubes, 59. The length of the tubes over which the heat flux are defined, are: first tube 9.9 m; second to the ninth tube: 9.4 m; tenth tube 9.9 m.

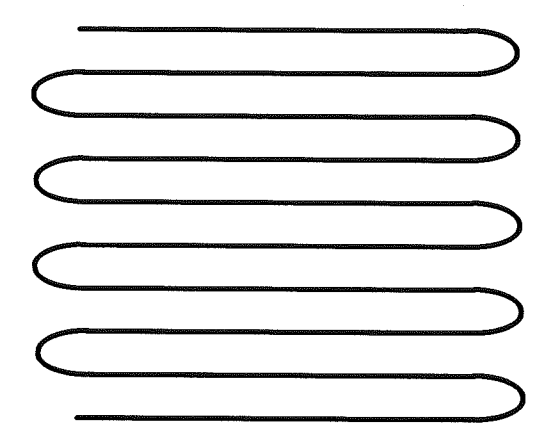


Figure 1: Schematically layout of the coil in the ethane cracker

The kinetic model used to model an ethane cracker is developed by Sundaram and Froment 1977. The scheme, together with the kinetic parameters, is given in Table 1.

<i>i</i> -th	Reaction	Order	$ko_{\rm i} [{\rm s}^{-1}] {\rm or} [{\rm m}^3 \cdot {\rm mol}^{-1} \cdot {\rm s}^{-1}]$	$E_{\rm i}$
				[J·mol ⁻¹]
1.	$\mathrm{C_2H_6} \rightarrow \mathrm{C_2H_4} + \mathrm{H_2}$	1	$4.65 \cdot 10^{13}$	273,020.0
2.	$C_2H_4 + H_2 \rightarrow C_2H_6$	2	$8.75 \cdot 10^{5}$	136,870.0
3.	$2C_2H_6 \rightarrow C_3H_8 + CH_4$	1	$3.85 \cdot 10^{11}$	273,190.0
4.	$C_3H_6 \rightarrow C_2H_2 + CH_4$	1	$9.81 \cdot 10^{8}$	154,580.0
5.	$C_2H_2 + CH_4 \rightarrow C_3H_6$	2	5.87·10 ¹	29,480.0
6.	$C_2H_2 + C_2H_4 \rightarrow C_4H_6$	2	1.03·10°	172,750.0
7.	$C_2H_4 + C_2H_6 \rightarrow C_3H_6 + CH_4$	2	$7.08 \cdot 10^{10}$	253,010.0

Table 1: Reaction scheme and kinetic parameters for thermal cracking of ethane (Froment 1979)

The viscosity [Pa·s] of the individual components is given by:

$$\mu_j = \frac{\sqrt{M_j} P c_j^{2/3}}{T c_j^{1/6} 1.0134^{2/3}} \left(1.9 \frac{T}{T c_j} - 0.29 \right) 10^{-7} Z c_j^{-2/3}$$
 for $: j = 1$ to 9

For the calculation of the dynamic viscosity the following critical data (Table 2) are required. This data is taken from Reid 1987. Besides the critical data of the nine components, the molecular mass and normal boiling point is given.

	CH₄	C_2H_2	C_2H_4	C_2H_6	C_3H_6	C_3H_8	C_4H_6	H_2	H ₂ O
Tc [K]	190.4	308.3	282.4	305.4	364.9	369.8	425.0	33.0	647.3
Pc [bar]	46.0	61.4	50.4	48.8	46.0	42.5	43.3	12.9	221.2
Zc [-]	0.288	0.270	0.280	0.285	0.274	0.281	0.270	0.303	0.235
Tb [K] at 1 atm	111.6	188.4	169.3	184.6	225.5	231.1	268.7	20.3	373.2
M [·10 ⁻³ kg·mol ⁻¹]	16.043	26.038	28.054	30.070	42.081	44.094	54.092	2.016	18.015

Table 2: Table of data needed to calculate the viscosity (Reid 1987).

The constants to calculate the isobaric heat capacity [J·mol⁻¹·K⁻¹] of the ideal gases are given below (Table 3), from (Reid 1987).

Component	A	В	C	D
CH ₄	19.250	5.213.10-2	1.197·10 ⁻⁵	-1.132·10 ⁻⁸
C_2H_2	26.820	$7.578 \cdot 10^{-2}$	-5.007·10 ⁻⁵	$1.412 \cdot 10^{-8}$
$\mathrm{C_2H_4}$	3.806	$1.566 \cdot 10^{-1}$	$-8.348 \cdot 10^{-5}$	$1.755 \cdot 10^{-8}$
C_2H_6	5.409	$1.781 \cdot 10^{-1}$	-6.938·10 ⁻⁵	8.713·10 ⁻⁹
C_3H_6	3.710	$2.345 \cdot 10^{-1}$	-1.160·10 ⁻⁴	$2.205 \cdot 10^{-8}$
C_3H_8	-4.224	$3.063 \cdot 10^{-1}$	-1.586·10 ⁻⁴	$3.215 \cdot 10^{-8}$
C_4H_6	-1.687	$3.419 \cdot 10^{-1}$	$-2.340 \cdot 10^{-4}$	$6.335 \cdot 10^{-8}$
$\mathrm{H_2}$	27.140	$9.274 \cdot 10^{-3}$	-1.381·10 ⁻⁵	7.645·10 ⁻⁹
$_{\rm LO}$	32.240	$1.924 \cdot 10^{-3}$	$1.055 \cdot 10^{-5}$	-3.569·10 ⁻⁹

Table 3: The constants for the isobaric heat capacity (Reid 1987).

The enthalpy of formation for the ideal gases at 298.2 Kelvin are shown below (Table 4), from (Reid 1987).

	CH₄	C_2H_2	C_2H_4	C_2H_6	C ₃ H ₆	C_3H_8	C ₄ H ₆	H_2	$\overline{\mathrm{H_{2}O}}$
$\Delta \mathrm{H_f}^{\circ}$	-7.490·10 ⁴	2.269·10 ⁵	5.234·10 ⁴	-8.474·10 ⁴	2.043·10 ⁴	-1.039·10 ⁵	1.102·10 ⁵	0	-2.420·10 ⁵

Table 4: Standard enthalpy of formation for the ideal gases at 298.2 K in [J·mol⁻¹] (Reid 1987).

APPENDIX 2: Discussion over Momentum Equation used by Froment

The aim of this appendix is to establish the difference in opinion between Froment and the author over the momentum equation in the simulation of an ethane cracker. The difference in opinion concerns the way in which the additional pressure drop due to the bends is accounted for in the momentum equation.

The equation used by Froment

The momentum equation with is used by Froment and Bischoff 79 is:

$$\frac{dP}{dz} = \frac{\frac{d}{dz} \left(\frac{1}{M_M}\right) + \frac{1}{M_M} \left[\frac{1}{T} \frac{dT}{dz} + \left(\frac{2f}{d} + \frac{f_{bend}}{\pi r_b}\right)\right]}{\frac{1}{M_M P} - \frac{P}{G^2 RT}}$$
(A-1)

$$\frac{d}{dz} \left(\frac{1}{M_M} \right) = \frac{\sum_{j=1}^{9} \frac{dF_j}{dz}}{GA_{coil}}$$
(A-2)

The original equation of equation (A-1) is given below. This equation will be used later in the discussion were the equations of the author is compared with this (A-3) one.

$$-\frac{dP}{dz} = \left[2\frac{f}{d} + \frac{f_{bend}}{\pi r_b}\right] \rho u^2 + \rho u \frac{du}{dz}$$
 (A-3)

The friction factor for straight tubes is given by

$$f = 0.046 \,\mathrm{Re^{-0.2}}$$
 when $\mathrm{Re} = \frac{dG}{\mu}$ (A-4)

The equation from the author

In Froment 79 (pp.396) the following equation to model the pressure drop is used. The fanning equation is used in the 'usual Bernoulli' equation.

$$-\frac{dp}{dz} = 2\frac{f}{d}\rho u^2 + \rho u \frac{du}{dz} \tag{A-5}$$

Expression (A-5) above can be derived from the well-known Bernoulli equation. That is given by:

$$-\Delta P = \frac{1}{2}\rho\Delta u^2 + g\rho\Delta h \tag{A-6}$$

The term on the left-hand side is the difference in pressure between level 2 and 1. The first term on the right-hand side gives the difference in kinetic energy between level 2 and 1. The second term on the right-hand side gives the difference in static pressure (Akker 96, Bird 60).

The assumptions for Bernoulli are:

- The fluid is incompressible
- Rotation free $\frac{dv_x}{dy} \frac{dv_y}{dx} = 0$ or in 3 dimensions $\nabla x = 0$. The fluid moves between two stream lines.
- Steady state
- The viscosity is zero; no friction

If the difference in height is assumed zero (no influence of the static pressure) and the Bernoulli equation (A-6) is corrected for friction due to the tube wall with the Fanning equation, we get:

$$-\Delta P = \frac{1}{2}\rho\Delta u^2 + 4f\frac{L}{d}\frac{1}{2}\rho u^2 \tag{A-7}$$

The second term on the right-hand side contains velocity u. This velocity (u) is the (u) on the place down stream (Akker 96). If the equation above is divided by Δz (which is the length of the tube (L)) and the limit of Δz goes to zero, equation (A-5) is obtained. Equation (A-7) can be expanded to account for the friction due to the bends in the tube. This is done as follows (Akker 96, Nekrasov 69, Bird 60) (Nekrasov is the source of Froment):

$$-\Delta P = \frac{1}{2}\rho\Delta u^2 + \left(4f\frac{L}{d} + f_{bend}\right)\frac{1}{2}\rho u^2 \tag{A-8}$$

If the equation above is divided by Δz and the limit of Δz goes to zero the following equation (A-9) is obtained. This expression spreads the friction due to the bend over the whole length of the tube.

$$-\frac{dP}{dz} = \left[2\frac{f}{d} + \frac{f_{bend}}{2L}\right]\rho u^2 + \rho u \frac{du}{dz}$$
 (A-9)

For nine bends f_{bend} (A-9) has to be multiplied by 9.

The difference between formula (A-9) and (A-3) is the way how, the friction of the bend(s) is accounted for. The difference in opinion between the author and Froment is discussed through the use of the Bernoulli equation. The reason for this is that the concept of friction factor holds for macroscopic balances. The equation stated by formula (A-5) is a simplified mechanical energy balance. It is of possible better to use equation (A-9) only in the bends, this results in

$$-\frac{dP}{dz} = \left[2\frac{f}{d} + \frac{f_{bend}}{2\pi r_b}\right] \rho u^2 + \rho u \frac{du}{dz}$$
 (A-10)

This formula is almost the same as the expression (A-3) used by Froment, the difference is a factor 2⁻¹. For the straight part the next equations should be used:

$$-\frac{dP}{dz} = \left[2\frac{f}{d}\right]\rho u^2 + \rho u \frac{du}{dz} \tag{A-11}$$

APPENDIX 3: Differentiation of Lagrange Interpolation Polynomial

The Lagrange interpolation polynomial is a continuous function and therefore can be differentiated. The Lagrange polynomial is not differentiated as easily as x^{j-1} . Taking the first and second derivatives of the Lagrange interpolation polynomial, we obtain

$$\frac{dy_{N+1}(x)}{dx} = \sum_{j=1}^{N+2} y_j \cdot \frac{dl_j(x)}{dx}$$
(A-1)

$$\frac{d^2 y_{N+1}(x)}{dx^2} = \sum_{j=1}^{N+2} y_j \cdot \frac{d^2 l_j(x)}{dx^2}$$
 (A-2)

In most practical problems, only the first two derivatives are required, so these are presented here. However, if higher derivatives are needed, the Lagrange interpolation polynomial can be differentiated further.

In particular, if we are interested in obtaining the derivative at the interpolation points, we have

$$\frac{dy_{N+1}(x_i)}{dx} = \sum_{j=1}^{N+2} \frac{dl_j(x_i)}{dx} \cdot y_j$$
(A-3)

for i = 1, 2, ..., N+1, N+2

Similarly, the second derivative is obtained as

$$\frac{d^2 y_{N+1}(x_i)}{dx^2} = \sum_{i=1}^{N+2} \frac{d^2 l_j(x_i)}{dx^2} \cdot y_j$$
 (A-4)

for i = 1, 2, ..., N+1, N+2

The summation format in the right hand side of equations (A-3) and (A-4) suggests the use of a vector representation for compactness, as we will show next.

We define the first derivative vector, composed of (N+2) first derivatives at the (N+2) interpolation (collocation) points, as

$$\mathbf{y'}_{N+1} = \left[\frac{dy_{N+1}(x_1)}{dx}, \frac{dy_{N+1}(x_2)}{dx}, \dots, \frac{dy_{N+1}(x_{N+1})}{dx} \frac{dy_{N+1}(x_{N+2})}{dx} \right]^T$$
(A-5)

Similarly, the second derivative vector is defined as

$$\mathbf{y''}_{N+1} = \left[\frac{d^2 y_{N+1}(x_1)}{dx^2}, \frac{d^2 y_{N+1}(x_2)}{dx^2}, \dots, \frac{d^2 y_{N+1}(x_{N+1})}{dx^2} \frac{d^2 y_{N+1}(x_{N+2})}{dx^2} \right]^T$$
(A-6)

The function vector is defined as values of y at N + 2 collocation points as

$$\mathbf{y} = [y_1, y_2, y_3, ..., y_{N+1}, y_{N+2}]^T$$
(A-7)

With these definitions of vector y and the derivative vectors, the first and second derivative vectors can be written in terms of the function vector y using matrix notation

$$\mathbf{y'} = \mathbf{A} \cdot \mathbf{y} \tag{A-8}$$

$$\mathbf{y}^{\prime\prime} = \mathbf{B} \cdot \mathbf{y} \tag{A-9}$$

where the matrices A and B are defined as

$$\mathbf{A} = \left\{ a_{ij} = \frac{dl_j(x_i)}{dx}; \qquad i, j = 1, 2, ..., N + 1, N + 2 \right\}$$
 (A-10)

$$\mathbf{B} = \left\{ b_{ij} = \frac{d^2 l_j(x_i)}{dx^2}; \qquad i, j = 1, 2, ..., N+1, N+2 \right\}$$
(A-11)

The matrices **A** and **B** are (N+2, N+2) square matrices. Once the N+2 collocation (interpolation) points are chosen, then the Lagrangian building blocks $l_j(x)$ are completely known, and thus the matrices **A** and **B** are also known. For computational purposes, a_{ij} and b_{ij} are calculated from [Rice 95]

$$a_{ij} = \frac{dl_{j}(x_{i})}{dx} = \begin{cases} \frac{1}{2} \frac{p_{N+2}^{(2)}(x_{i})}{p_{N+2}^{(1)}(x_{i})} & j = i\\ \frac{1}{(x_{i} - x_{j})} \frac{p_{N+2}^{(1)}(x_{i})}{p_{N+2}^{(1)}(x_{j})} & i \neq j \end{cases}$$
(A-12)

and

$$b_{ij} = \frac{d^{2}l_{j}(x_{i})}{dx^{2}} = \begin{cases} \frac{1}{3} \frac{p_{N+2}^{(3)}(x_{i})}{p_{N+2}^{(1)}(x_{i})} & j = i\\ 2a_{ij} \left[a_{ii} - \frac{1}{(x_{i} - x_{j})} \right] & i \neq j \end{cases}$$
(A-13)

where $p_{N+2}^{(1)}$, $p_{N+2}^{(2)}$ and $p_{N+2}^{(3)}$ are calculated from the following recurrence formula $p_0(x) = 1$

$$p_{j}(x) = (x - x_{j})p_{j-1}(x); \quad j = 1, 2, ..., N + 2$$

$$p_{j}^{(1)}(x) = (x - x_{j})p_{j-1}^{(1)}(x) + p_{j-1}(x)$$

$$p_{j}^{(2)}(x) = (x - x_{j})p_{j-1}^{(2)}(x) + 2p_{j-1}^{(1)}(x)$$

$$p_{j}^{(3)}(x) = (x - x_{j})p_{j-1}^{(3)}(x) + 3p_{j-1}^{(2)}(x)$$
(A-14)

with

$$p_0^{(1)}(x) = p_0^{(2)}(x) = p_0^{(3)}(x) = 0 (A-15)$$

APPENDIX 4: Adaptive Collocation on Finite Elements

In this appendix a method is described to achieve a more accurate placement of the elements. Generally, the approximation error for a given collocation scheme of a reactor depends on the shape and the characteristics of the approximated composition, temperature and pressure profiles. However, the features of the state profiles of the solution are unknown a priori and therefore it can be difficult to select the elements sizes. An estimate of the approximation error, that will be updated as the optimal solution is approached, may give a measure of the local 'goodness' of the approximation.

The choice of equally spaced finite elements does not necessarily result in an optimal element placement. For steep profiles of the state variables, a large number of collocation points is required for an accurate representation of the actual solution. On the other hand, a few collocation points would be sufficient to match the solution when changes with small slope occur. A criterion for the adaptive element breakpoint placement may be the distribution of the approximation error equally throughout the reactor. An element partition methodology based on error equidistribution, with a given number of elements per reactor and a given number of collocation points per element, will attempt to place small elements in those regions where steep changes in the state variables occur and larger elements in those regions where relatively small changes occur.

According to the methodology of de Boor 78 the breakpoints are located such that a local error term associated with each element is made constant. The function y which satisfies an first order differential equation, is approximated by piecewise polynomials of order N+1 (degree < N+1) with breakpoint sequence:

$$a = W_1 < W_1 < \dots < W_{NE+1} = b$$
 (A-1)

The breakpoints W correspond to the boundaries of the finite elements.

If y is sufficiently smooth then the local approximation error satisfies the following inequality Seferlis 95:

$$\|y - \hat{y}\|_{W_s, W_{s+1}} \le C\Delta W_s^{N+1} \|y^{(N+1)}\|_s + O(\Delta W^{N+2})$$
 with: $s = 1, 2, ..., NE$ (A-2)

where:

 $\|y - \hat{y}\|_{W_s, W_{s+1}}$ is the max-norm of the local approximation error term between the function y and the piecewise polynomial approximation \hat{y} . In the case of a reactor, the function y represents the composition, temperature and pressure profiles determined by for instance gPROMS or MATLAB or an analytic solution (if there is one). The \hat{y} represents the solution obtained by the OCFE model. The ΔW_s is the length of the s-th interval. $\|y^{(N+1)}\|_s$ is the max-norm of the

(N+1)-th derivative of the function y in the interval $[W_s, W_{s+1}]$. C is a constant that depends only upon N and the order of the differential equation for a given collocation scheme. The global error term is $O(W^{N+2})$ and for sufficiently small elements it can be neglected Seferlis 95.

The accuracy of the approximation can be improved by reducing the size of those elements where the (N+1)-th derivative of y is large, for a given number of collocation points within each element, or by adding more collocation points. In the development of the adaptive OCFE models, the number of collocation points per element is kept constant. The inequality given by equation (A-2) suggests for sufficiently small elements (global error can be neglected), that the breakpoints W_2, \ldots, W_{NE} be placed so as to:

$$\min_{W_r} \max_{s} \left(\Delta W_s \| y^{(N+1)} \|_{s}^{\frac{1}{(N+1)}} \right) \quad r = 2, ..., NE \qquad s = 1, 2, ..., NE$$
 (A-3)

The expression given by formula (A-3) states that per element the maximum of the product of the (N+1)-th derivative times the length of an element should be minimized to obtain the optimum W_r . The elements W_1 and W_{NE+1} are respectively 0 and the total length of the element Γ (see theory 2.1.2).

The problem given by equation (A-3) is difficult to solve since it contains non-differentiable functions (max-norm) and the function y which is only known approximately. The goal is not to locate each breakpoint to attain a global optimum, but rather to obtain a local optimal distribution of elements lengths for which the approximation error associated within each element is constant. The breakpoints are chosen so that:

$$\Delta W_s \| y^{(N+1)} \|_{s}^{\frac{1}{(N+1)}} = \text{constant} \quad \text{for } s = 1, 2, ..., NE$$
 (A-4)

The determination of the break point according to problem (A-3) and by the method given by equation (A-4) are asymptotically the same. This is shown by De Boor 78:

$$\int_{W}^{W_{s+1}} \left| y^{(N+1)}(x) \right|^{\frac{1}{(N+1)}} dx = \frac{1}{NE} \int_{a}^{b} \left| y^{(N+1)}(x) \right|^{\frac{1}{(N+1)}} dx \tag{A-5}$$

The collocation solution is used to approximate $y^{(N+1)}$ in the elements. However, the (N+1)-th derivative of the collocation solution is equal to zero. The reason for this is that the order of the approximating polynomial is (N+1) but the degree of the polynomial is at most N. Hence the piecewise constant N-th derivative of the collocation solution is used to estimate $y^{(N+1)}$, the estimation will be denoted with $\hat{y}^{(N+1)}$. The approximation of the (N+1)-th derivative $\hat{y}^{(N+1)}$, is done according to the Boor 78:

$$\hat{y}^{(N+1)}(x) = \frac{\frac{2|\Delta\Theta_{3/2}|}{W_3 - W_1}}{\frac{|\Delta\Theta_{s-1/2}|}{W_{s+1} - W_{s-1}} + \frac{|\Delta\Theta_{s+1/2}|}{W_{s+2} - W_s}} \quad \text{on } [W_1, W_2]$$

$$\frac{2|\Delta\Theta_{s-1/2}|}{W_{s+1} - W_{NE-1}} \quad \text{on } [W_s, W_{s+1}] \quad s = 2, \dots, NE-1$$

$$\frac{2|\Delta\Theta_{NE-1/2}|}{W_{NE+1} - W_{NE-1}} \quad \text{on } [W_{NE}, W_{NE+1}]$$

$$(A-6)$$

where $\Theta_{s+1/2} = \hat{y}^N(x)$ on $[W_s, W_{s+1}]$, and $\Delta\Theta_{s-1/2} = \Theta_{s+1/2} - \Theta_{s-1/2}$. A schematic of the approximation of the (N+1)-th derivative of the true solution is given in Figure A-1.

y ^(N+1) Derivative approximation

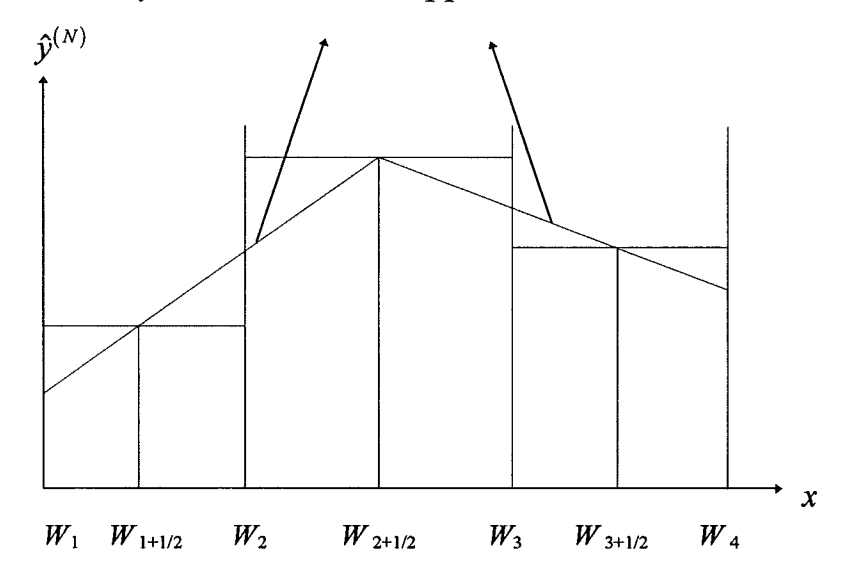


Figure A-1: Approximation of the (N+1)-th derivative of the state variable profile Seferlis 95.

In the case of a reactor or a distillation column, there are multiple state variable profiles to be approximated. The objective is to equidistribute the approximation error associated with all the variables. This is done by using equation (A-4). The value of $y^{(N+1)}$ is estimated from the N-th derivative of the approximation piecewise polynomial \hat{y} , given by equation (A-6). The approximation polynomial is the Lagrange interpolation polynomial. The N-th derivative of the Lagrange polynomial must be calculated. The Lagrange polynomial is equivalent to:

$$\hat{y}(x_i) = \sum_{i=1}^{N+1} d_j x_i^{j-1} = \mathbf{Q} \cdot \mathbf{d} \quad \text{for } i = 1, 2, ..., N+1$$
(A-7)

Where i stand for the i-th collocation point. The matrix \mathbf{Q} and vector \mathbf{d} are defined by expression (A-8).

$$Q_{ij} = x_i^{j-1}$$

$$\mathbf{d} = \mathbf{Q}^{-1} \cdot \hat{\mathbf{y}}$$
(A-8)

The parameter vector \mathbf{d} can be solved because the solution $\hat{\mathbf{y}}$ at the collocation points x_i within each element are known.

The N-th derivative in each element can then be calculated as follows:

$$\hat{y}^{(N)} = N! d_{N+1} \tag{A-9}$$

The norm in equation (A-4) is the max-norm. The 2-norm will be used to determine the total approximation error Seferlis 95. The max-norm is desirable, but non differentiable. However, the 2-norm is considered to be a good compromise. In this way some form of averaging is obtained. The element lengths are not related to one extreme (if there is one of course). Equation (A-4) transforms into:

$$\Delta W_s \left[\sum_{j=1}^{M} \left\{ \left(\hat{y}_{j,s}^{(N+1)} \right)^{\frac{1}{(N+1)}} \right\} \right]^{1/2} = \text{constant} \quad \text{for } s = 1, 2, ..., NE$$
 (A-10)

where M is the total number of state variables that are approximated. $\hat{y}_{j,s}^{(N+1)}$ is the (N+1)-th derivative, calculated with (A-6) of equation j in finite element s.

It is assumed that $|\hat{y}^{(N+1)}|$ behaves like $|y^{(N+1)}|$ Seferlis 95. The local error term is equidistributed among the finite elements in e.g. a reactor or distillation column. A continuous and monotonically increasing function G(x), that calculates the additive local error term as a function of the position in the reactor is constructed.

$$G(x) = \int_{a}^{x} (\hat{y}^{(N+1)}(x))^{\frac{1}{(N+1)}} dx$$
 (A-11)

The normalized cumulative error per finite element is defined through:

$$\Omega(W_s) = \frac{G(W_s)}{G(b)}$$
 for $i = 1, 2, ..., NE$ (A-12)

G(b) is the cumulative error of the whole domain over which collocation on finite elements is applied, s indicates which breakpoint is calculated.

The new locations of the breakpoints are determined by the following expression Koster 93:

$$\Omega(W_1^{new}) = 0$$

$$\Omega(W_{s+1}^{new}) = \frac{s}{NE} \qquad \text{for } s = 1, 2, ..., NE$$
(A-13)

The new elements W_s^{new} have to be determined by linear interpolation. This is schematically shown in figure A-2.

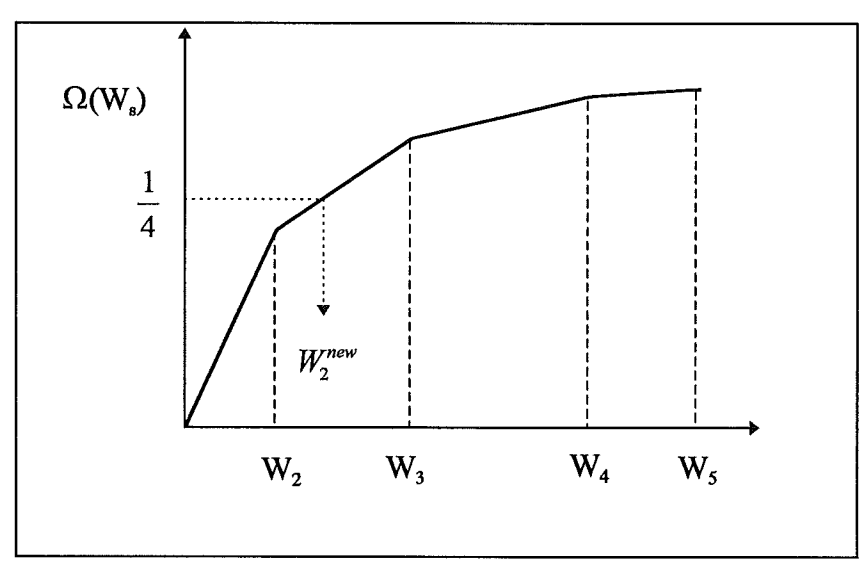


Figure A-2: Example of breakpoint placement

The algorithm that calculates the optimal placement of the breakpoints is utilized in an outer-loop of the solver, that determines the solution of a mathematical model e.g. a reactor or distillation column.

The algorithm consists of the following steps:

- i. Obtain a solution of the reactor model with equidistributed elements.
- ii. Estimate the error within each element using the obtained solution (eq. A-6)
- iii. Adjust the elements lengths so that the error is equiditributed (eq. A-11,12,13)
- iv. If the element lengths do not change more than a defined tolerance, stop. Otherwise continue.
- v. Solve the mathematical model with the new partition.
- vi. Go to step ii.

The method of adaptive orthogonal collocation on finite elements is tested on the problem stated by:

$$\frac{d^2y}{dx^2} - \phi^2 y = 0 \tag{A-14}$$

With the boundary conditions:

$$x = 0 \qquad \frac{dy}{dx} = 0$$

$$x = 1 \qquad y = 1$$
(A-15)

For this problem the exact solution is also known:

$$y(x) = \frac{\cosh(\phi x)}{\cosh(\phi)} \tag{A-16}$$

A steep curve is obtained when $\phi = 100$. In the table below some results are shown:

Table A-1: Results of testing the adaptive OCFE on problem (A-14) with $\phi = 100$.

	N=2				N=6				
NE	With opt	With optimization		No optimization		With optimization		No optimization	
	f	f _m	f	f_m	f	f_{m}	f	f_m	
3	0.0233	0.1382	0.0221	0.1528	0.0038	0.0202	0.0054	0.0420	
4	0.0133	0.0603	0.0192	0.1230	8.10.10-5	3.72.10-4	0.0038	0.0220	
5	0.0056	0.0139	0.0170	0.1003	7.57.10-6	3.48.10-5	0.0023	0.0118	
6	0.0025	0.0051	0.0150	0.0827	1.05.10-6	4.78.10-6	0.0014	0.0065	
7	0.0011	0.0020	0.0131	0.0688	2.29.10 ⁻⁷	1.04.10-6	7.94.10-4	0.0036	
10	1.62·10-4	2.99.10-4	0.0088	0.0419	5.49·10 ⁻⁹	2.46.10-8	1.69·10-4	7.60.10-4	

Where N is the number of interior collocation points within each element and NE is the number of elements. 'With optimization' means that the elements are placed such that the error within each element is the same. The difference between the analytic solution and the collocation solution at the collocation points is given by f. The difference between the collocation solution, in the middle of two collocation points, obtained with the Lagrange polynomial and the analytic solution is given by f_m .

$$f = \sqrt{\frac{\sum_{j}^{NE(N+1)+1} (y_{j}^{analytic} - \hat{y}_{j}^{col})^{2}}{NE(N+1)+1}}$$
(A-17)

$$f_{m} = \sqrt{\frac{\sum_{j=1}^{NE(N+1)} (y_{j}^{Analytic} - \hat{y}_{j}^{Lag})^{2}}{NE(N+1)}}$$
(A-18)

The total number of collocation points is NE(N+1)+1, the double values at the junctions are eliminated, there are NE(N+1) values between collocation points.

From the table above we conclude that the optimization of the elements lengths improves the collocation accuracy in the case of OCFE on the problem stated by (A-14), with ϕ =100. This improvement is for the calculation of the y-values at the collocation points as well as for the values calculated with the resulting Lagrange polynomials.

APPENDIX 5: Path Parameterization by Arclength

A problem with continuation technique may arise if the homotopy path doubles back on itself, in that case the homotopy equation does not have an unique solution for some values of t. These point were the path doubles back on itself are called turning points or (regular) limit points. At these turning points the Jacobian $\mathbf{H}_{\mathbf{x}}$ is singular, we can either perturb \mathbf{x} slightly so that $\mathbf{H}_{\mathbf{x}}$ is nonsingular or we try recasting the differential equations in another form. This recasting can be accomplished by assuming that both \mathbf{x} and t can be written as functions of the arclength, s, of the path (Klopfenstein 1961). If the homotopy equation is differentiated with respect to arclength, s, the following IVPs are obtained:

$$\mathbf{H}_{x} \cdot \frac{d\mathbf{x}}{ds} + \mathbf{h}_{t} \frac{dt}{ds} = 0 \tag{I-1}$$

This set (I-1) is made determinant by addition of the arclength of the tangent vector (Seider and Brengel 1991):

$$\frac{d\mathbf{x}^{T}}{ds} \cdot \frac{d\mathbf{x}}{ds} + \left(\frac{dt}{ds}\right)^{2} = 1$$
(I-2)

The initial conditions for the IVPs defined by (I-1) and (I-2) are:

$$\mathbf{x}(0) = \mathbf{x}_0$$

$$t(0) = 0$$
(I-3)

We define that $\frac{dt}{ds}$ and $\frac{dx}{ds}$ are denoted by respectively: t and \dot{x}

These IVPs can be solved conveniently by a simple Euler predictor and Newton correction in the hyperplane orthogonal to the Euler predictor. This is only possible when we are far from a turning point with respect to homotopy parameter, t. Near or at a turning point the \mathbf{H}_{x} matrix may become ill-conditioned or singular. We now discuss the means for dealing with this circumstance. We can derive the following equations by applying equations (I-1) and (I-2) (Wayburn and Seader 1984).

$$\left[\frac{\mathbf{H}_{x}}{\dot{\mathbf{x}}^{T}} \middle| \frac{\partial \mathbf{h}}{\dot{t}_{i}} \right] \cdot \left[\frac{I}{0^{T}} \middle| \dot{\dot{\mathbf{x}}} \right] = \left[\frac{\mathbf{H}_{x}}{\dot{\mathbf{x}}^{T}} \middle| \frac{\mathbf{H}_{x} \cdot \dot{\mathbf{x}} + \frac{\partial \mathbf{h}}{\partial t} \dot{t}}{\dot{\mathbf{x}}^{T} \cdot \dot{\mathbf{x}} + \dot{t}^{2}} \right] = \left[\frac{\mathbf{H}_{x}}{\dot{\mathbf{x}}^{T}} \middle| \frac{0}{1} \right]$$
(I-4)

The first matrix on the left hand side, call it χ , is nonsingular because $\left[\dot{\mathbf{x}}^T\middle|\dot{t}\right]$ is orthogonal to every

row of $\left[\mathbf{H}_{x} \middle| \frac{\partial \mathbf{h}}{\partial t}\right]$, which itself has rank n. This results in:

$$\det(\chi) \cdot \det\left(\frac{I}{0^T} \middle| \frac{\dot{\mathbf{x}}}{\dot{t}}\right) = \det\left(\frac{\mathbf{H}_x}{\dot{\mathbf{x}}^T} \middle| \frac{0}{1}\right) \tag{I-5}$$

or

$$i\det(\chi) = \det(\mathbf{H}_{x}) \tag{I-6}$$

This shows that \mathbf{H}_x is singular if and only if t = 0. A point where t = 0 is called a turning point with respect to t. Equation (I-5) shows that, at a point on the homotopy path far from a turning point with respect to t, \mathbf{H}_x should be far from singular, in which case the solution of the set (I-1) and (I-2) can be obtained as follows.

Set i = 1, this changes equation (I-1) and (I-2) in:

$$\left[\frac{\mathbf{H}_{x} \middle| \frac{\partial \mathbf{h}}{\partial t}}{\left(\mathbf{e}^{n+1}\right)^{T}}\right] \cdot \mathbf{v} = \begin{bmatrix} 0 \\ \vdots \\ 0 \\ 1 \end{bmatrix} = \mathbf{e}^{n+1} \tag{I-7}$$

Solve system (I-7) for \mathbf{v} , results in the solution to equation (I-1), the last equation of expression (I-7) can of course be eliminated. To obtain the solution which satisfies both (I-1) and (I-2) vector \mathbf{v} should be normalized, to give the unit tangent vector, \mathbf{u} , of the homotopy path:

$$\mathbf{u} = \frac{\mathbf{v}}{\|\mathbf{v}\|} \tag{I-8}$$

An step along the unit tangent vector is made to obtain an estimate of the vector \mathbf{x} at s_{i+1} . Alternatively, the Newton correction can be taken in the hyperplane orthogonal to the coordinate axis corresponding to a suitable local parameter, which is either t, itself, or, in case t is close to zero, some x_i such that x_i is not close to zero. The process of switching parameters on a local basis is referred to as reparameterization (Reinboldt 1983). This reparameterization is discussed in detail in the next paragraph. We continue the discussion here in analogy with the previous.

Even through \mathbf{H}_x is singular, we expect $[\mathbf{H}_x \mathbf{h}_t]$ to be of full rank, n, because of Sard's theorem and the parameterized Sard's theorem, for further information the reader is referred to appendix C of Wayburn and Seader 1987 and Garcia and Zangwill 1981. Identify t with x_{n+1} ($x_{n+1} = t$); let \mathbf{H}_{-i}^* be the $n \cdot (n+1)$ matrix, $[\mathbf{H}_x \mathbf{h}_t]$, with the i-th column removed. The size of \mathbf{H}_{-i}^* is $n \cdot n$. Let $\dot{\mathbf{x}}_{-i}$ be the n+1 dimensional column vector $\dot{\mathbf{x}}$ with the i-th component removed (t is part of t !). Then we can write according to (I-4):

$$\left[\frac{\mathbf{H}_{-i}^{*}}{\dot{\mathbf{x}}_{-i}^{T}}\middle|\frac{\partial \mathbf{h}}{\partial x_{i}}\right] \cdot \left[\frac{I}{0^{T}}\middle|\dot{\mathbf{x}}_{-i}\right] = \left[\frac{\mathbf{H}_{-i}^{*}}{\dot{\mathbf{x}}_{-i}^{T}}\middle|\frac{\mathbf{H}_{-i}^{*} \cdot \dot{\mathbf{x}}_{-i} + \frac{\partial \mathbf{h}}{\partial x_{i}}\dot{x}_{i}}{\dot{\mathbf{x}}_{-i}^{T} \cdot \dot{\mathbf{x}}_{-i} + \dot{x}_{i}^{2}}\right] = \left[\frac{\mathbf{H}_{-i}^{*}}{\dot{\mathbf{x}}_{-i}^{T}}\middle|0\right]$$
(I-9)

The first matrix on the left hand side, call it χ , is nonsingular because $\left[\dot{\mathbf{x}}_{-i}^T\middle|\dot{x}_i\right]$ is orthogonal to

every row of $\left[\mathbf{H}_{-i}^* \middle| \frac{\partial \mathbf{h}}{\partial x_i}\right]$, which itself has rank n. This results in:

$$\det(\chi) \cdot \det\left(\frac{I}{0^T} \middle| \frac{\dot{\mathbf{x}}_{-i}}{\dot{x}_i} \right) = \det\left(\frac{\mathbf{H}_{-i}^*}{\dot{\mathbf{x}}_{-i}^T} \middle| \frac{0}{1}\right) \tag{I-10}$$

or

$$\dot{x}_i \det(\chi) = \det(\mathbf{H}_{-i}^*) \tag{I-11}$$

This shows that \mathbf{H}_{-i}^* is singular if \dot{x}_i is zero. In other words, far from turning points with respect to x_i , i.e. far from a point on the homotopy path were, \mathbf{H}_{-i}^* should be far from singular, and x_i can be used as a local parameter for purposes of solving equations (I-1) and (I-2) for the unit tangent vector. Also, Newton corrections can be made safely in the hyperplane orthogonal to the x_i -axis.

The above remarks can be illustrated by the following example. The homotopy equation is:

$$h(x,t) = x^3 - 30x^2 + 280x - 860t = 0$$
 (ex-1)

and can be differentiated with respect to arclength s, to obtain:

$$\frac{\partial h}{\partial s} = \frac{\partial h}{\partial x}\frac{dx}{ds} + \frac{\partial h}{\partial t}\frac{dt}{ds} = \left[\frac{\partial h}{\partial x}\middle|\frac{\partial h}{\partial t}\right] \cdot \begin{bmatrix} \dot{x} \\ \dot{t} \end{bmatrix} = \left[3x^2 - 60x + 280\middle| - 860\right] \cdot \begin{bmatrix} \dot{x} \\ \dot{t} \end{bmatrix}$$
(ex-2)

At x = 0, $\left[\frac{\partial h}{\partial x}\right] = 280 \neq 0$. To compute the unit tangent vector, u, we first solve:

$$280v_1 - 860v_2 = 0 (ex-3)$$

corresponding to equation (I-1), where v_1 and v_2 are placeholders for \dot{x} and \dot{t} (the derivatives of x and t to arclength s). Since t does not vanish, we may set $v_2 = 1$. Then, $v_1 = 860/280 = 3.0714286$. Therefore,

$$\mathbf{u} = \frac{(v_1, v_2)^T}{\|v_1, v_2\|} = \frac{(3.07, 1)^T}{\|3.07, 1\|}$$
 (ex-4)

which satisfies both equation (I-1) and (I-2). The resulting tangent vector, **u**, which is the solution of equation (ex-1) is unity due to the constraint equation (I-2).

Given a steplength, the Euler predictor step can be taken followed by a Newton correction parallel to the x-axis with t fixed. This procedure can be repeated until $t \approx 0.97$. At t = 0.9702634 and x = 7.4180111, the 1·1 matrix representing \mathbf{H}_x is singular, i.e.

 $3x^2 - 60x + 280 = 0$. This is a turning point with respect to t; and, at such point, i = 0. In this 1-D case, it is clear that the unit tangent vector is just $(1, 0)^T$; nevertheless, we shall go through the formalities.

We must change the local parameter from x_2 to x_1 , where x_1 is to be identified with x and x_2 is to be identified with t. The 1·1 matrix \mathbf{H}_{-i}^* consisting of the element -860, is nonsingular and the scalar \dot{x}_1 is nonzero. Normally we would set v_1 equal to 1 and compute the remaining components of v other then v_{n+1} , the placeholder for t. In this 1-D case, there are no additional components of v (other then v_{n+1} which is zero). Therefore,

$$\mathbf{u} = \frac{(v_1, v_2)^T}{\|v_1, v_2\|} = \frac{(1, 0)^T}{\|1, 0\|}$$
 (ex-5)

Reparameterization of homotopy differential equations

The equation given by (I-1) can be written in the next matrix notation:

$$\begin{bmatrix}
\frac{\partial h_{1}}{\partial x_{1}} & \frac{\partial h_{1}}{\partial x_{2}} & \cdots & \frac{\partial h_{1}}{\partial x_{n}} & \frac{\partial h_{1}}{\partial t} \\
\frac{\partial h_{2}}{\partial x_{1}} & \frac{\partial h_{2}}{\partial x_{2}} & \cdots & \frac{\partial h_{2}}{\partial x_{n}} & \frac{\partial h_{2}}{\partial t} \\
\vdots & & \vdots & \vdots & \vdots \\
\frac{\partial h_{n}}{\partial x_{1}} & \frac{\partial h_{n}}{\partial x_{2}} & \cdots & \frac{\partial h_{n}}{\partial x_{n}} & \frac{\partial h_{n}}{\partial t}
\end{bmatrix} \cdot
\begin{bmatrix}
\frac{dx_{1}}{ds} \\
\frac{dx_{2}}{ds} \\
\vdots \\
\frac{dx_{n}}{ds} \\
\frac{dt}{ds}
\end{bmatrix} =
\begin{bmatrix}
0 \\
0 \\
\vdots \\
0
\end{bmatrix}$$
(I-12)

This set (I-12) is made determinant by addition of the definitive equation for arclength of the tangent vector (Rion and Brunt 1990):

$$(ds)^{2} = (dx_{1})^{2} + (dx_{2})^{2} + \dots + (dx_{n})^{2} + (dt)^{2}$$
(I-13)

which also can be written as:

$$1 = \left(\frac{dx_1}{ds}\right)^2 + \left(\frac{dx_2}{ds}\right)^2 + \dots + \left(\frac{dx_n}{ds}\right)^2 + \left(\frac{dt}{ds}\right)^2$$
 (I-14)

Euler Prediction

In order to avoid singularities in the Jacobian matrix in equation (I-12), as turning points are approached, the local continuation variable technique of Rheinboldt and Burkardt (1983) can be used. The local continuation variable is chosen as the one whose component of the tangent vector from the previous iteration has the largest absolute value. First we identify t with x_{n+1} , the expressions (I-12) and (I-14) transform to:

$$\begin{bmatrix}
\frac{\partial h_{1}}{\partial x_{1}} & \frac{\partial h_{1}}{\partial x_{2}} & \cdots & \frac{\partial h_{1}}{\partial x_{n}} & \frac{\partial h_{1}}{\partial x_{n+1}} \\
\frac{\partial h_{2}}{\partial x_{1}} & \frac{\partial h_{2}}{\partial x_{2}} & \cdots & \frac{\partial h_{2}}{\partial x_{n}} & \frac{\partial h_{2}}{\partial x_{n+1}} \\
\vdots & & \vdots & \vdots \\
\frac{\partial h_{n}}{\partial x_{1}} & \frac{\partial h_{n}}{\partial x_{2}} & \cdots & \frac{\partial h_{n}}{\partial x_{n}} & \frac{\partial h_{n}}{\partial x_{n+1}}
\end{bmatrix} \cdot \begin{bmatrix}
\frac{dx_{1}}{ds} \\
\frac{dx_{2}}{ds} \\
\vdots \\
\frac{dx_{n}}{ds} \\
\frac{dx_{n+1}}{ds}
\end{bmatrix} = \begin{bmatrix} 0 \\ 0 \\
\vdots \\
0 \end{bmatrix}$$
(I-15)

$$1 = \left(\frac{dx_1}{ds}\right)^2 + \left(\frac{dx_2}{ds}\right)^2 + \dots + \left(\frac{dx_n}{ds}\right)^2 + \left(\frac{dx_{n+1}}{ds}\right)^2$$
 (I-16)

Consider the k-th variable($x_1, x_2, ..., x_{n+1}$) of equations (I-15) to be the continuation variable; then (I-15) can be reduced with respect to the continuation variable, x_k , to the following $n \cdot n$ system:

$$\begin{bmatrix}
\frac{\partial h_{1}}{\partial x_{1}} & \dots & \frac{\partial h_{1}}{\partial x_{k-1}} & \frac{\partial h_{1}}{\partial x_{k+1}} & \dots & \frac{\partial h_{1}}{\partial x_{n+1}} \\
\frac{\partial h_{2}}{\partial x_{1}} & \dots & \frac{\partial h_{2}}{\partial x_{k-1}} & \frac{\partial h_{2}}{\partial x_{k+1}} & \dots & \frac{\partial h_{2}}{\partial x_{n+1}} \\
\vdots & & \vdots & & \vdots & & \vdots \\
\frac{\partial h_{n}}{\partial x_{1}} & \dots & \frac{\partial h_{n}}{\partial x_{k-1}} & \frac{\partial h_{n}}{\partial x_{k+1}} & \dots & \frac{\partial h_{n}}{\partial x_{n+1}}
\end{bmatrix} \cdot \begin{bmatrix}
\frac{dx_{1}}{ds} \\
\frac{dx_{k-1}}{ds} \\
\frac{dx_{k-1}}{ds} \\
\frac{dx_{k+1}}{ds}
\end{bmatrix} = -\begin{bmatrix}
\frac{\partial h_{1}}{\partial x_{k}} \\
\frac{\partial h_{2}}{\partial x_{k}} \\
\frac{\partial h_{2}}{\partial x_{k}} \\
\frac{\partial h_{n}}{\partial x_{k}}
\end{bmatrix} = -\begin{bmatrix}
\frac{\partial h_{1}}{\partial x_{k}} \\
\frac{\partial h_{2}}{\partial x_{k}} \\
\frac{\partial h_{2}}{\partial x_{k}} \\
\frac{\partial h_{2}}{\partial x_{k}}
\end{bmatrix} = -\begin{bmatrix}
\frac{\partial h_{1}}{\partial x_{k}} \\
\frac{\partial h_{2}}{\partial x_{k}} \\
\frac{\partial h_{2}}{\partial x_{k}} \\
\frac{\partial h_{2}}{\partial x_{k}}
\end{bmatrix} = -\begin{bmatrix}
\frac{\partial h_{1}}{\partial x_{k}} \\
\frac{\partial h_{2}}{\partial x_{k}} \\
\frac{\partial h_{2}}{\partial x_{k}} \\
\frac{\partial h_{2}}{\partial x_{k}}
\end{bmatrix} = -\begin{bmatrix}
\frac{\partial h_{1}}{\partial x_{k}} \\
\frac{\partial h_{2}}{\partial x_{k}} \\
\frac{\partial h_{2}}{\partial x_{k}}
\end{bmatrix} = -\begin{bmatrix}
\frac{\partial h_{1}}{\partial x_{k}} \\
\frac{\partial h_{2}}{\partial x_{k}} \\
\frac{\partial h_{2}}{\partial x_{k}}
\end{bmatrix} = -\begin{bmatrix}
\frac{\partial h_{1}}{\partial x_{k}} \\
\frac{\partial h_{2}}{\partial x_{k}} \\
\frac{\partial h_{2}}{\partial x_{k}}
\end{bmatrix} = -\begin{bmatrix}
\frac{\partial h_{1}}{\partial x_{k}} \\
\frac{\partial h_{2}}{\partial x_{k}} \\
\frac{\partial h_{2}}{\partial x_{k}}
\end{bmatrix} = -\begin{bmatrix}
\frac{\partial h_{1}}{\partial x_{k}} \\
\frac{\partial h_{2}}{\partial x_{k}} \\
\frac{\partial h_{2}}{\partial x_{k}}
\end{bmatrix} = -\begin{bmatrix}
\frac{\partial h_{1}}{\partial x_{k}} \\
\frac{\partial h_{2}}{\partial x_{k}} \\
\frac{\partial h_{2}}{\partial x_{k}}
\end{bmatrix} = -\begin{bmatrix}
\frac{\partial h_{1}}{\partial x_{k}} \\
\frac{\partial h_{2}}{\partial x_{k}} \\
\frac{\partial h_{2}}{\partial x_{k}}
\end{bmatrix} = -\begin{bmatrix}
\frac{\partial h_{1}}{\partial x_{k}} \\
\frac{\partial h_{2}}{\partial x_{k}} \\
\frac{\partial h_{2}}{\partial x_{k}}
\end{bmatrix} = -\begin{bmatrix}
\frac{\partial h_{1}}{\partial x_{k}} \\
\frac{\partial h_{2}}{\partial x_{k}} \\
\frac{\partial h_{2}}{\partial x_{k}}
\end{bmatrix} = -\begin{bmatrix}
\frac{\partial h_{1}}{\partial x_{k}} \\
\frac{\partial h_{2}}{\partial x_{k}} \\
\frac{\partial h_{2}}{\partial x_{k}}
\end{bmatrix} = -\begin{bmatrix}
\frac{\partial h_{1}}{\partial x_{k}} \\
\frac{\partial h_{2}}{\partial x_{k}} \\
\frac{\partial h_{2}}{\partial x_{k}}
\end{bmatrix} = -\begin{bmatrix}
\frac{\partial h_{1}}{\partial x_{k}} \\
\frac{\partial h_{2}}{\partial x_{k}} \\
\frac{\partial h_{2}}{\partial x_{k}}
\end{bmatrix} = -\begin{bmatrix}
\frac{\partial h_{1}}{\partial x_{k}} \\
\frac{\partial h_{2}}{\partial x_{k}} \\
\frac{\partial h_{2}}{\partial x_{k}}
\end{bmatrix} = -\begin{bmatrix}
\frac{\partial h_{1}}{\partial x_{k}} \\
\frac{\partial h_{2}}{\partial x_{k}}
\end{bmatrix} = -\begin{bmatrix}
\frac{\partial h_{1}}{\partial x_{k}} \\
\frac{\partial h_{2}}{\partial x_{k}}
\end{bmatrix} = -\begin{bmatrix}
\frac{\partial h_{1}}{\partial x_{k}} \\
\frac{\partial h_{2}}{\partial x_{k}}
\end{bmatrix} = -\begin{bmatrix}
\frac{\partial h_{1}}{\partial x_{k}} \\
\frac{\partial h_{2}}{\partial x_{k}}
\end{bmatrix} = -\begin{bmatrix}
\frac{\partial h_{1}}{\partial x_{k}} \\
\frac{\partial h_{2}}{\partial x_{k}}
\end{bmatrix} = -\begin{bmatrix}\frac{\partial h_{1}}{\partial x_{k}} \\
\frac{\partial h_{2}}{\partial x_{k}}
\end{bmatrix} = -\begin{bmatrix}\frac{\partial h_{1}}{\partial x_{k}} \\
\frac{\partial h_{2}}{\partial x_{k}}
\end{bmatrix} = -$$

Choose $\frac{dx_k}{ds} = 1$ and solve set (I-17) for the other $\frac{dx_i}{ds}$. This results does not satisfy equation (I-16).

This is solved via calculation of the unit tangent vector, u,

$$\mathbf{u} = \frac{\left(\frac{dx_1}{ds}, \dots, \frac{dx_{n+1}}{ds}\right)^T}{\left\|\frac{dx_1}{ds}, \dots, \frac{dx_{n+1}}{ds}\right\|}$$
(I-18)

which satisfies both equations (I-15) and (I-16).

The estimate of x at s_{i+1} denoted by $\tilde{\mathbf{x}}(s_{i+1})$, where i is the current iteration step, is calculated as follows with an Euler step.

$$\widetilde{\mathbf{x}}(s_{i+1}) = \mathbf{x}(s_i) + \Delta s \cdot \mathbf{u} \tag{I-19}$$

Correction procedure

Once an estimate to the homotopy path is generated as above, Newton's method is employed to correct back to the exact homotopy path. The homotopy equations form a set of n equations in n+1 unknowns. In the correction procedure the following set has to solved, where j is the j-th iteration of the Newton loop:

$$\begin{bmatrix}
\frac{\partial h_{1}}{\partial x_{1}} & \frac{\partial h_{1}}{\partial x_{2}} & \cdots & \frac{\partial h_{1}}{\partial x_{n}} & \frac{\partial h_{1}}{\partial x_{n+1}} \\
\frac{\partial h_{2}}{\partial x_{1}} & \frac{\partial h_{2}}{\partial x_{2}} & \cdots & \frac{\partial h_{2}}{\partial x_{n}} & \frac{\partial h_{2}}{\partial x_{n+1}} \\
\vdots & \vdots & \vdots & \vdots \\
\frac{\partial h_{n}}{\partial x_{1}} & \frac{\partial h_{n}}{\partial x_{2}} & \cdots & \frac{\partial h_{n}}{\partial x_{n}} & \frac{\partial h_{n}}{\partial x_{n+1}}
\end{bmatrix} \cdot \begin{bmatrix}
x_{1}^{j+1} - x_{1}^{j} \\
x_{2}^{j+1} - x_{2}^{j} \\
\vdots \\
x_{n+1}^{j+1} - x_{n+1}^{j}
\end{bmatrix} = -\begin{bmatrix}
h_{1}(\mathbf{x}^{j}) \\
h_{2}(\mathbf{x}^{j}) \\
\vdots \\
h_{n}(\mathbf{x}^{j})
\end{bmatrix}$$
(I-20)

This system (I-20) is made determinant during application of Newton's method in one of two ways. The first method is to hold one of the variables constant. This yields an $n \cdot n$ determinant system. Rheinboldt (1980) recommends that the variable with the largest gradient be held constant to prevent numerical instability. This can be accomplished by supplementing the equation set (I-20) by the equations:

$$\left[\mathbf{e}^{i} \cdot \left(\mathbf{x} - \mathbf{x}^{k}\right)\right] = 0 \tag{I-21}$$

where

$$\mathbf{e}^{i} = [0, 0, 0, ..., 1_{i}, 0, ..., 0]$$
 (I-22)

and i represents the variable with the largest gradient to the homotopy path.

In the second method the equation set is supplemented by the equations:

$$\left[\mathbf{u}^T \cdot \mathbf{N}_{cor}\right] = 0 \tag{I-23}$$

where N_{cor} is the vector of Newton correctors, short for the column vector given in (I-20) on the left hand side. The vector \mathbf{u} is the unit tangent vector given by (I-18). This is a geometric constraint that forces corrections to be made in the hyperplane orthogonal to the tangent vector (see Allgower and Georg 1990).

APPENDIX 6: Equations used for Index Determination.

This appendix contains all the equations which are used in MAPLE V release 5 for determination of the index of the ethane cracker model. All the following equations are found in Froment 79. The variation of the molar flow of the components is given by:

$$\frac{dF_j}{dz} = A_{coil} \left(\sum_{i=1}^{7} \alpha_{ij} r_i \right) \quad j = 1 \text{ to } 9$$
(A.1-A.9)

The heat balance:

$$\frac{dT}{dz} = \frac{\left[q(z)\pi d + A_{coil}\sum_{i=1}^{7}(-\Delta H_i)r_i\right]}{\sum_{j=1}^{9}F_jCp_j}$$
(A.10)

The momentum equation is expressed as:

$$-\frac{dP}{dz} = \left[2\frac{f}{d} + \frac{9f_{bend}}{2L}\right]\rho u^2 + \rho u \frac{du}{dz}$$
(A.11)

The velocity can be represented by the following equations:

$$u = \frac{G}{\rho} \tag{A.12}$$

The density of the gas mixture:

$$\rho = \frac{M_m P}{RT} \tag{A.13}$$

The mean molar mass of the reaction mixture

$$M_m = \frac{GA_{coil}}{sumF} \tag{A.14}$$

$$sumF = \sum_{i=1}^{9} F_i \tag{A.15}$$

The friction factor:

$$f = 0.046 \left(\frac{dG}{\mu}\right)^{-0.2} \tag{A.16}$$

$$\mu_{j} = \frac{\sqrt{M_{j}} P c_{j}^{2/3}}{T c_{j}^{1/6}} \left(1.9 \frac{T}{T c_{j}} - 0.29 \right) 10^{-7} Z c_{j}^{-2/3}$$
(A.17-A.25)

$$\mu = \frac{\sum_{j=1}^{9} F_j \mu_j}{sumF} \tag{A.26}$$

The rate of the reactions:

$$r_1 = ko_1 \exp\left(-\frac{E_1}{RT}\right) \frac{F_4}{sumF} \frac{P}{RT} \tag{A.27}$$

$$r_2 = ko_2 \exp\left(-\frac{E_2}{RT}\right) F_3 F_8 \frac{P^2}{(RTsumF)^2}$$
 (A.28)

$$r_3 = ko_3 \exp\left(-\frac{E_3}{RT}\right) \frac{F_4}{sumF} \frac{P}{RT} \tag{A.29}$$

$$r_4 = ko_4 \exp\left(-\frac{E_4}{RT}\right) \frac{F_5}{sumF} \frac{P}{RT} \tag{A.30}$$

$$r_5 = ko_5 \exp\left(-\frac{E_5}{RT}\right) F_1 F_2 \frac{P^2}{\left(RTsumF\right)^2}$$
(A.31)

$$r_6 = ko_6 \exp\left(-\frac{E_6}{RT}\right) F_2 F_3 \frac{P^2}{(RTsumF)^2}$$
 (A.32)

$$r_7 = ko_7 \exp\left(-\frac{E_7}{RT}\right) F_3 F_4 \frac{P^2}{(RTsumF)^2}$$
 (A.33)

The heat of reaction is:

$$\Delta H_i = \sum_{i=1}^{9} \alpha_{ij} \Delta H_{f,i}$$
 for : $i = 1$ to 7 (A.34-A.40)

The heat of formation at temperature T of component j is:

$$\Delta H_{f,j} = \Delta H_{f,j}^{o} + \int_{T_{e,j}}^{T} Cp_{j} dT$$
 for $: j = 1 \text{ to } 9$ (A.41-A.49)

The specific heat of the gas is given by:

$$Cp_j = A_j + B_j T + C_j T^2 + D_j T^3$$
 for $: j=1 \text{ to } 9$ (A.50-A.58)

APPENDIX 7: Momentum and Heat Balance Applied to Heated Tubes

The aim of this appendix is to derive the momentum and heat balance used to describe the flow in a tube. The balances are derived from the equation of motion and the finite difference energy balance (vector-tensor equations) given in Bird 60. First we start with the momentum balance.

Momentum Balance

For an infinitesimal volume with dimensions dx, dy and dz, the following differential momentum balance can be derived. The fluid is able to move through all six faces of the volume in any arbitrary direction. The equation below is a vector-tensor equation in rectangular coordinates (x, y, z) (Bird 60):

(a) (b) (c) (d) (e)
$$\frac{\partial}{\partial t} \rho \mathbf{v} = -[\nabla \cdot \rho \mathbf{v} \mathbf{v}] - \nabla P - [\nabla \cdot \tau] + \rho \mathbf{g}$$
 (2-1)

The density and the velocity of the fluid is represented respectively by ρ and the vector \mathbf{v} . The pressure of the system is given by the scalar P. The vector \mathbf{g} is the acceleration of gravity. The tensor τ is the momentum flux tensor or stress tensor. The term (a) gives the rate of increase of momentum per unit of volume. Term (b) is the rate of momentum gain by convection per unit of volume. The pressure force on the element per unit of volume is given by term (c). The rate of momentum gain by viscous transfer per unit of volume is represented by term (d). Term (e) is the gravitation force on the element per unit of volume.

We consider a system with a single fluid entrance (at plane "1" with cross section A_1) and a single exit (at plane "2" with cross section A_2), a heat input Q and Mechanical work W out. This system does not move with respect to the coordinate system. This is schematically given by Figure 2.

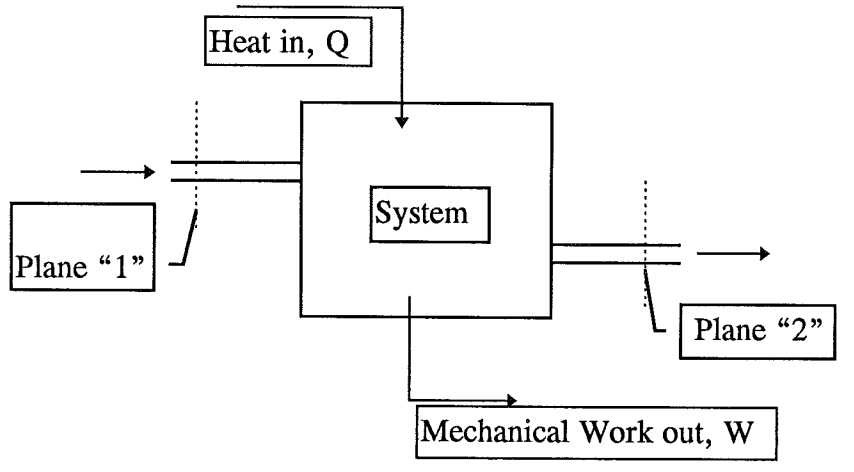


Figure 2: Macroscopic flow system with fluid entering at plane "1" and leaving at plane "2".

These reference planes are chosen to be perpendicular to the tube walls. The following assumptions are made:

- At the planes "1" and "2" the time-smoothed velocity is parallel to the conduit walls
- At the planes "1" and "2" the density ρ and other physical properties do not vary across the cross section.

Integration of the equation of motion (2-1) over the volume V results in:

$$\frac{d}{dt}\mathbf{p}_{tot} = \rho_1 \langle \overline{v}_1^2 \rangle \mathbf{A}_1 - \rho_2 \langle \overline{v}_2^2 \rangle \mathbf{A}_2 + P_1 \mathbf{A}_1 - P_2 \mathbf{A}_2 - \mathbf{F} + m_{tot} \mathbf{g}$$
(2-2)

With:

$$\mathbf{p}_{tot} = \int_{V} \rho \overline{v} dV \tag{2-3}$$

$$m_{tot} = \int_{V} \rho dV \tag{2-4}$$

For a circular tube $\langle \overline{v}^n \rangle$ is given by:

$$\left\langle \overline{v}^{n}\right\rangle =\frac{\int\limits_{0}^{2\pi R}\overline{v}^{n}rdrd\theta}{\int\limits_{0}^{2\pi R}rdrd\theta} \tag{2-5}$$

To indicate that a variable is a vector, they are written in boldface. The $\overline{\mathbf{v}}$ is the time-smoothed velocity vector. This concept will be explained via turbulent flow in a pipe. If the flow is turbulent the velocity will fluctuate both in time as well as in space. Focus on the fluid at one point in the tube, where turbulent flow exists. If we imagine that while watching this spot the pressure drop causing the flow, is increased slowly so that the mean axial velocity will slowly increase. The instantaneous velocity \mathbf{v}_z is an irregular (chaotic) oscillating function. The time-smoothed velocity $\overline{\mathbf{v}}_z$ is defined by taking a time average of \mathbf{v}_z over a time interval \mathbf{t}_o with respect to the time scale of turbulent oscillation, but small with respect to time-changes in the imposed pressure drop causing the flow:

$$\overline{v}_z = \frac{1}{t_o} \cdot \int_t^{t+t_o} v_z dt \tag{2-6}$$

The Force F in formula (2-2) is the force of the fluid on the solid and is made up of all viscous and pressure forces. The derivation of formula (2-2) from the equation of motion is given in the next section.

Transformation of equation of motion to macroscopic balance

We integrate formula (2-1) to derive the macroscopic momentum balance for a flow system such as Figure 2. Consider the situation that the time-smoothed behavior is steady. Use the Gauss divergence theorem to transform volume integrals to surface integrals:

$$\int_{V} (\nabla \cdot U) dV = \int_{A_{u}} U_{n} dA + \int_{A_{1}} U_{n} dA + \int_{A_{2}} U_{n} dA$$
(2.1-1)

in which V is the volume between "1" and "2" containing the fluid. It is convenient to split up the surface of V into the wetted solid surface $A_{\rm w}$ (one phase flow only) and the cross-sectional areas at "1" and "2" $(A_1 A_2)$. Note that $U_{\rm n}$ is the outward normal component of U. With the assumption that the time-smoothed behavior is steady, the equation of motion can be written in terms of the time-smoothed quantities

(a) (b) (c) (d) (e)
$$\frac{\partial}{\partial t} \rho \overline{\mathbf{v}} = -\left[\nabla \cdot \rho \overline{\mathbf{v}} \overline{\mathbf{v}}\right] - \nabla \overline{P} - \left[\nabla \cdot \overline{\mathbf{\tau}}\right] + \rho \mathbf{g}$$
 (2.1-2)

For completeness there should be mentioned that the term (d) is a summation of the viscous and turbulent momentum flux $[\nabla \cdot \overline{\tau}] = [\nabla \cdot \overline{\tau}^{(t)}] + [\nabla \cdot \overline{\tau}^{(t)}]$. The turbulent momentum flux $\overline{\tau}^{(t)}$ are usually referred to as the Reynolds stresses. More information over these two momentum fluxes can be found in Bird 60.

This equation is valid for turbulent as well as viscous flow. Expression (2.1-2) will be integrated term by term, over the volume of the entire flow system:

(a)
$$\int_{V} \frac{\partial}{\partial t} \rho \overline{v} dV = \frac{d}{dt} \int_{V} \rho \overline{v} dV = \frac{d}{dt} \mathbf{p}_{tot}$$
 (2.1-3)

The definition of P_{tot} is given in formula (2-3). This integral vanishes when the system does not change with time. Equation (2.1-3) only holds when the system does not move with respect to the coordinate system.

(b)
$$\int_{V} \nabla \cdot \rho \overline{v} \overline{v} dV = \int_{A_{w} + A_{1} + A_{2}} (\rho \overline{v} \overline{v})_{n} dA = -\rho \langle \overline{v}_{1}^{2} \rangle A_{1} + \rho \langle \overline{v}_{2}^{2} \rangle A_{2}$$
 (2.1-4)

The mean velocity of the time-smoothed velocity is given for a circular tube by expression (2-5). The integral over A_w is zero because v is zero on the wetted surfaces. The "1" term acquires a minus sign, since the flow velocity is inwardly directed, that is, opposed to the outward normal vector

(c)
$$\int_{V} \nabla P dV = \int_{A_{w} + A_{1} + A_{2}} (P)_{n} dA = -P_{1} \cdot A_{1} + P_{2} \cdot A_{2}$$
 (2.1-5)

The Gauss divergence theorem can also be applied to scalars. Here the integral over A_w is identically zero.

(d)
$$\int_{V} \left[\nabla \cdot \overline{\tau} \right] dV = \mathbf{F}$$
 (2.1-6)

No further manipulations are performed on this integral. It represents the force of the fluid on the solid and is made up of the sum of all viscous and pressure forces.

(e)
$$\int_{V} \rho \mathbf{g} dV = \int_{V} \rho dV \mathbf{g} = m_{tot} \mathbf{g}$$
 (2.1-7)

The m_{tot} is defined by equation (2-4).

Application of momentum equation to tube flow

Equation (2-2) can be applied to prescribe the pressure profile in pipe-flow. In steady state the expression given by (2-2) reduces to:

$$0 = \rho_1 \langle \overline{v}_1^2 \rangle \mathbf{A}_1 - \rho_2 \langle \overline{v}_2^2 \rangle \mathbf{A}_2 + P_1 \mathbf{A}_1 - P_2 \mathbf{A}_2 - \mathbf{F} + m_{tot} \mathbf{g}$$
(3-1)

If the force F is the sum of all the viscous and pressure forces. The volume integral of the momentum flux given by formula (2.1-6) states the force F. Application of the Gauss theorem results in:

$$\int_{V} \left[\nabla \cdot \overline{\tau} \right] dV = \int_{A_{w} + A_{1} + A_{2}} \overline{\tau}_{n} dV = \tau_{f \to w} \cdot A_{w} = F$$
(3-2)

The outward component of the stress at the planes "1" and "2" is zero. The momentum flux of the fluid to the wall can be modeled with the Fanning equation. This is given by Akker 96:

$$\tau_{f \to w} = f \cdot \frac{1}{2} \cdot \rho \langle \overline{v}^2 \rangle \tag{3-3}$$

Substitution of (3-3) in (3-2) and substitution of the result in expression (3-1) gives:

$$\rho_1 \langle \overline{v}_1^2 \rangle A - \rho_2 \langle \overline{v}_2^2 \rangle A + P_1 A - P_2 A = f \cdot \frac{1}{2} \cdot \rho \langle \overline{v}^2 \rangle \cdot S \cdot L + m_{tot} g$$
(3-4)

The cross-sectional area for planes "1" and "2" is the same and the tube considered has a single entrance and a single exit. For the acceleration of gravity we take the component in the direction of the flow. The area of the wetted surface A_w is equal to the product of circumference $(S=2\pi R)$ and the length of the tube L.

The velocity in the term on the right hand side is the velocity at the plane downstream ("2") Akker 96. Application of equation (3-4) to a section of a tube with length Δz gives the following formula. The velocity u is short for $\langle \overline{v} \rangle$.

$$\rho_z u_z^2 A - \rho_{z+\Delta z} u^2_{z+\Delta z} A + P_z A - P_{z+\Delta z} A = f \cdot \frac{1}{2} \cdot \rho \cdot u^2_{z+\Delta z} \cdot S \cdot \Delta z + \left(\int_z^{z+\Delta z} \rho A dz \right) \cdot g$$
 (3-5)

With the limit of Δz going to zero the following differential equation is obtained.

$$\frac{d}{dz}(P \cdot A + \rho \cdot u^2 A) = -\frac{1}{2} \cdot f \cdot \rho \cdot u^2 \cdot S + \rho \cdot A \cdot g \tag{3-6}$$

Expression (3-6) states the change along the tube of the momentum production. The Fanning friction factor (f) can be calculated with the usual equations, given in for instance Akker 96. If the assumption is made that the velocity profile is flat (plug flow), equation (3-6) can be written as:

$$\frac{d}{dz}(P \cdot A + \Phi_m \cdot u) = -\frac{1}{2} \cdot f \cdot \rho \cdot u^2 \cdot S + \rho \cdot A \cdot g \tag{3-7}$$

The following assumptions are made to obtain formula (3-7):

- Flat velocity profile (plug flow)
- The time-smoothed velocity profile can be applied (steady velocity profile)
- The time-smoothed velocities at plane "1" and "2" are parallel to the conduit walls
- The fluid properties do not vary across the cross section
- The system is in steady state.
- The Fanning equation can be used to model the momentum flux from the fluid to the tubes wall

In order to neglect the influence of the gravitation force the following criteria can be used. We want to neglect the gravitation contribution relative to the Fanning contribution. This gives the next comparison:

$$f \cdot u^2 \cdot R \qquad \sim \qquad R^2 \cdot g \tag{3-8}$$

The criteria defined as C_{mb} gives the ratio of the gravitation and the Fanning contribution to the derivative of the total momentum.

$$C_{mb} = \frac{R \cdot g}{f \cdot u^2} = \frac{d \cdot g}{2 \cdot f \cdot u^2} \tag{3-9}$$

If, for instance, $C_{\rm mb}$ smaller is than ε (is a criteria for instance 10^{-3}), the gravitation contribution can be neglected.

Heat Balance

For an infinitesimal volume with dimensions dx, dy and dz, the following finite difference energy balance can be given. The fluid is able to move through all six faces of the volume in any arbitrary direction. The equation below is a vector-tensor equation in rectangular coordinates (x, y, z) (Bird 60):

(a) (b) (c) (d) (e)
$$\frac{\partial}{\partial t} \rho \cdot \hat{E} = -(\nabla \cdot \rho \mathbf{v} \hat{E}) - (\nabla \cdot \mathbf{q}) - (\nabla \cdot P \mathbf{v}) - (\nabla \cdot [\tau \cdot \mathbf{v}])$$
(4-1)

Term (a) is the rate of gain of energy per unit volume. The term (b) represents the rate of energy input per unit volume by conduction. The rate of energy input per unit volume by conduction is given by term (c). The rate of work done on the fluid per unit volume by pressure forces is represented with (d). The term (e) gives the rate of work done on the fluid per unit volume by viscous forces. The expression (4-1) is the first law of thermodynamics for an "open", instationary system. Actually this statement of the first law is not complete in that other forms of energy and energy transport such as nuclear, radiative, and electromagnetic, are not included.

With \hat{E} defined as total energy:

$$\hat{E} = \hat{U} + \hat{K} + \hat{\Phi} \tag{4-2}$$

The term \hat{K} represents the kinetic energy and is given by:

$$\hat{K} = \frac{1}{2}v^2 \tag{4-3}$$

The potential energy is expressed in terms of the gradient of a scalar function, that is:

$$g = -\nabla \hat{\Phi} \tag{4-4}$$

By internal energy (\hat{U}) we understand the energy associated with the random translation and internal motion of the molecules plus the energy of interaction between the molecules; that is, the internal energy is dependent on local temperature and density of the fluid. Kinetic energy (\hat{K}) is interpreted as the energy associated with the observable fluid motion. The potential energy of the fluid is denoted with $\hat{\Phi}$.

We consider the system sketched in Figure 2, and assume, as is done in the chapter 2, that the time-smoothed velocities at "1" and "2" are parallel to the conduit walls and that the fluid properties do not vary across the cross section.

Integration of equation (4-1) over the volume results in the next macroscopic expression:

$$\frac{d}{dt}(U_{tot} + K_{tot} + \Phi_{tot}) = \rho_1 \cdot \langle \overline{v}_1 \rangle \cdot \hat{U}_1 \cdot A_1 - \rho_2 \cdot \langle \overline{v}_2 \rangle \cdot \hat{U}_2 \cdot A_2
+ \frac{1}{2} \cdot \rho_1 \cdot \langle \overline{v}_1^3 \rangle A_1 - \frac{1}{2} \cdot \rho_2 \cdot \langle \overline{v}_2^3 \rangle A_2
+ \rho_1 \cdot \langle \overline{v}_1 \rangle \cdot \hat{\Phi}_1 \cdot A_1 - \rho_2 \cdot \langle \overline{v}_2 \rangle \cdot \hat{\Phi}_2 \cdot A_2
+ Q - W
+ P_1 \cdot \langle \overline{v}_1 \rangle \cdot A_1 - P_2 \cdot \langle \overline{v}_2 \rangle \cdot A_2$$
(4-5)

The term Q is the heat entering the fluid via the solid surface and by conduction or radiation in the fluid at the inlet and outlet. The term W is the work transferred by means of moving parts (e.g. a turbine or compressor) and work needed to introduce new material at "1" and remove material at "2". In expression (4-5) U_{tot} , K_{tot} and Φ_{tot} are the total internal, kinetic and potential energies in the system. These quantities are defined as:

$$U_{tot} = \int_{V} \rho \hat{U} dV \tag{4-6}$$

$$K_{tot} = \int_{V} \frac{1}{2} \rho \bar{v}^2 dV \tag{4-7}$$

$$\Phi_{tot} = \int_{V} \rho \hat{\Phi} dV \tag{4-8}$$

Transformation of energy balance to macroscopic energy balance.

Integration of formula (4-1) results in the macroscopic energy balance for a flow such as Figure 2. Consider the situation that the time-smoothed behavior is steady. Use the Gauss divergence theorem to transform volume integrals to surface integrals:

$$\int_{V} (\nabla \cdot U) dV = \int_{A_{n}} U_{n} dA + \int_{A_{n}} U_{n} dA + \int_{A_{n}} U_{n} dA$$
(4.1-1)

in which V is the volume between "1" and "2" containing the fluid. It is convenient to split up the surface of V into the wetted solid surface $A_{\rm w}$ (one phase flow only) and the cross-sectional areas at "1" and "2" $(A_1 A_2)$. Note that $U_{\rm n}$ is the outward normal component of U. With the assumption that the time-smoothed behavior is steady, the energy balance can be written in terms of the time-smoothed quantities.

(a) (b) (c) (d) (e)
$$\frac{\partial}{\partial t} \rho \cdot \hat{E} = -\left(\nabla \cdot \rho \overline{\mathbf{v}} \hat{E}\right) - \left(\nabla \cdot \overline{\mathbf{q}}\right) - \left(\nabla \cdot \overline{P} \overline{\mathbf{v}}\right) - \left(\nabla \cdot [\overline{\tau} \cdot \overline{\mathbf{v}}]\right)$$
(4.1-2)

It should be mentioned that the terms (c) and (e) are summations of viscous and turbulent quantities. In the further discussion the term kinetic energy is also not completely correct because energy by turbulent fluctuations is not accounted for. Because they are generally small, compared to the kinetic energy of the main flow velocity. No further explanation is given, the author refers the reader for some more information to Bird 60.

Expression (4.1-2) will be integrated term by term, over the volume of the entire flow system. The system is assumed not to move with respect to the coordinate system.

(a)
$$\int_{V} \frac{\partial}{\partial t} \rho \hat{E} dV = \frac{d}{dt} \int_{V} \rho \hat{E} dV = \frac{d}{dt} \left(U_{tot} + K_{tot} + \Phi_{tot} \right)$$
 (4.1-3)

The definition of U_{tot} , K_{tot} and Φ_{tot} are given by the formulas (4-6), (4-7) and (4-8). This integral vanishes when the system does not change with time.

$$\int_{V} (\nabla \cdot \rho \overline{\mathbf{v}} \hat{E}) dV = \int_{A_{w} + A_{1} + A_{2}} (\rho \overline{\mathbf{v}} \hat{E})_{n} dA = -\rho_{1} \cdot \langle \overline{v}_{1} \rangle \cdot \hat{U}_{1} \cdot A_{1} + \rho_{2} \cdot \langle \overline{v}_{2} \rangle \cdot \hat{U}_{2} \cdot A_{2}$$
(b)
$$-\frac{1}{2} \rho_{1} \cdot \langle \overline{v}_{1}^{3} \rangle \cdot A_{1} + \frac{1}{2} \rho_{2} \cdot \langle \overline{v}_{2}^{3} \rangle \cdot A_{2}$$

$$-\rho_{1} \cdot \langle \overline{v}_{1} \rangle \cdot \hat{\Phi}_{1} \cdot A_{1} + \rho_{2} \cdot \langle \overline{v}_{2} \rangle \cdot \hat{\Phi}_{2} \cdot A_{2}$$
(4.1-4)

The surface mean value of the time-smoothed velocity is given for a circular tube by expression (2-5). The integral over $A_{\rm w}$ is zero because ${\bf v}$ is zero on the wetted surfaces (no slip condition). The "1" term acquires a minus sign, since the flow velocity is inwardly directed, that is, opposed to the outward normal. The 'total' energy in (4.1-4) is given by: $\hat{E} = \hat{U} + \hat{K} + \hat{\Phi}$.

(c)
$$\int_{V} -(\nabla \cdot \mathbf{q}) dV = Q$$
 (4.1-5)

No further manipulations are performed on this integral. Q represents the heat entering the fluid via the solid surface and by conduction and radiation in the fluid at the inlet and outlet.

(d)
$$\int_{V} (\nabla \cdot P\overline{\mathbf{v}}) dV = \int_{A_{1}+A_{1}+A_{2}} (P\overline{\mathbf{v}})_{n} dA = -P_{1} \cdot \langle \overline{v}_{1} \rangle \cdot A_{1} + P_{2} \cdot \langle \overline{v}_{2} \rangle \cdot A_{2}$$
 (4.1-6)

The integral over $A_{\mathbf{w}}$ is zero because \mathbf{v} is zero on the wetted surfaces.

(e)
$$\int_{V} (\nabla \cdot [\overline{\tau} \cdot \overline{\mathbf{v}}]) dV = \int_{A_{w} + A_{1} + A_{2}} (\overline{\tau} \cdot \overline{\mathbf{v}})_{n} dA \approx 0$$

Here the integral on A_w is identically zero; the integrals on A_1 and A_2 represent the work being done by viscous forces to push fluid into or out of the system and this contribution can be safely neglected (Bird 60).

Application of the heat balance to tube flow

A heated tube, for instance by fire, is of interest in the process of steam cracking of hydrocarbons. In the steady state of a process equation (4-5) changes to:

$$0 = \rho_{1} \cdot \langle \overline{v}_{1} \rangle \cdot \hat{U}_{1} \cdot A_{1} - \rho_{2} \cdot \langle \overline{v}_{2} \rangle \cdot \hat{U}_{2} \cdot A_{2}$$

$$+ \frac{1}{2} \cdot \rho_{1} \cdot \langle \overline{v}_{1}^{3} \rangle A_{1} - \frac{1}{2} \cdot \rho_{2} \cdot \langle \overline{v}_{2}^{3} \rangle A_{2}$$

$$+ \rho_{1} \cdot \langle \overline{v}_{1} \rangle \cdot \hat{\Phi}_{1} \cdot A_{1} - \rho_{2} \cdot \langle \overline{v}_{2} \rangle \cdot \hat{\Phi}_{2} \cdot A_{2}$$

$$+ Q - W$$

$$+ P_{1} \cdot \langle \overline{v}_{1} \rangle \cdot A_{1} - P_{2} \cdot \langle \overline{v}_{2} \rangle \cdot A_{2}$$

$$(5-1)$$

Application of equation (5-1) to a section of a tube with length Δz gives the following formula. The velocity u is short for $\langle \overline{v} \rangle$.

$$0 = \rho_{z} \cdot u_{z} \cdot \hat{U}_{z} \cdot A_{z} - \rho_{z+\Delta z} \cdot u_{z+\Delta z} \cdot \hat{U}_{z+\Delta z} \cdot A_{z+\Delta z}$$

$$+ \frac{1}{2} \cdot \rho_{z} \cdot u^{3}_{z \cdot A_{z}} - \frac{1}{2} \cdot \rho_{z+\Delta z} \cdot u^{3}_{z+\Delta z} \cdot A_{z+\Delta z}$$

$$+ \rho_{z} \cdot u_{z} \cdot \hat{\Phi}_{z} \cdot A_{z} - \rho_{z+\Delta z} \cdot u_{z+\Delta z} \cdot \hat{\Phi}_{z+\Delta z} \cdot A_{z+\Delta z}$$

$$+ Q_{wall} \cdot S \cdot \Delta z$$

$$+ P_{z} \cdot u_{z} \cdot A_{z} - P_{z+\Delta z} \cdot u_{z+\Delta z} \cdot A_{z+\Delta z}$$

$$(5-2)$$

The term Q_{wall} is the heat flux through the tube wall to the fluid in the tube. The heat input by conduction and radiation via the inlet and outlet is not accounted for. The work done by the fluid in the tube is assumed zero. With the limit of Δz going to zero the following differential equation is obtained.

$$\frac{d}{dz}\left(\rho \cdot u \cdot \hat{U} \cdot A + P \cdot u \cdot A + \frac{1}{2} \cdot \rho \cdot u^{3} \cdot A + \rho \cdot u \cdot \hat{\Phi} \cdot A\right) = Q_{wall} \cdot S$$
(5-3)

The expression given by (5-3) gives the change along the tube of the heat production. If plug flow is assumed, the equation given by (5-3) can be written as:

$$\frac{d}{dz}\left(\Phi_{m}\cdot\hat{U} + \Phi_{m}\cdot P\cdot\hat{V} + \Phi_{m}\frac{1}{2}\cdot u^{2} + \Phi_{m}\cdot\hat{\Phi}\right) = Q_{wall}\cdot S$$
(5-4)

The term \hat{V} is the reciprocal density ρ . The quantity $\hat{U} + P \cdot \hat{V}$, which appears in the foregoing equations, is called the enthalpy (per unit mass) and is given the symbol \hat{H} . Substitution of the enthalpy gives:

$$\frac{d}{dz}\left(\Phi_{m}\cdot\hat{H} + \Phi_{m}\frac{1}{2}\cdot u^{2} + \Phi_{m}\cdot\hat{\Phi}\right) = Q_{wall}\cdot S \tag{5-5}$$

If there is production of heat in the tube by a chemical reaction, equation (5-5) can be modified as follows.

$$\frac{d}{dz}\left(\Phi_m \cdot \hat{H} + \Phi_m \frac{1}{2} \cdot u^2 + \Phi_m \cdot \hat{\Phi}\right) = Q_{wall} \cdot S + \Delta H_r \cdot A \tag{5-6}$$

With ΔH_r the production of heat by a chemical reaction per unit volume. The potential energy can be neglected in most tube flow problems. This gives:

$$\frac{d}{dz}\left(\Phi_m \cdot \hat{H} + \Phi_m \frac{1}{2} \cdot u^2\right) = Q_{wall} \cdot S + \Delta H_r \cdot A \tag{5-7}$$

If the fluid is an ideal gas then the enthalpy can be calculated as follows:

$$\hat{H}(T) = \int_{T_{ref}}^{T} Cp(T)dT + \hat{H}(T_{ref})$$
(5-8)

The following assumption have been made to obtain the equation (5-7):

- The potential energy does not play an important role
- The flow regime is turbulent (plug flow)
- The work done by the fluid is zero
- The time-smoothed velocities at plane "1" and "2" are parallel to the conduit walls
- The fluid properties do not vary across the cross section
- The system is in steady state.
- The time-smoothed velocity profile can be applied.

In order to neglect the influence of the potential energy, the following criteria can be used. We want to neglect the potential energy contribution relative to the kinetic energy contribution. The potential energy $\hat{\Phi}$ is approximated with $h \cdot g$, the term h is some measure for the height relative to the earth (h=0 at the lowest part of the system). This gives the next comparison:

$$\frac{1}{2} \cdot u^2 \quad \sim \quad h \cdot g \tag{5-9}$$

Of course we can use the sum of the enthalpy and the kinetic energy as comparison, but in general the kinetic term is smaller than the enthalpy term. This results in a more sensitive criteria C_{hb} . The criteria defined as C_{hb} gives the ratio of the potential energy due to gravity and the kinetic energy contribution to the derivative of the total heat.

$$C_{hb} = \frac{2 \cdot h \cdot g}{u^2} \tag{5-10}$$

If for instance C_{hb} is smaller than ϵ the energy contribution due to gravitation can be neglected.

APPENDIX 8: Maximum Velocity of Compressible Fluid in a Tube

Picture a gas flowing at steady-state in a straight, constant-diameter pipe. Take as our system the contents of the pipe between lines a and b in Figure 3. An energy balance written over an accounting period equal to the time for 1 kg of gas to flow through the system, becomes:

$$0 = \left(\hat{H} + \frac{1}{2}u^2\right)_b - \left(\hat{H} + \frac{1}{2}u^2\right)_a - \hat{Q}$$
 (II-1)

or, for a differential-sized length of pipe:

$$d(\hat{H}) + ud(u) = d(\hat{Q}) \tag{II-2}$$

The " $^{"}$ " indicates that the properties H and Q are given per unit of mass. The property Q is the heat supplied by the surrounding to the tube.

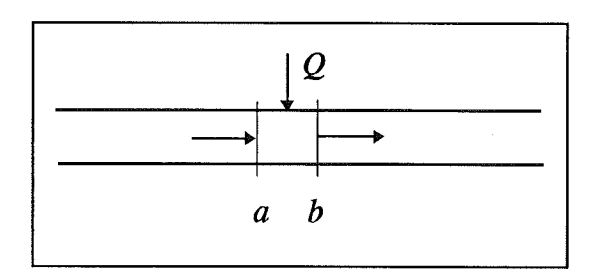


Figure 3: Gas flowing in constant-area pipe

The equation of continuity for a steady state process is:

$$Ad\left(\frac{u}{\hat{V}}\right) = 0 \tag{II-3}$$

The volume is denoted by V. The cross section A is a constant and therefore eliminated. Solving for the differential velocity u:

$$d(u) = \frac{ud(\hat{V})}{\hat{V}} \tag{II-4}$$

Substitution of (II-4) in (II-2) results in:

$$d\hat{H} = -u^2 \frac{d(\hat{V})}{\hat{V}} + d(\hat{Q})$$
 (II-5)

The thermodynamic states that the enthalpy can be written as:

$$d(\hat{H}) = Td(\hat{S}) + \hat{V}d(P) \tag{II-6}$$

Substitution of (II-5) in (II-6) gives:

$$Td(\hat{S}) = -\frac{u^2d(\hat{V})}{\hat{V}} - \hat{V}d(P) + d(\hat{Q})$$
(II-7)

As gas flows along a pipe in the direction of decreasing pressure, its specific volume increases, as its velocity increases in accord with equation (II-3). Thus in the direction of increasing velocity, d(P) is negative and d(V) is positive, and the first and the second term on the right hand side of the preceding equation contribute in opposite directions to the entropy change. For an adiabatic process, d(S) must be positive (with a limiting value of zero) according to the second law of thermodynamics. This condition is met as long as the second term in the equation makes a sufficiently large positive contribution to overbalance the negative contribution of the first term. However, as the pressure decreases, the specific volume increases ever more rapidly.

Thus it is possible to reach a pressure such that the negative contribution of the first term on the right hand side becomes equal to the positive contribution of the second. In this case a maximum velocity is reached at that differential length of pipe for which d(S) = 0. For an adiabatic (and isentropic) or reversible process expression (II-7) gives the maximum velocity:

$$u_{\text{max}}^2 = -\hat{V}^2 \left(\frac{\partial P}{\partial \hat{V}}\right)_{\text{S}} = \left(\frac{\partial P}{\partial \rho}\right)_{\text{S}}$$
 (II-8)

This is identical to the equation in physics for the speed of sound in the fluid (Smith and Van Ness 1987). Therefore, the maximum fluid speed obtainable in a pipe of constant cross-sectional area is the speed of sound.

The velocity of sound is the maximum value that can be reached in a conduit of constant cross section, provided the entrance velocity is subsonic. The sonic velocity must be reached at the exit of the pipe. If the pipe length is increased, the mass rate of flow decreases so that the sonic velocity is still obtained at the outlet of the lengthened pipe.

An other way to obtain the maximum attainable velocity in a tube, given by expression (II-8) is to consider formula (II-7) in the next form:

$$u^{2} = -\hat{V}^{2} \frac{d(P)}{d(\hat{V})} - \hat{V} \left(T \frac{d(\hat{S})}{d(\hat{V})} - \frac{d(\hat{Q})}{d(\hat{V})} \right) = \left(\frac{dP}{d\rho} \right) + \rho \left(T \frac{d\hat{S}}{d\rho} - \frac{d\hat{Q}}{d\rho} \right)$$
(II-9)

The second law of thermodynamics is prescribed as:

$$d(\hat{S}) \ge \frac{d(\hat{Q})}{T} \tag{II-10}$$

If the process is reversible and isentropic (speed of sound conditions) then equation (II-8) is obtained. For an irreversible process equation (II-10) holds without the equal sign. This results in a lower velocity due to the fact that $d(\rho)$ is negative, in combination with the second law. The velocity in a tube is lower or equal to the speed of sound:

$$u^{2} \le \left(\frac{\partial P}{\partial \rho}\right)_{S} \tag{II-11}$$

For an ideal gas the following equation for the pressure can be used:

$$P = \frac{\rho RT}{M} \tag{II-12}$$

At the end of this section it will be shown that equation (II-8) is equal to the next expression:

$$u_{\text{max}}^2 = \frac{Cp}{Cv} \left(\frac{\partial P}{\partial \rho} \right)_{\text{T}}$$
 (II-13)

The maximum velocity of an ideal gas is:

$$u_{\text{max}} = \sqrt{\frac{Cp}{Cv} \frac{RT}{M}}$$
 (II-14)

At isothermal conditions this reduces to:

$$u_{\text{max}} = \sqrt{\frac{RT}{M}} \tag{II-15}$$

The values resulting from equations (II-14) and (II-15) are an indication for the applicability of the momentum and heat balances described in this report. If the velocity of the gas is bigger than the velocity calculated with equations (II-14) and (II-15) the momentum and/or energy balance can not be applied anymore.

We will now derive expression (II-13). With the chain rule, (II-8) can be broken into:

$$\left(\frac{\partial P}{\partial V}\right)_{S} = \left(\frac{\partial P}{\partial T}\right)_{S} \left(\frac{\partial T}{\partial V}\right)_{S} \tag{II-16}$$

Each derivative on the right hand side of (II-16) is split into its entropy derivatives:

$$\left(\frac{\partial P}{\partial T}\right)_{S} = -\left(\frac{\partial S}{\partial T}\right)_{P} \left(\frac{\partial P}{\partial S}\right)_{T} \quad \text{and} \quad \left(\frac{\partial T}{\partial V}\right)_{S} = -\left(\frac{\partial S}{\partial V}\right)_{T} \left(\frac{\partial T}{\partial S}\right)_{V}$$
(II-17)

The following Maxwell's equations are used (Smith and Van Ness 1987):

$$\left(\frac{\partial P}{\partial S}\right)_{T} = -\left(\frac{\partial \Gamma}{\partial V}\right)_{P} \quad \text{and} \quad \left(\frac{\partial S}{\partial V}\right)_{T} = \left(\frac{\partial P}{\partial \Gamma}\right)_{V}$$
 (II-18)

From d(H) = Td(S) + Vd(P) and d(U) = Td(S) - Pd(V) it can be shown that:

$$\left(\frac{\partial S}{\partial T}\right)_{P} = \frac{Cp}{T}$$
 and $\left(\frac{\partial S}{\partial T}\right)_{V} = \frac{Cv}{T}$ (II-19)

Combination of (II-16) to (II-19) gives:

$$\left(\frac{\partial P}{\partial V}\right)_{S} = -\frac{Cp}{Cv} \left(\frac{\partial T}{\partial V}\right)_{P} \left(\frac{\partial P}{\partial T}\right)_{V} \tag{II-20}$$

Application of the same mathematics as to derive (II-17) yields:

$$\left(\frac{\partial P}{\partial V}\right)_{S} = \frac{Cp}{Cv} \left(\frac{\partial P}{\partial V}\right)_{T} \tag{II-21}$$

Substitution of (II-21) in (II-8) gives(II-13).

We have proven that the partial derivative of the pressure to the specific volume with constant entropy is equal to the ratio Cp over Cv times the partial derivative of the pressure to the specific volume at isothermal conditions.